AN INVESTIGATION OF TURBOGENERATOR DYNAMICS AND CONTROL

THESIS
SUBMITTED TO THE DEPARTMENT OF
ELECTRONICS AND ELECTRICAL ENGINEERING
OF GLASGOW UNIVERSITY

FOR THE DEGREE
DOCTOR OF PHILOSOPHY

BY

ZAKARIA FADLALMOULA MOHAMMED

ABSTRACT :

This thesis provides an investigation of the dynamics and control of turbogenerators from a multivariable control viewpoint. The multivariable control framework chosen -Individual Channel Analysis and Design- is particularly appropriate since it encapsulates the dynamical characteristics of the uncontrolled system with a view to exposing the potential and limitations for subsequent closed-loop control. The main contribution of the thesis is a complete new insight into why excitation/governor control with Power System Stabilisers (PSS) has been so successful for the control of turbogenerators connected to an infinite bus is provided by the small-signal multivariable analysis framework, Individual Channel Analysis and Design. The multivariable analysis justifies treating the turbogenerator system as a pseudo- Single-Input Single-Output, (SISO) system where the governor loop is first closed and the exciter loop is treated as a SISO system for the prime purpose of rejecting voltage disturbances. The function of the PSS is identified as that of overcoming an awkward switch-back frequency-domain characteristic of the excitation channel so as to permit high-performance excitation channel bandwidths up to 10 rad/sec that otherwise could not be obtained. Thus, in addition to the control requirements of set point regulation of the terminal voltage and shaft speed, the PSS provides for a second control requirement of strong voltage disturbance rejection over the important frequency range of 0 to 10 rad/sec. The PSS control option is also assessed against other control options. Several other results concerning stability robustness to system uncertainties in different system configurations follow from the analysis in a transparent and immediate way.

Acknowledgements

During the course of this research, I have been assisted by many individuals to whom I am personally, and intellectually greatly indebted.

In Glasgow, Professor John O'Reilly, my Supervisor, offered me unfailing guidance, encouragement and friendliness, without which this work would have been very difficult to undertake.

In Sudan, I am indebted to the late Dr. Mohmoud Sharief, of the National Electric Corporation, Sudan, who introduced me to the world of Power Systems, by shifting my academic interests from the field of Electronics.

This research has also been greatly influenced by discussion with Dr. William Leithead of the Industrial Control Centre, at Strathclyde University.

And lastly, and above all, I am greatly indebted to the Sudanese People, who despite their difficulties provided funds for me (and hundreds like me) through the Ministry of Education

Table of Contents

Chapter 1 : Introduction

1.1- *Power System Stability*

Since the early days of the electric power industry, it was recognized that, the electric energy supplied to the consumer must have quality, be a reliable service, as well as be produced economically. The quality is related to the voltage magnitude level and its electric frequency; both must be within a narrow range with respect to their rated values, so that consumers can expect that electromechanical devices and other types of electrical loads perform according to their specification. Reliability, on the other hand, is a concept associated with the availability of the service whenever consumers need it. In short, power supplied to consumer must be stable.

Power system stability is a complex subject that has challenged power system engineers for many years, and early stability problems were associated with remote hydraulic generating stations feeding into metropolitan load centers over long-distance transmission [1]. For economic reasons, such systems were operated close to their steady-state stability limits, (a power system is in a steady-state operation when it is applying power to consumer loads at a fixed frequency and voltage). Steady-state stability, in the past, was normally deduced from consideration of the power angle curve [2]. This procedure ignores damping, both positive and negative, in the machine and consequently doesn't provide a complete picture or solution of the stability problem. This is particularly true for a machine with a voltage regulator, when operating in the dynamic-stability region with positive synchronizing torque,

because the movement of the rotor, subsequent to a small displacement, is largely dependent upon the damping in the system. If positive damping is present the rotor oscillation will die away. If there is no damping the machine will hunt, and if the damping is negative the rotor oscillations will increase in amplitude and may eventually cause the machine to become unstable.

With the continual growth in power systems and in interconnections, there is a corresponding continual economic pressure to install larger and larger generating units, and there was no avoiding the fact that this process tends in turn to result in higher reactances, lower inertias being used; and that this tendency sometimes makes the job of designing a reliable and stable system more difficult [3]. Available tools to the power system engineer for system analysis and planning or system operation have evolved through the years, and the methods of analysis and the models used were dictated by developments in the art of computation and the stability theory of dynamic systems. Models and analysis methods started very simple (slide rules and mechanical calculators were used). As power system evolved and interconnections between independent systems were found to be economically attractive, the complexity of the stability problems increased. The use of analogue computer boards gave the means of study and limited size networks were analyzed to solve power flows, fault currents and transient stability problems. For instance, using simplified models for synchronous machine, the "first swing" under transient conditions was studied. No modeling for the field or torque control was included,

not only because the time constants of these loop were recognized to be long, but also due to limitations imposed by the hardware, so that the implementation of field or torque control loops was not easy to accomplish. Therefore, it was necessary to keep the overall machine parameters of a power system within bounds, if a reasonable degree of stability is to be preserved, and Power Engineers turn to control action (voltage regulators and turbine valves) to increase the stability limits.

In the early 1950s, engineers became aware of the instabilities introduced by the "then" modern voltage regulators, and stabilizing feedback circuits came into action [4]. In the 1960s, large interconnected systems experienced growing oscillations, and it was thought that the inherently weak natural damping of large and weakly-coupled systems was the main cause [5], and it was suggested that the system damping could be enhanced by artificial signals introduced through the excitation systems [6]. Improvements to system stability also came about by way of faster-fault clearing and continuous-acting voltage regulators with no dead band, with the benefits of excitation system with a high degree of response for increasing steady-state stability been recognized since the early 1940s.

Other methods of improving power system stability known to engineers in the 1950s was the technique of replacing the system loads, when faults occur in the transmission lines, by braking resistors, short-circuit current limiters, and fast valving [7].

1.2- *The synchronous machine*

One of the main components of an electric power station is the synchronous machine, in which the mechanical-electric energy conversion takes place. Usually it is a 3-phase synchronous type, and is based on Faraday's induction law [8]. Its essential components are :-

(1) an armature winding, (2) a magnetic field, and (3) a mechanical energy input, in the form of a force or a torque which causes a relative motion of the armature winding with respect to the field. This motion produces voltage in the armature, and an electric torque is generated opposite to the mechanical torque of the prime mover when the generator has a load. The power system dynamic problems are mainly those of the synchronous machines in power systems. For instance, the low-frequency oscillations of a large electric power system are due to the mechanical mode oscillations of the synchronous machine. Therefore, in order to have a high quality service, the synchronous machine is made to perform in a closed-loop or feedback form, Fig. 1.1.

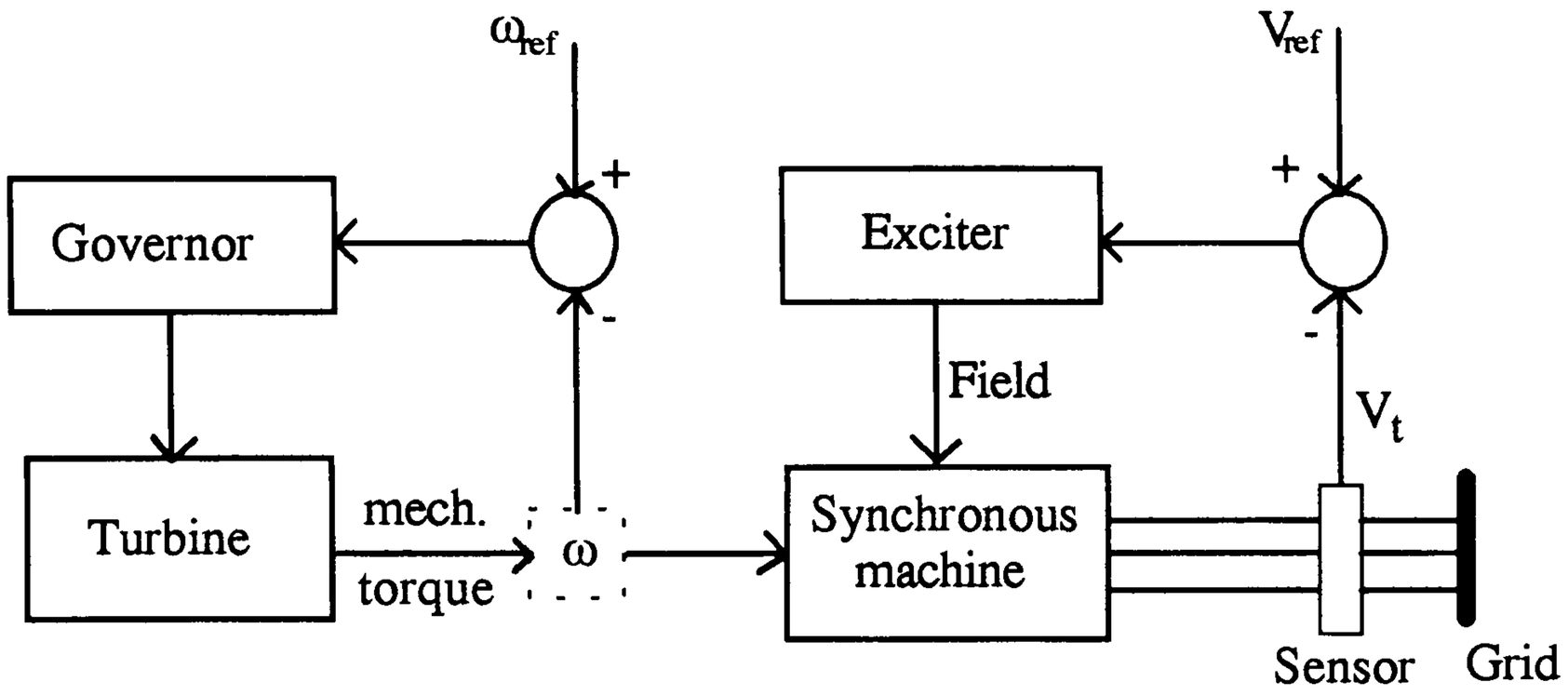

Fig. 1.1 Turbogenerator system

Traditionally, advantage is taken of the relative weak interaction between the dc field current (which affects mainly the voltage magnitude at the machine terminals) with respect to the prime mover (turbine) torque (whose direct effect is on the electrical power output), when the generator is connected to an isolated electric load or when it is acting in parallel with other generators in a system form. Small deviations from the fixed references are corrected by governor and voltage regulator controls. In a conventially-controlled turbogenerator system, an automatic voltage regulator (AVR) provides continuous control action for the exciter field current, to keep the generator terminal voltage constant, and the governor positions the steam inlet valves to control the prime mover (turbine) torque.

1.3- *Damping and synchronizing torques*

When a synchronous machine loses synchronism or "falls out of step" with the rest of the system, its rotor runs at a higher or lower speed than that required to

generate voltages at system frequency. The "slip" between rotating stator field (corresponding to system frequency) and the rotor field results in large fluctuations in the machine power output, current, and voltage; this causes the protection system to isolate the unstable machine from the system.

With electric power systems, the change in electrical torque of a synchronous machine following a perturbation can be resolved into two components :

$$\Delta T_e = T_s \Delta\delta + T_D \Delta\omega$$

where

$T_s \Delta\delta$ is the component of torque change in phase with the rotor angle perturbation $\Delta\delta$ and is referred to as the *synchronizing torque* component; T_s is the synchronizing torque coefficient.

$T_D \Delta\omega$ is the component of torque change in phase with the speed deviation $\Delta\omega$ and is referred to as the damping torque component; T_D is the damping torque coefficient.

System stability depends on the existence of both components of torque for each of the synchronous machines. Lack of sufficient synchronizing torque results in instability through an *aperiodic drift* in rotor angle. On the other hand, lack of sufficient damping torque results in *oscillatory instability*.

1.4- *Power system stabilizer*

The availability of thyristor exciters and the use of electrohydraluic governors with fast valving, provide the means for achieving significant

improvements in turbogenerator control. The effects of high-gain, fast-acting excitation systems have been studied by many authors [9], with the low-frequency oscillations due to the creation of large electric power systems being the main cause for concern. Subsequent investigations revealed that automatic voltage regulation as well as heavy power flows were aggravating the dynamic stability problem. Various additional stabilizing signal have been suggested to dampen these low oscillations. In particular, a stabilizing signal derived from speed error [10] has been found to be very effective in damping system oscillations, and many methods have been suggested to design this signal by way of a so called "*Power System Stabilizer*, PSS". One common design approach to the PSS is based on eigenvalue analysis, whereby eigen patterns are used to identify the modes of oscillations which are close to the region of instability in the s-domain and which are likely to be a source of instability; additional dynamics through new PSS poles and zeros are then introduced to shift those poles away from the danger zone. Other methods include the root-locus, pole placement, adaptive control ...etc.

Most of the methods use the concept of synchronizing and damping torques in the machine described above in Section (1.3). DeMello and Concordia [11] were the first to use phase compensation theory to analyze the damping effect provided by a lead-lag controller for damping machine oscillations. Nowadays the lead-lag controller is the most widely employed excitation controller for providing damping characteristics of a synchronous machine. The conventional approach to AVR-PSS

design can basically be classified as a sequential design consisting of two stages : Firstly, the AVR is designed to meet the required voltage regulation performance. Then, the PSS is designed to meet the required damping performance. Basically, faster excitation with higher voltage ceilings provide increased synchronising torques with improved transient performance, but at the expense of injecting negative damping into the system. The PSS supplies a supplementary phase-advanced speed (power) signal which is considered to provide additional damping to the lightly damped machine. Stabilizers using shaft speed as an input signal were successfully designed and applied, since they avoid direct disturbances from load fluctuations. However, they are sensitive to local mode oscillations, which complicate their design and restrict their effectiveness. A combination of power and speed was introduced and they are now replacing the speed PSS. Many more recent studies have been published on various methods of tuning the PSS (eg [12]), the additional use of a notch filter in the exciter path [13], and the advantages or otherwise of supplementary exciter transient gain reduction [14],[15]. Kundur [14], analyze the PSS in Ontario Hydro, in which no Transient Gain Reduction (TGR) is used in the exciter; while Larsen [15], of the General Electric Co. advocates the use of TGR. More recently, Grondin et.el. [16] of Hydro-Quebec replaces the conventional PSS with a 3-term compensator.

The above works are representative but by no means exhaustive. These works indicate that interest in the use of the PSS for turbogenerator control shows

little sign of diminishing. In 1995, several authors suggest new approaches to design suitable PSS which are robust and easy to implement; and two of the most recent methods are:-

(a) *Robust PSS design* [17,18]

The objective of designing a robust power system stabilizer (RPSS) is to make the overall system stable both within the normal operating conditions and within some extreme situation such as a fault, and at the same time maintain a certain degree of system performance. In designing an RPSS, each individual parameter K_1 .....K_6 of the synchronous machine, (see Chapter 3), is replaced by its corresponding parameteric uncertainty.

Within the power system operating range of interest, the K's parameters are bounded with lower and upper values.

The control design model of a robust PSS is developed to fit into the standard configuration of H_∞ analysis and synthesis as shown in Fig. 1.2. In Fig. 1.2, P is the interconnected system which consist of nominal plant G_o, uncertainties weighting function R_u, and performance weighting function W_p. In 1.2, W_d represents the combination of disturbance weighting functions of the mechanical torque and the field voltage. Δ denotes the uncertainties which are unknown but bounded; K is the HPSS controller needed to be specified.

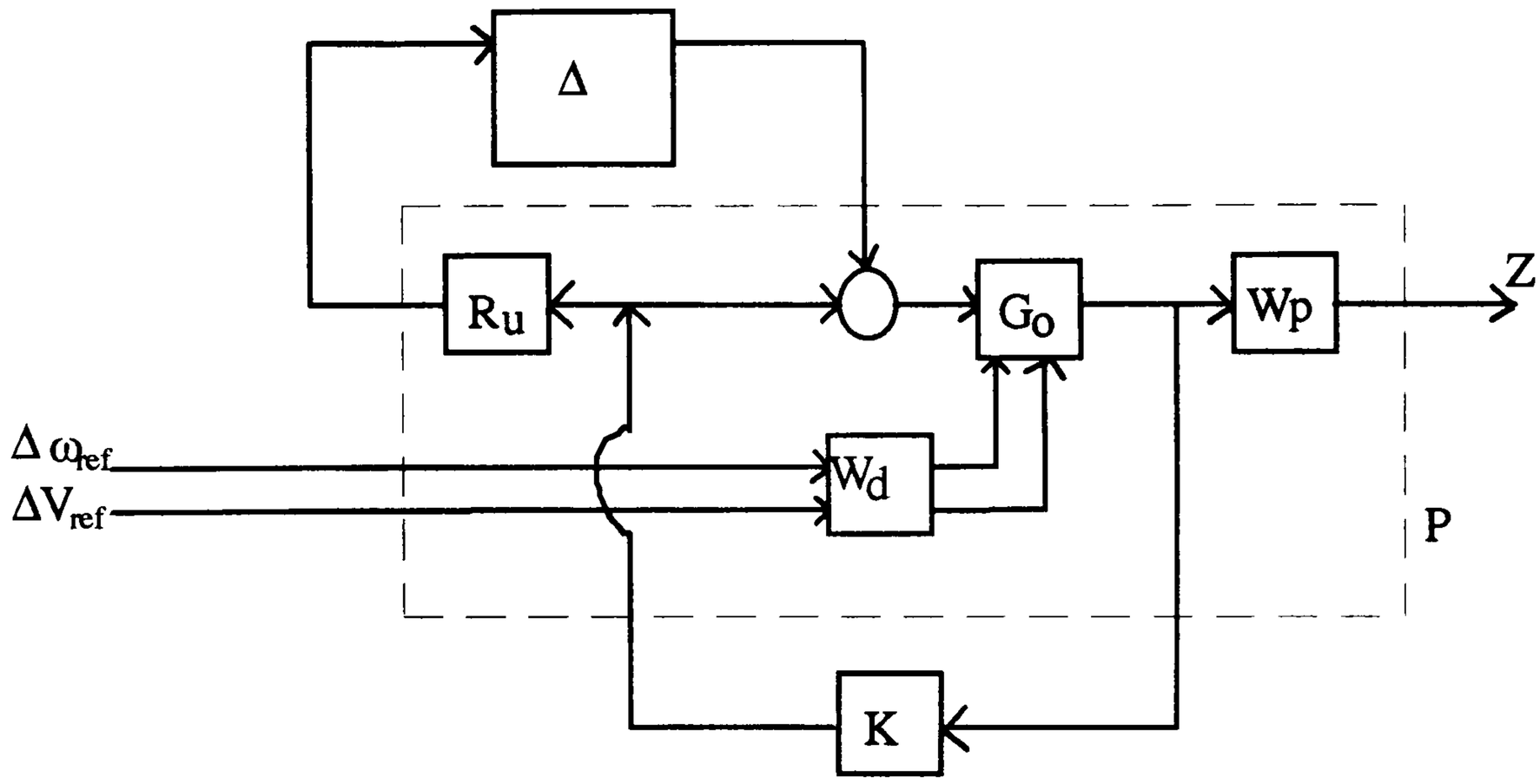

Fig. 1.2 General Interconnection structure

(b) *Fuzzy logic power system stabiliser (FPSS)* : [19,20]

A new type of PSS based on fuzzy set theory is proposed in reference [20] to improve the dynamic performance of a power system by allowing the PSS to have good damping characteristic over a wide range of operating conditions.

The first step in designing a fuzzy controller is to decide which state variables representative of system dynamic performance must be taken as the input signals to the controller. In power systems, based on previous experience, generator speed deviation ($\Delta\omega$) and acceleration ($\Delta\omega$) are chosen to be the input signals of the fuzzy PSS. The input to the excitation system would be the control variable which is actually the output of the fuzzy PSS. After choosing the proper variables as input and output of the fuzzy controller, it is required to decide on the linguistic variables. These variables transform the numerical values of the input of the fuzzy controller, to fuzzy quantities. For power systems, seven linguistic variables for each of the

input and output variables are used to describe them. These are, LP (large positive), MP (medium positive), SP (small positive), VS (very small), SN (small negative), MN (medium negative), and LN (large negative). In order to find the minimum of stabiliser inputs, an open loop simulation for different initial conditions is performed. The results are used to find the minimum and maximum of $(\Delta\omega)$ and $(\Delta\omega)$. After specifying the fuzzy sets, it is required to determine the membership functions for these sets, (e.g. bell-shaped function, triangle-shaped function ...etc.). The degree of membership can be defined as functions when the control variable amplitude is continuous.

	PSS output						
$\Delta\omega$ / $\Delta\omega$	LN	MN	SN	VS	SP	MP	LP
LP	VS	SP	MP	LP	LP	LP	LP
MP	SN	VS	SP	MP	MP	LP	LP
SP	MN	SN	VS	SP	SP	MP	LP
VS	MN	MN	SN	VS	SP	MP	MP
SN	LN	MN	SN	SN	VS	SP	MP
MN	LN	LN	MN	MN	SN	VS	SP
LN	LN	LN	LN	LN	MN	SN	VS

Table 1.1 Decision table for PSS output

A set of rules which define the relation between the input and output of fuzzy controller can be found using the available knowledge in the area of designing PSS. These rules are defined using the linguistic variables. The two inputs, speed and acceleration, result in 49 rules for each synchronous machine. These rules are shown in Table 1.1 above where all the symbols are defined in the basic fuzzy logic terminology. A typical rule has the following structure : **Rule 1**

" *If speed deviation is LP (large positive) AND acceleration is LN (large negative) then Vpss (output of fuzzy PSS) is VS (very small)*".

Now it is required to find the fuzzy region for the output for each fuzzy rule using methods like Minimum-Maximum, or Maximum-Product ...etc. Fuzzy rules are connected using AND operators. The AND operator is used to obtain the minimum between input membership functions. Later, the minimum between this result and the output membership function is found. Finally, the output membership function of a rule is calculated. This procedure is carried out for all the rules and for every rule an output membership function is obtained. To find the output membership function due to all of these rules, the maximum among all of these rules is calculated.

Since a nonfuzzy signal is needed for the excitation system, by knowing the membership function of the fuzzy controller its numerical value can be determined. There are different techniques for defuzzification of fuzzy quantities such as Maximum Method, Height Method, and Centroid Method.

1.5- *Research of this thesis*

The function of excitation/governor control with PSS appears to be well understood from a power systems analysis perspective [10],[21],[22], following the celebrated paper by DeMello and Concordia [11].

From a control engineering point of view, as opposed to a power systems point of view, the function of the PSS is less clear and indeed raises a number of fundamental issues; not the least of which is if the supposed role of the PSS is to provide system damping, why is it that phase compensation (damping) cannot be applied directly to the excitation system rather than indirectly by way of the PSS.

While a number of control-oriented studies have appeared [23-27], they confine themselves to control design of various types and provide supporting evidence of improved system damping often in terms of the conventional synchronising and damping torque analysis described above. One notable exception is the very interesting work by Hamdan and Hughes [28] which uses the multivariable frequency-response methods of Rosenbrock [29] and MacFarlane [30] and pole-zero analysis to demonstrate why the PSS is effective. There will be occasion to refer to this work again for it essentially complements the control explanation reported herein which, as we shall see, is very different from that offered by conventional synchronising and damping torque analysis. In short, this work demonstrate that the PSS, originally conceived in [31],[32], is an ingenious

control device which obviates an extremely awkward excitation control characteristic, at small price, so as to meet an overall desired control specification.

The key to uncovering the function of the PSS and what control specification it is designed to meet is to recognise from the outset that a single turbogenerator connected to an infinite bus is a 2-input, 2-output multivariable system. A thorough and readily understandable multivariable analysis of the turbogenerator system and the function of the PSS is provided by the multivariable control framework known as Individual Channel Analysis and Design [33],[34],[35],[36].

The thesis is organised as follows. After introducing the Individual Channel Analysis and Design (ICAD) in Chapter 2, Chapter 3 provides an in-depth multivariable analysis of the turbogenerator. Further multivariable analysis of turbogenerator regulation in Chapter 4 identifies the fundamental role played by the PSS in facilitating single-loop control of the multivariable system to meet a certain control specification and analyses the stability robustness of the combined control scheme to system uncertainties. The PSS control option is also assessed against two other control options. Chapter 5 analyses two recent control methods for stabilising a turbognerator connected to an infinite bus, Conclusions are presented in Chapter 6.

Chapter 2 : Review of Individual Channel Analysis and Design

2.1- *Introduction*

In this chapter a concise review of the Individual Channel Analysis and Design (ICAD) framework is presented. It contains the basic aspects of the framework in terms of a 2-input 2-output system, which can then be extended to the general case of multivariable systems (multi-input multi-output cases).

In a typical control design task, once it is specified which system input is intended to derive which system output, certain design goals need to be met. These include : steady state response, disturbance rejection, transient response, actuator protection, closed-loop stability and robustness. In SISO systems these goals can easily be achieved by using the classical Nyquist/Bode methodology; multi-input multi-output (MIMO) systems, on the other hand, have the problem of cross-coupling which hampers the direct application of classical analysis and design methods. ICAD, a new application oriented framework developed by O'Reilly and Leithead [33], enables the application of Nyquist/Bode analysis and design to multivariable system by overcoming problems preventing such application which arise from the very nature of m-input m-output systems, such as: the determination of the influence of the

plant structure on the controller, the application of phase and gain margins to multivariable systems, and the design of each individual controller element even though it depends on all other individual elements in the controller matrix.

2.2- *Multivariable Analysis using ICAD*

Consider the multivriable feedback control configuration of Fig. 2.1.

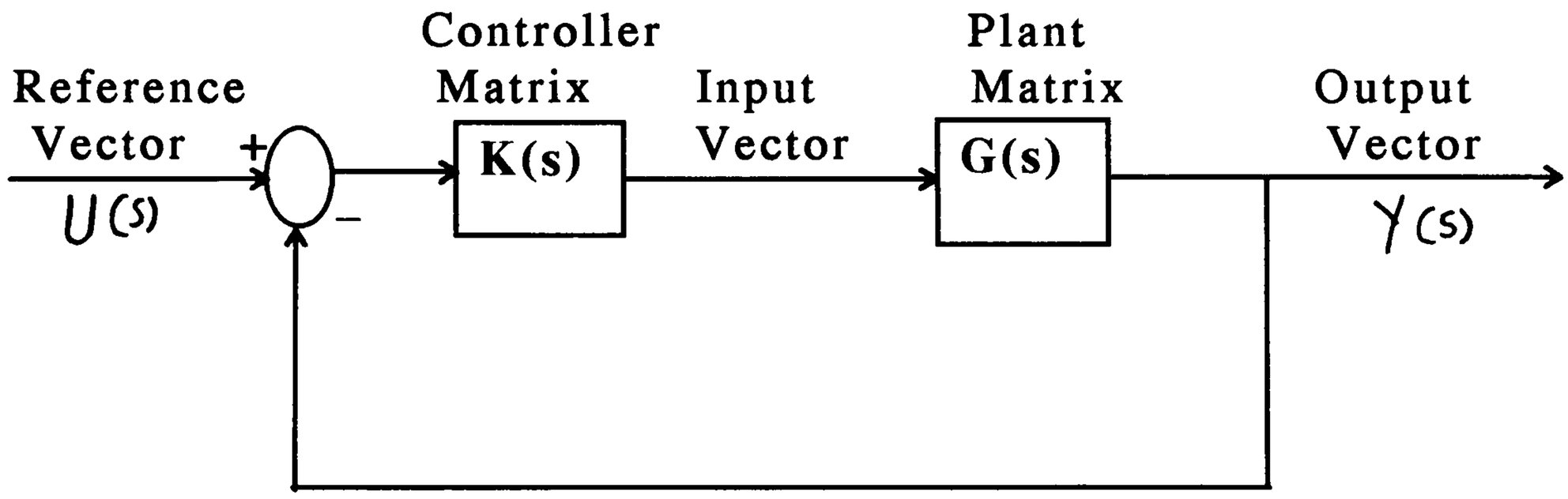

Fig. 2.1 Standard multivariable control problem

where G(s) is the matrix transfer function representing the plant, K(s) is the controller transfer function matrix, U(s) is the plant input vector and Y(s) is the plant output vector. In accord with the customer specification, input u_i is paired with output y_i; this individual input-output pairing is called a channel. Focusing our attention on the 2-input 2-output multivariable problem with diagonal controller; then Fig. 2.1 can be redrawn as in Fig. 2.2

where k_i are the diagonal elements of the diagonal controller matrix K(s), and g_{ij} are the elements of the plant matrix G(s) for i,j=1,2.

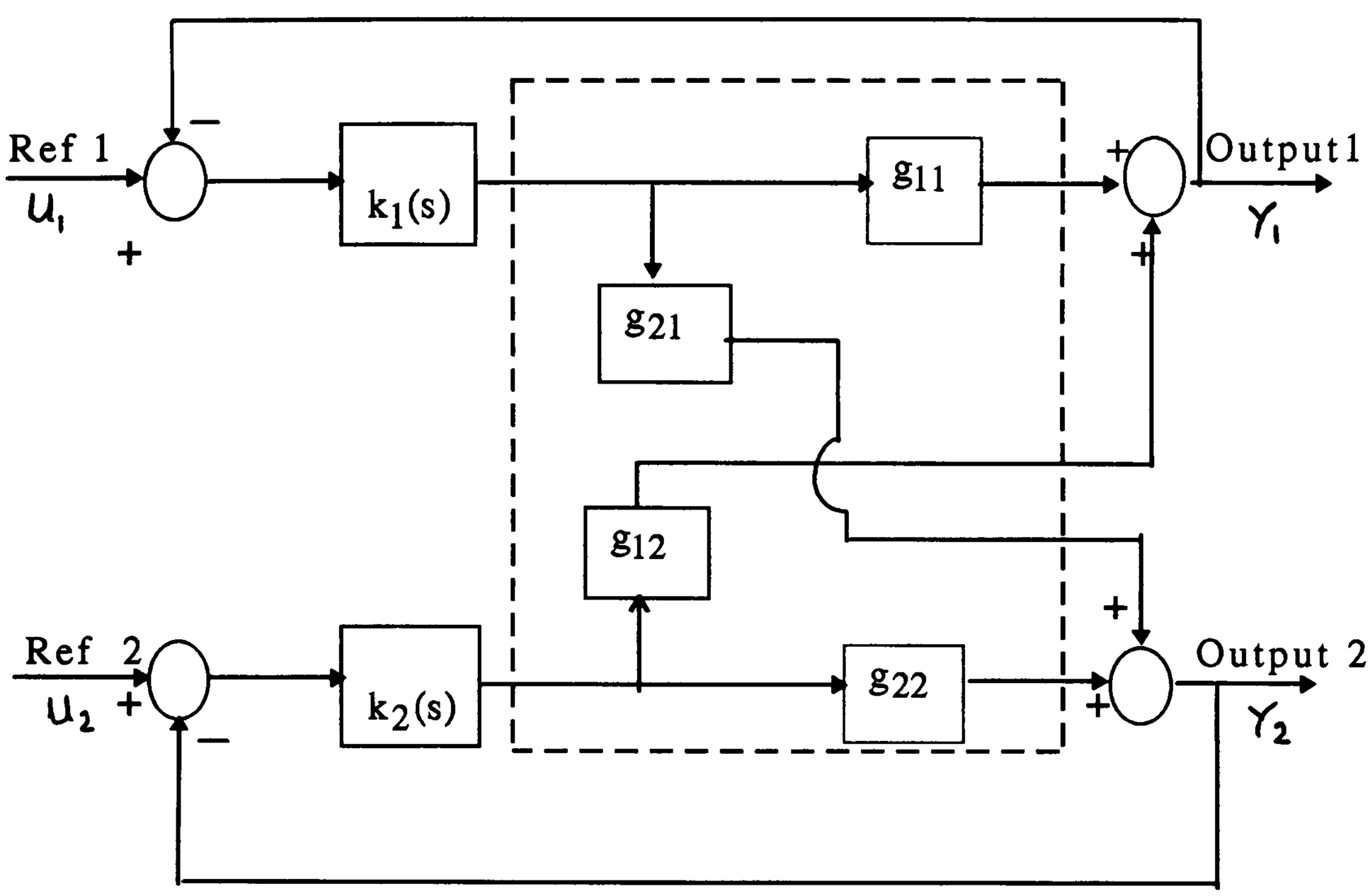

Fig. 2.2 The 2-input 2-output multivariable control problem with diagonal feedback

Consider the forward signal transmission from the first reference r_1 to its associated output y_1. This forward signal transmission follows two parallel paths: one directly through $g_{11}(s)$; the other via $g_{21}(s)$, the bottom feedback subsystem and $g_{12}(s)$. We observe also in Fig. 2.2 that the forward cross-signal transmission from the second reference r_2 to y_1 is via the bottom feedback

subsystem and $g_{12}(s)$ .These signal transmissions from r_1 to y_1 and from r_2 to y_1 can, after a little block algebra, the details of which are described in [33], be represented as in Fig. 2.3.

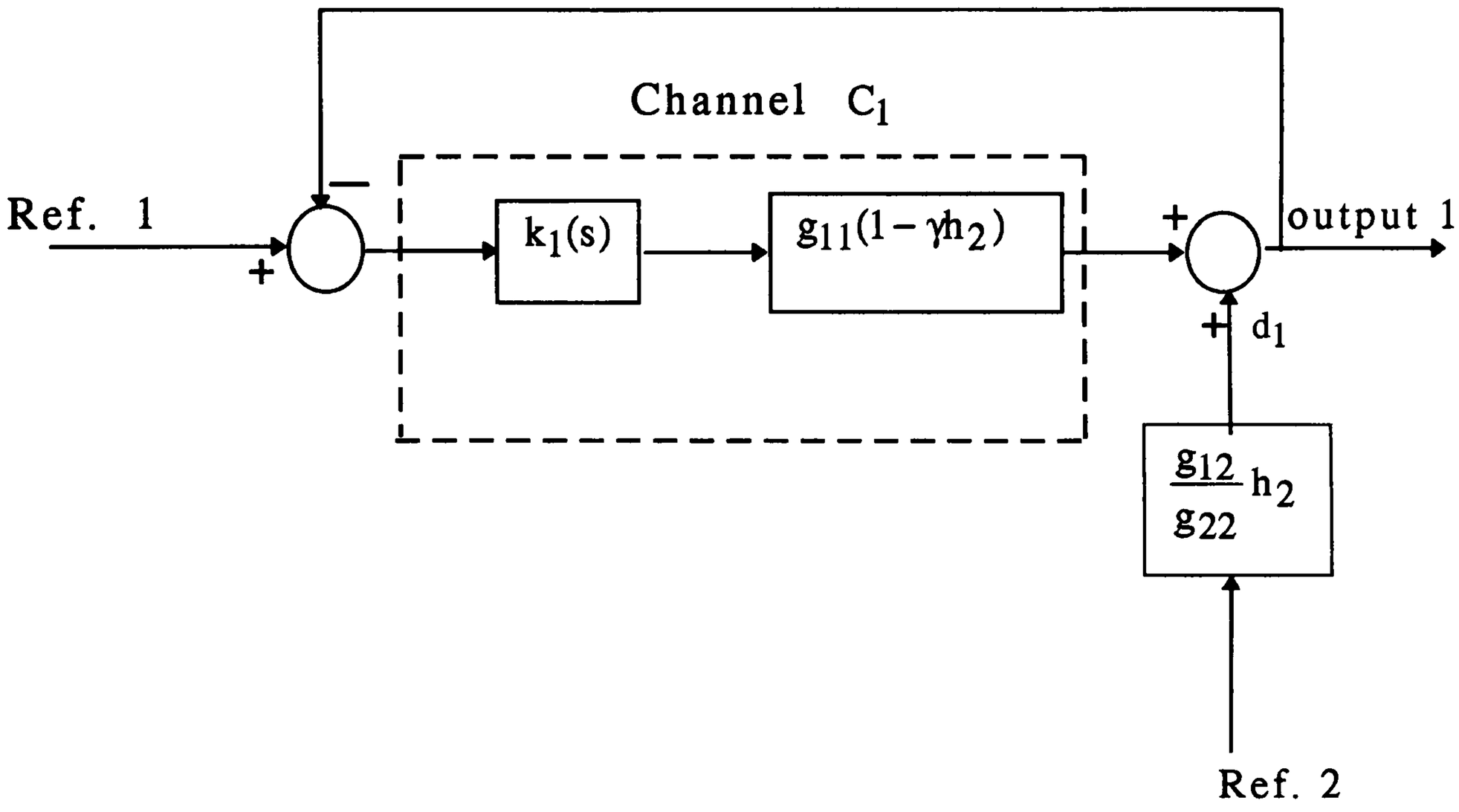

Fig. 2.3 Individual channel design structure : Channel C_1

In other words, Fig. 2.3. depicts the individual signal transmission Channel C_1 between reference 1 and its associated output 1 together with the additive cross-reference 'disturbance' signal $g_{12}g_{22}^{-1}h_2r_2$ at output 1. Likewise, by symmetry of the topological structure of Fig. 2.2., Channel C_2 between reference 2 and its associated output 2, together with a unity negative feedback

control loop and a cross-reference 'disturbance' signal $g_{21}g_{11}^{-1}h_1r_1$ is represented by Fig. 2.4.

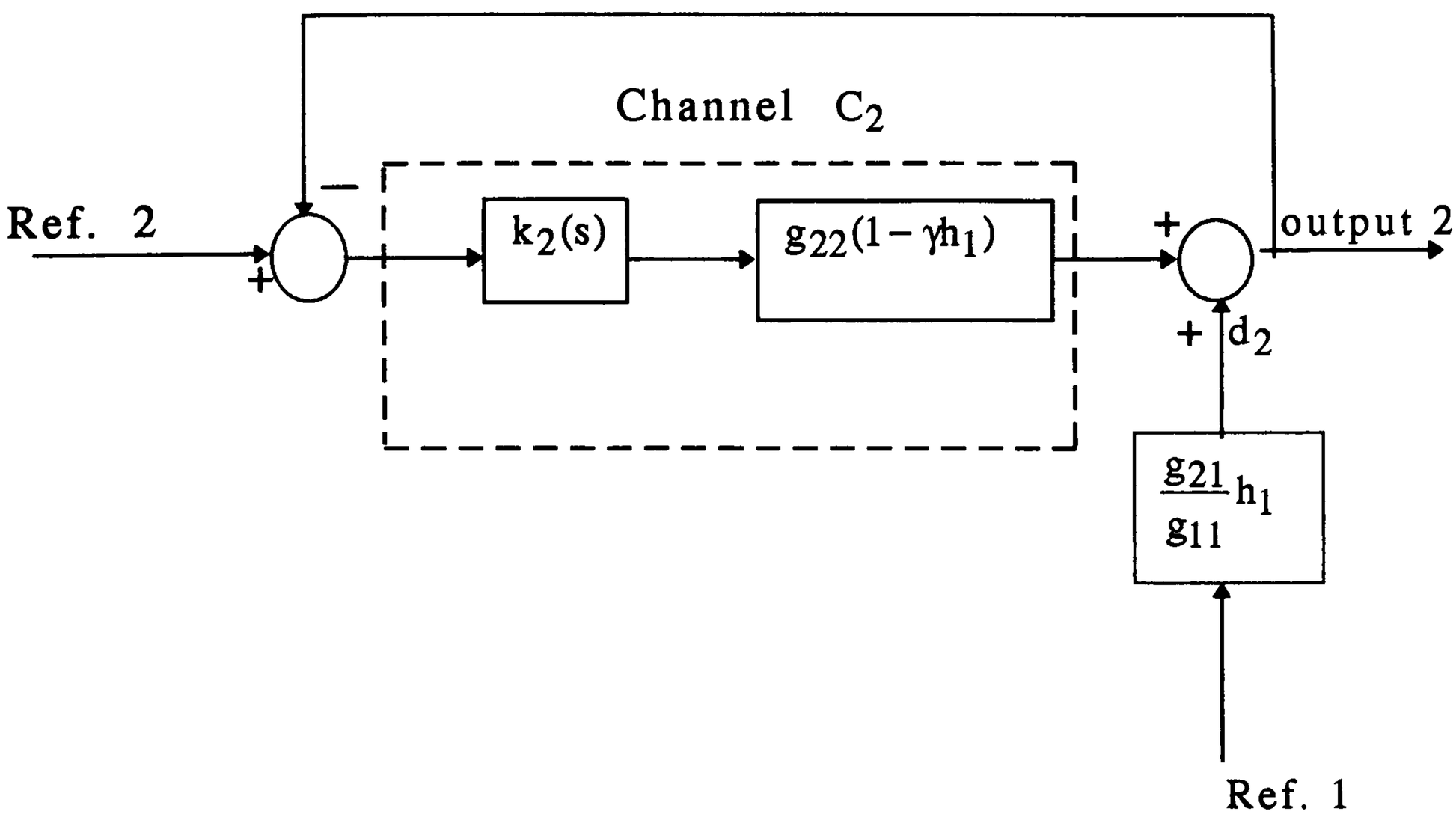

Fig. 2.4 Individual channel design structure : Channel C_2

Thus, we have established [33] that the two individual channel feedback control problems of Fig. 2.3 and 2.4, are together structurally equivalent to the original 2-input 2-output feedback control problem of Fig. 2.2; all signal interactions via $g_{12}(s)$ and $g_{21}(s)$ are retained and no structural information is lost.

From Fig. 2.3, Channel C_1 has the forward path single-input single-output (SISO) transfer function

$$C_1 = k_1 g_{11}(1-\gamma h_2) \qquad (2.1)$$

where

$$\gamma(s) = \frac{g_{12}g_{21}}{g_{11}g_{22}} \tag{2.2}$$

$$\text{and } h_2 = \frac{k_2 g_{22}}{1 + k_2 g_{22}} \tag{2.3}$$

Similarly, from Fig. 2.4, Channel C_2 has the forward path SISO transfer function

$$C_2 = k_2 g_{22}(1 - \gamma h_1) \tag{2.4}$$

where

$$h_1 = \frac{k_1 g_{11}}{1 + k_1 g_{11}} \tag{2.5}$$

In particular, the multivariable nature of the turbogenerator SISO channels C_1 and C_2 is described [33] by the complex frequency multivariable structure function $\gamma(s)$. When $\gamma(s)$ is small in magnitude, signal interaction between the loops is low (in which case, the two channels behave almost like two independent loops); when $\gamma(s)$ is large in magnitude, interaction between the loops is high. Thus, the 2-input 2-output multivariable system is decomposed into two equivalent set of SISO system. Each SISO system is the open-loop channel transmittance between input i and output i, with the feedback loop between output i and input i open but the other

feedback loop closed. Although such a decomposition of multivariable systems is not new; ICAD ensures that these SISO channel transmittances are reformulated to make explicit the role of the plant structure. The significant aspects of the plant structure are encapsulated in the scalar multivariable structure function $\gamma(s)$ to which the individual channel transmittances are simply related. The multivariable structure of the original plant is maintained in the equivalent SISO systems by-way of this multivariable structure function with no loss of information. The closed-loop response of Channel C_1 to reference r_i and r_j is described by

$$y_i(s) = t_{ii}(s)r_i(s) + d_i(s)r_2(s) \tag{2.6}$$

where

$$t_{ii}(s) = \frac{C_i}{1+C_i} \tag{2.7}$$

$$d_i(s) = \frac{g_{ij}h_j}{g_{jj}}\left(\frac{1}{1+C_i}\right) \qquad i \neq j \tag{2.8}$$

Assuming $\gamma \neq 0$, the transient dynamic and disturbance rejection performance of the output response $y_i(s)$ can be characterised entirely by the transmittance $C_i(s)$; namely,

* for stable reference inputs and disturbance inputs, $y_i(s)$ is stable provided $\frac{C_i}{1+C_i}$ is stable.

* for reference input $r_i(s)$, the tracking performance of $y_i(s)$ is indicated by $\frac{C_i}{1+C_i}$

* for disturbance input $d_i(s)$, disturbance rejection on $y_i(s)$ performance is indicated by $\frac{1}{1+C_i}$

Hence given a diagonal controller, the transmittance $C_i(s)$, can be used to assess the dynamic performance achieved by the controller in the usual manner with such frequency domain parameters as the crossover frequencies of $C_i(s)$ and bandwidths of $t_{ii}(s)$ retaining their usual significance [34].

Assuming no pole/zero cancellations occur within the channel transmittances, the pole-zero structure of the channels is specified by Table 2.1 below

	Zeros	Poles
Channel C_1	Zeros of $(1-\gamma h_2)$	Poles of $g_{11}, g_{12}, g_{21}, h_2$
Channel C_2	Zeros of $(1-\gamma h_1)$	Poles of $g_{22}, g_{12}, g_{21}, h_1$

Table 2.1 Open-loop channel structure

As in classical SISO systems, the possible closed-loop dynamical performance of the individual channels in the 2-input 2-output case is adversely affected by the presence of channel RHPZs. From Table 2.1, the number of right half plane zeros (RHPZs) of channel C_i is the number of RHPZs of $(1-\gamma h_j)$ and is determined from Result 2.1 as follows

Result 2.1

Suppose that the Nyquist plot of the multivariable structure function γh_j encircles the (1,0) point N times more in a clockwise direction than in an anti-clockwise direction. Then Z, the number of RHPZs of $(1-\gamma h_j)$ is given by

$$N=Z-P$$

where P is the number of RHPPs of γh_j

Whether Channel C_i is minimum phase depends on γh_j. When the structure of γh_j and γ are the same and the magnitude of the control gain $k_j(s)$ is large, the RHPZ's of $(1-\gamma h_j)$ are essentially the RHPZ's of $(1-\gamma)$ which are the 2-input 2-output plant RHP system zeros. From a result similar to Result 2.1, the latter correspond to the encirclement of the point (1,0) by the Nyquist plot of $\gamma(s)$. The

channel zeros are different from each other and are different from the plant system zeros.

In a very direct manner the multivariable structure function γ, particularly its Nyquist plot, indicates those structural aspects of the plant associated with its multivariable nature. By its magnitude it indicates the strength of the cross coupling. By its closeness of approach to the (1,0) point it indicates the extent to which the plant is ill-conditioned. The significant RHPP's and RHPZ's of the transfer function elements are those which are RHPP's of γ. The presence of these RHPP's are indicated by the number of encirclements of the point (1,0) by the Nyquist plot of $\gamma(s)$.

Similarly, the multivariable structure function γh_j, particularly its Nyquist plot, indicates structural aspects of Channel C_i. The significant RHPP's and RHPZ's of the transfer function elements and $h_j(s)$ are those which are RHPP's of γh_j. The presence of these RHPP's are indicated by the number of encirclements of the point (1,0). Whether or not Channel C_i is minimum phase, is indicated by the number of encirclements of the point (1,0). Thus, the multivariable structure functions γh_j are important indicators of actual closed-loop performance achieved by the controller. Hence

given a diagonal controller, Table 2.1 and Result 2.1 can be used to assess the structural aspects of the channel. Two main results concerning the role of single-loop subsystem in multivariable control by ICAD of 2-input 2-output systems are [33]:

Result 2.2

Multivariable systems have Nyquist-Bode gain and phase margins associated with each individual SISO signal transmission channel

Result 2.3

The gain and phase margins associated with each Channel $C_i = k_i g_{ii}\left(1 - \gamma h_j\right)$, $i, j = 1,2$, $(i \neq j)$ *of (2.1) and (2.4) are robustness measures provided that the polar diagram of the multivariable structure function* γh_j *does not come close to the (1,0) point.*

Although, the influence of the structure of the scalar channel C_i transmittance on the control gain $k_i(s)$ is readily assessed, this structure itself depends on the control gain $k_j(s)$, $i \neq j$. An existence result is required to establish that there exists a diagonal controller which stabilises the closed-loop system and to relate the structure of the scalar Channel C_i transmittances to the structure of the original 2-input 2-output plant.

ICAD, [34] gives a set of results on the existence of diagonal controllers which stabilises the closed-loop system and relate the structure of C_i to the structure of the original 2-input 2-output plant .

2.3- *Non-diagonal Control* :-

Plants with poor structure are readily identified from the multivariable structure functions. Normally attempts are made to amend this poor structure by two approaches; namely pre(post)-compensation and feedforward of the controller output to the plant output. By way of analysis, ICAD shows that [34] restriction to diagonal control in ICAD or elsewhere is not a significant restriction on performance; and that lack of robustness (meeting performance specification in the face of plant uncertainties) is not alleviated by non-diagonal control. A fundamental restriction in the use of pre(post)-compensation with multivariable plants, however, is that its presence weakens the link between the gain and phase margins and robustness. In general, whenever possible, it is preferable to improve structure by feedforward control.

Some plants may exhibits either excessive phase sensitivity or excessive structural sensitivity or both. These sensitivities do arise

when the Nyquist plots of the multivariable functions, $\gamma h_i(s)$, go too near the (1,0) point; when this is the case it is tempting to use non-diagonal compensation to shift the Nyquist plots far from the point (1,0) and so cause the stability of feedback control to be more robust. Sometimes, it might be anticipated that a design with different cost weighting matrices, which diagonalises the system in the frequency range of interest and so displaces the Nyquist plot of the multivariable function $\gamma(s)$ from the vicinity of the point (1,0), might remove the lack of

robustness due to excessive sensitivities.

Unfortunately, this is not always the case. From Leithead and O'Reilly [36], the utility on non-diagonal feedback control is summarised by the following :

(I) it cannot improve performance when attempting to achieve high-performance control (i.e. with channel bandwidth greater than all significant system dynamics).

(ii) it achieves no more than that achieved by swapping the assignment of inputs to outputs with diagonal control when attempting to achieve low-performance control (i.e. low channel bandwidth) in the presence of structural difficulties when the individual) transfer function elements, $g_{ij}(s)$ are minimum phase; but

it may make possible improvements in performance when the individual transfer function elements, $g_{ij}(s)$ are non-minimum phase.

(iii) it achieves no more than that achieved by swapping the assignment of inputs to outputs with diagonal control when attempting to improve robustness.

(iv) it cannot alleviate lack of robustness due to excessive phase sensitivity or excessive structural sensitivity.

(v) it can improve the ability of a fixed controller to cater for an uncertain plant or a family of plants with uncertain structure.

(vi) it can improve the ability of a controller to achieve system integrity.

Finally, ICAD as an application-oriented framework, is used to investigate, analyse and recommend a number of design techniques to various applications, such as single main rotor helicopter control system [37], submarine operating at shallow submergence [38], and gas turbine [33].

Chapter 3 : Modelling and Multivariable Analysis of the Turbogenerator system

3.1- *Introduction*

Turbogenerator system stability may broadly be defined as the property of the system that enables it to remain in a state of operating equilibrium under normal operating conditions and to regain an acceptable state of equilibrium after being subjected to a disturbance. Since power systems rely on synchronous machines for generation of electrical power, a necessary condition for satisfactory system operation is that all synchronous machines in a power system remain in synchronism.

A synchronous machine has two essential elements: the field and the armature. Normally, the field is on the rotor and the armature is on the stator. The field winding is excited by direct current. When the rotor is driven by a prime mover (turbine), the rotating magnetic field of the field winding induces alternating voltages in the three-phase armature windings of the stator. The frequency of the induced alternating voltages and of the resulting currents that flow in the stator windings when a load is connected depends on the speed of the rotor. The frequency of the stator

electrical quantities is thus synchronised with the rotor mechanical speed: hence the designation "synchronous machine".

This chapter addresses the following questions :- How can each component or group of components of a power system be represented so that an analysis of the system performance can be made; which of the several possible representations, or *models*, of the given components will best describe the system to meet the objectives of a given study; and what mathematical expressions will describe the characteristics of each system element so that it can be quantified for the analysis.

The modelling and analysis of the synchronous machine has always been a challenge. The problem was worked on intensely in the 1920s and 1930s [39] and has been the subject of several more recent investigations [40-42]. There are infinite number of possible synchronous machine configurations . But as mentioned in [22], it is neither adequate nor practical to devise a "universal" model for all power system dynamic problems. Nevertheless, a study conducted by the North East Power Co-ordinated Council in the USA, in a report named "Effects of synchronous machine modelling" published in 1971, concludes that "in general, it is more important in stability studies to use accurate machine data

than to use a more elaborate machine model" [21]. Other findings support this. One finding by Anderson & Fouad [21] state that "the models developed with (F, D, and Q) windings, i.e. high order models, provide practically no improvement over a simpler model with only F & Q windings". Another, is a comparison made by E.L.Busby et.el, [43] between an eight-order linear model which includes the synchronous, transient, and subtransient circuits of the generator in both d, and q axis; and a third order linear model. The conclusion is that, the third order model is in most cases adequate for dynamic stability simulation and is *nearly* as close as the 8th order model in matching the test result. Also Dandeno et.el.[44] remark "when using the standard machine data, a more complex model of a synchronous machine did not always give more accurate results in the stability studies performed". ICAD offers, as we shall see, further insight and comparison, through the analysis of the γ-function for different model orders at the same operating conditions.

3.2- *Park's Equations for a synchronous machine* :-

Fig. 3.1 shows the schematic of the cross section of a three-phase synchronous machine with one pair of field poles.

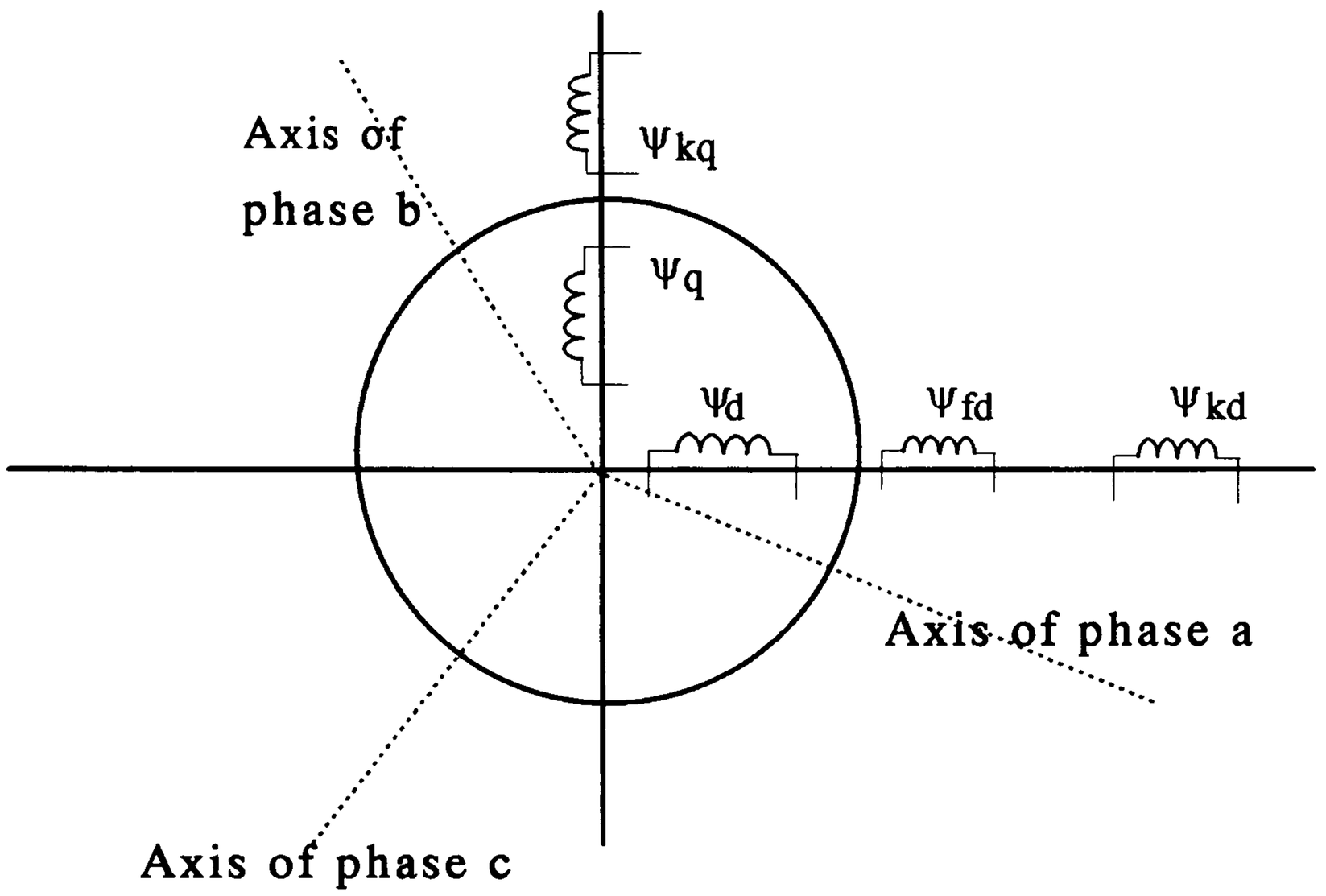

Fig 3.1 Synchronous machine

The machine consists of two essential elements: the field winding and the armature winding. The field winding carries direct current and produces a magnetic field which induces alternating voltages in the armature winding. The design of a large interconnected system to ensure stable operation at minimum cost is a very complex problem, and the economic gains to be realized through the solution to this problem are enormous. From a control theory point of view, the power system is a very high-order multivariable process, operating in a constantly changing

environment. Because of the high dimensionality and complexity of the system, it is essential to make simplifying assumptions and to analyze specific problems using the right degree of detail of system representation. this requires a good grasp of the characteristics of the overall system as well as of those of its individual elements.

The linearised equations for the dynamic behavior of the synchronous machine are based upon the equations proposed by Park [8]. Many publications have appeared in the last 50 years which use Park's model with varying assumptions to derive turbogenerator models. One or more of the following assumptions have been used [45] :

(1) voltage behind transient reactance is constant.

(2) derivatives of axis currents and flux linkage with respect to time are negligible in comparison with rotational terms.

(3) stator resistance is negligible and the stator windings are sinusoidally distributed round the air-gap.

(4) effect of change in speed in the voltage equations is neglected.

(5) magnetic hysteresis is negligible.

(6) magnetic saturation effects are negligible.

On the other hand, the mechanical equations of the machine are very well established [46], and three basic assumptions are

made in deriving these equations : (1) machine rotor speed does not vary greatly from synchronous speed (1 pu). (2) machine rotational power losses due to windage and friction are ignored. (3) shaft power is constant except as a result of speed power generation action. Assumption 1 allows per unit power to be equated with per unit torque. From Assumption 2, the acceleration power of the machine is the difference between the shaft power (P_m) as supplied by the prime mover and the electrical power (P_e).

The machine electrical circuit is shown in Fig. 3.2.

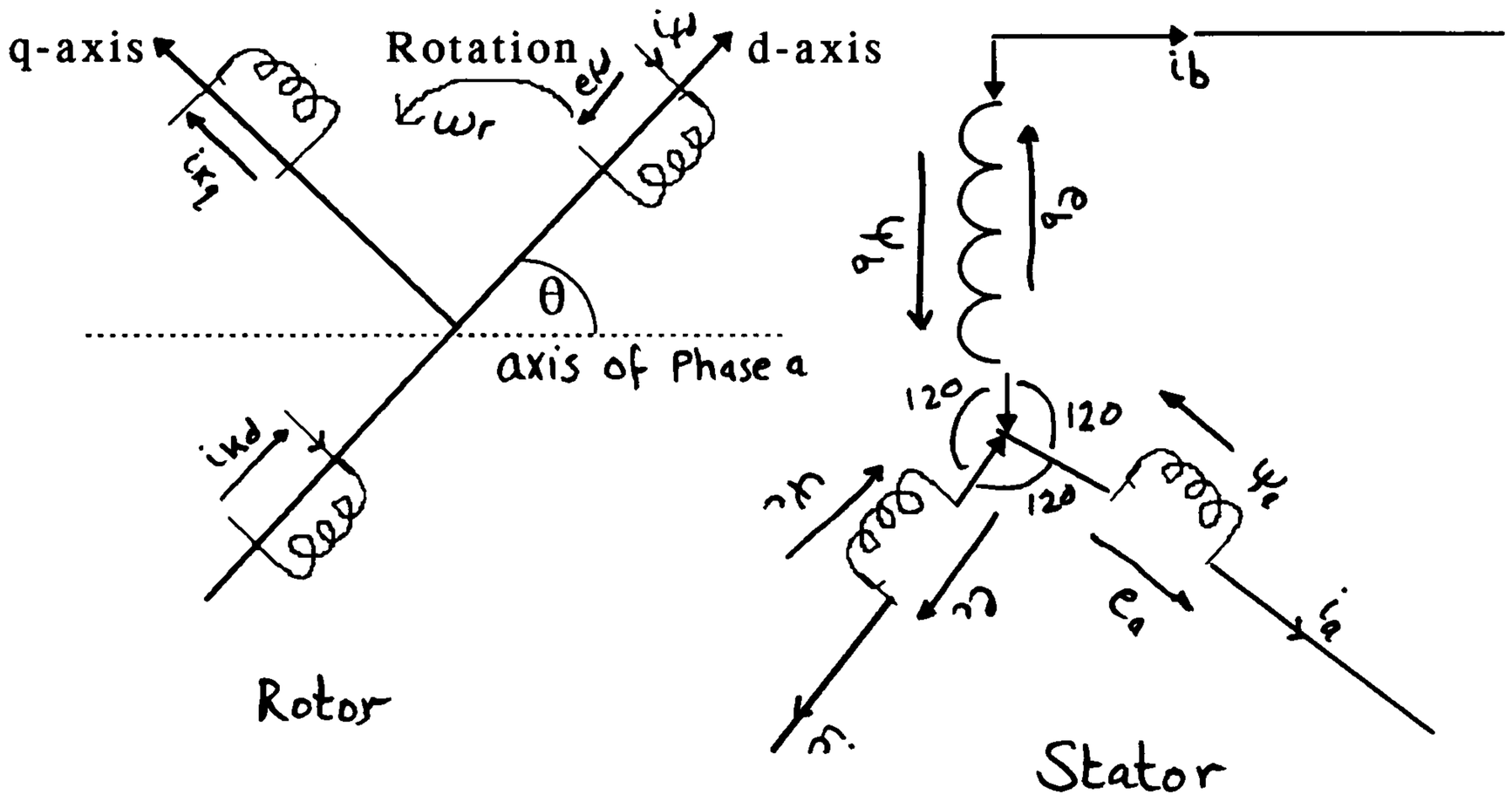

Fig.3.2 Machine electric circuit

The stator circuit consist of 3-phase armature windings carrying alternating currents. The rotor circuits comprise field and damper windings. The field winding is connected to a source of

direct current. There are three armature phase windings a, b, and c on the stator of the machine, which have been replaced by two equivalent armature phase windings: a d winding on the d-axis, and a q winding on the q-axis. Some damper windings on the rotor, k_d on the d-axis and k_q on the q-axis, which are permanently short-circuited are available, and there is also a field winding fd on the d-axis, which is dc-excited.

The linearised Park's equations in pu may be written as follows [47]:-

$$\Delta V_d = -\Delta \psi_q \tag{3.1}$$

$$\Delta V_q = \Delta \psi_d \tag{3.2}$$

$$\Delta \psi_d = x_{ad}\Delta I_{fd} + x_{ad}\Delta I_{kd} - x_d \Delta I_d \tag{3.3}$$

$$\Delta \psi_q = x_{aq}\Delta I_{kq} - x_q \Delta I_q \tag{3.4}$$

$$\Delta \psi_{kd} = x_{ad}\Delta I_{fd} + x_{kkd}\Delta I_{kd} - x_{ad} \Delta I_d \tag{3.5}$$

$$\Delta \psi_{kq} = x_{kkq}\Delta I_{kq} - x_{aq} \Delta I_q \tag{3.6}$$

$$\Delta \dot{\psi}_{kd} + \omega R_{kd}\Delta I_{kd} = 0 \tag{3.7}$$

$$\Delta \dot{\psi}_{kq} + \omega R_{kq}\Delta I_{kq} = 0 \tag{3.8}$$

$$\Delta E_{fd} = \Delta \dot{\psi}_{fd} + \omega R_{fd}\Delta I_{fd} \tag{3.9}$$

$$\Delta \psi_{fd} = x_{ffd}\Delta I_{fd} + x_{ad}\Delta I_{kd} - x_{ad} \Delta I_d \tag{3.10}$$

Where V denotes voltage in volts, I a current in amperes, R a resistance in ohms, ψ a flux linkage in webers, and ω a speed in electrical radians per second.

3.3- *Synchronous machine model for low-frequency oscillation studies:*

The circuit shown in Fig. 3.3 may be considered as a simplification of a multigenerator system from the viewpoint of studying the stability performance of only one machine in the system. Thus the external reactance and infinite-bus represent the system as seen from the terminals of the machine studied.

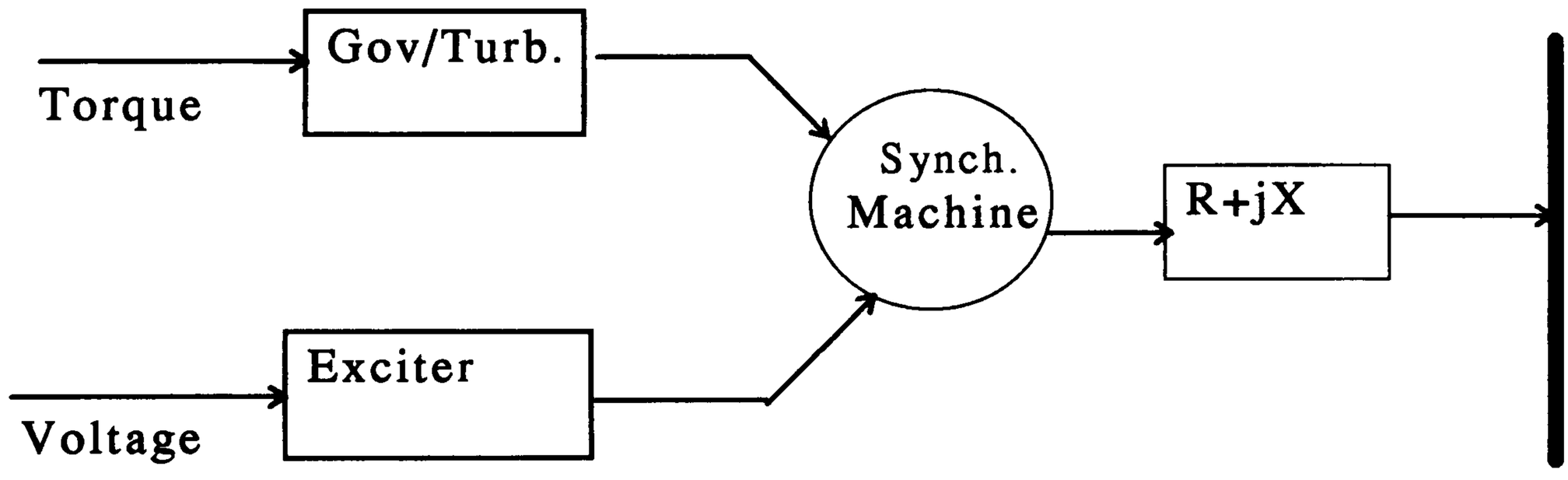

Fig. 3.3 Single generator connected to an infinite bus

The machine contains two channels, one from the exciter through the synchronous machine, and it is usually associated with the terminal voltage; the other is from the prime mover, again through the machine, and it is linked to the shaft speed. So, there

are two system outputs, the terminal voltage (V_t) and the shaft speed (ω); while the two system inputs are the reference input to the exciter (E_{ref}) and the reference position of the prime mover (T_{ref}). All the multivariable interactions take place within the synchronous machine and in ICAD context, the problem of stability for the whole system should be addressed considering only the structural dynamics of the synchronous machine and the customer specifications.

The dynamical characteristics of the synchronous machine in both its electric and mechanical aspects are obtained from Park's equations which describe the interaction between the electrical properties of the generator and its mechanical dynamics through the turbogenerator speed (ω) and the electric torque (T_{el}) transferred. During low-frequency oscillations, the current induced in a damper winding (k_d, k_q) is negligibly small; hence the damper winding can be completely ignored in system modelling. As for the d-axis and q-axis windings, their natural oscillating frequency is extremely high, their eignmodes will not affect the low-frequency oscillations, and hence they can be simply described by algebraic equations. What is left is the field

windings (f_d) circuit of the machine which must be described, not only because of its low eignmodes frequency, but also because it is directly connected to the exciter system. Finally, the torque differential equation of the synchronous machine must be included in the model. This configuration constitutes the basic low-order linear model (third order) representing the synchronous machine, and could be used for the low-frequency oscillations studies [22]. Hefferon and Philips [48], have presented a set of linearised equations involving special parameters [K_1 ..... K_6] based on Park's equations to describe the synchronous machine, and when the equations representing the prime mover (turbine) and exciter subsystems are added to the synchronous machine equations, an overall interacting turbogenerator system is obtained. Shackshaft [49] derived a general purpose turbogenerator model, in which none of the assumptions listed in Section (3.2) were used, but more simplified models were later developed by different authors using one or more of the assumptions, [50],[51],[52]. These authors have emphasized the need of Matrix methods and state-space formulation in turbogenerators control analysis and synthesis because of the wide spread use of digital computer. The general equations describing the performance of a synchronous

machine with no damper windings and with negligible resistance based on H-P model, are given in the Appendix (3). From Appendix (3), the linear equations representing the system are

$$\left(Ms^2 + Ds\right)\Delta\delta = \Delta T_m - K_2\Delta\psi_{fd} - K_1\Delta\delta \tag{3.11}$$

$$\Delta\psi_{fd} = \frac{K_3}{1+K_3T'_{do}s}\Delta E_{fd} - \frac{K_4}{1+K_3T'_{do}s}\Delta\delta \tag{3.12}$$

$$\Delta V_t = K_6\Delta\psi_{fd} + K_5\Delta\delta \tag{3.13}$$

where $s=j\omega$ is the complex frequency, ΔT_m is the mechanical torque input, ΔE_{fd} is the field voltage input, $\Delta\omega$ is the rotor speed output, $\Delta\delta$ is the rotor angle and ΔV_t is the terminal voltage output, M is the inertia constant. The coefficient D is a rather general term allowing, not only for damper windings, but also for prime-mover damping and variations in load torque with changes in speed. In general, D is not a constant and varies with speed and power flow. However, for any particular speed and power when only small changes about a mean value arise, D can be assumed to remain constant. The block diagram of Fig. 3.4 below shows schematically these equations.

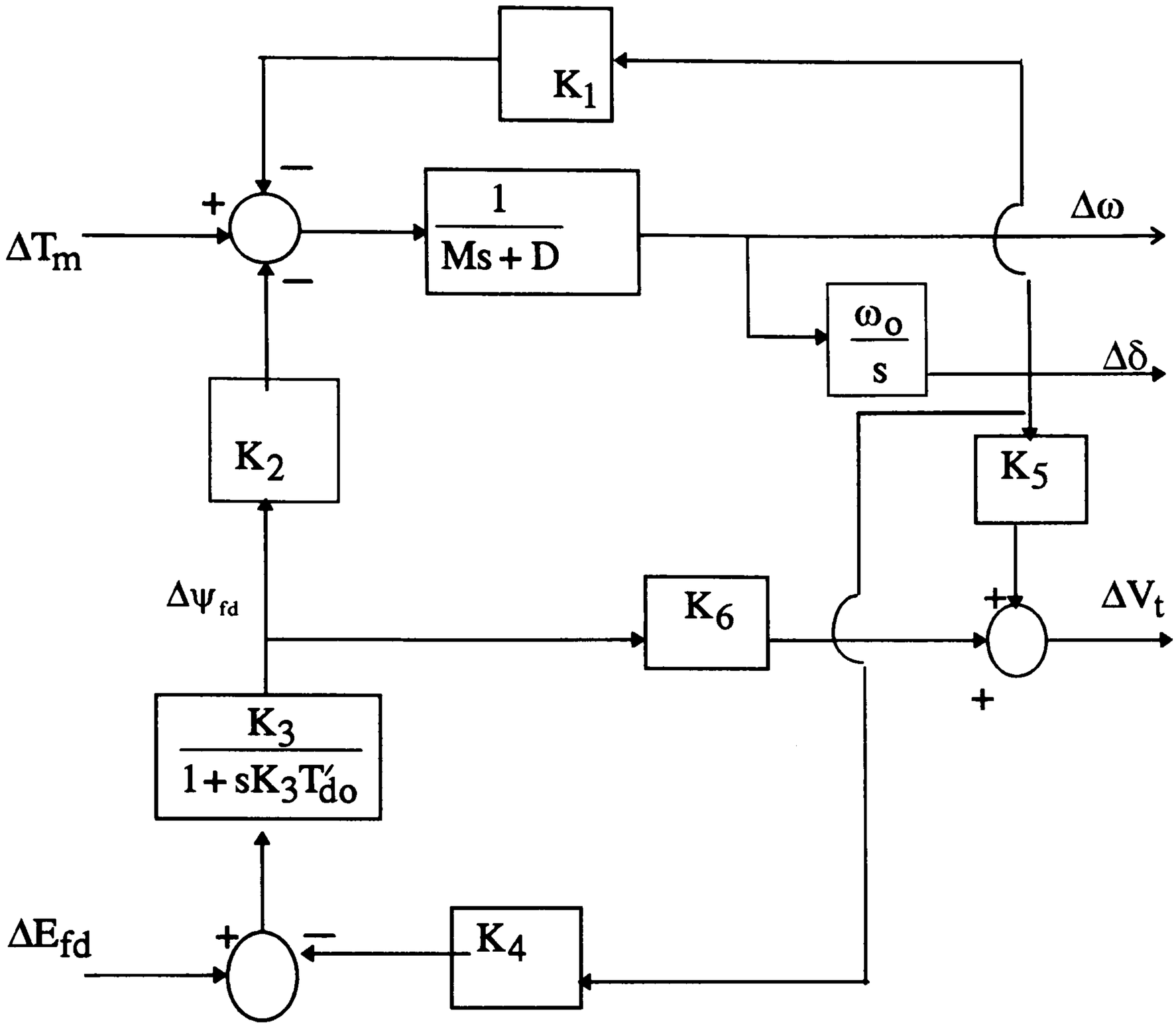

Fig. 3.4 Third order linearised model of the synchronous machine

The constants K_1 and K_2 are derived from the electric torque expressions; K_3 and K_4 are derived from the field winding circuit equations; K_5 and K_6 are derived from the generator terminal voltage. Except K_3 - which is an impedance factor- the parameters K_1, K_2, K_4, K_5, K_6 depend on the operating conditions of the machine. This model constitutes the basic model

for synchronous machines, and it is of third order. From equations (3.10 - 3.13), the transfer-matrix form, is shown in Fig. 3.5.

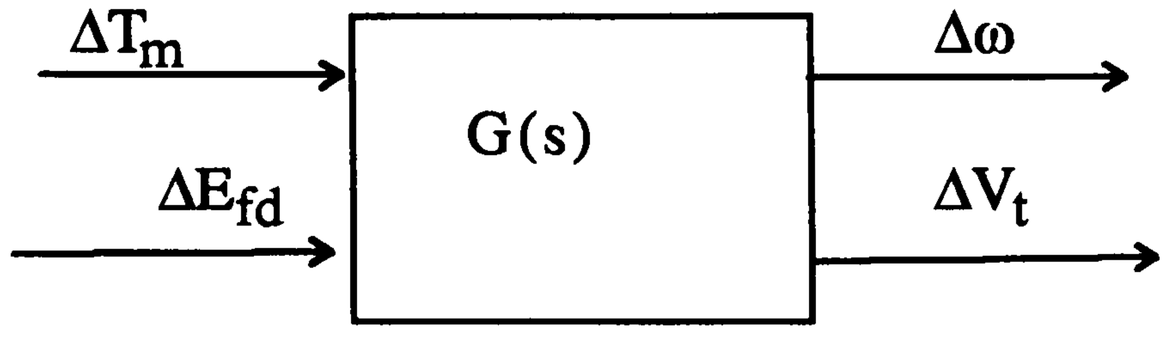

Fig. 3.5 Transfer function matrix model of synchronous machine

where

$$G(s) = \frac{1}{\Delta}\begin{bmatrix} g_{11}(s) & g_{12}(s) \\ g_{21}(s) & g_{22}(s) \end{bmatrix} \tag{3.14}$$

and

$$\Delta\omega = g_{11}(s)\Delta T_m + g_{12}(s)\Delta E_{fd} \tag{3.15}$$

$$\Delta V_t = g_{22}(s)\Delta E_{fd} + g_{21}(s)\Delta T_m \tag{3.16}$$

where the numerator polynomials

$g_{11}(s)$: transfer function between $\Delta\omega$ and ΔT_m.

$g_{12}(s)$: transfer function between $\Delta\omega$ and ΔE_{fd}.

$g_{21}(s)$: transfer function between ΔV_t and ΔT_m.

$g_{22}(s)$: transfer function between ΔV_t and ΔE_{fd}.

are given by :-

$$g_{11}(s) = s(1 + sK_3T'_{do}) \tag{3.17}$$

$$g_{12}(s) = -K_2K_3s \tag{3.18}$$

$$g_{21}(s) = K_5(1 + sK_3T'_{do})\omega_o - K_3K_4K_6\omega_o \qquad (3.19)$$

$$g_{22}(s) = K_3K_6(Ms^2 + Ds) + K_3(K_1K_6 - K_2K_5)\omega_o \qquad (3.20)$$

and the open-loop system characteristic polynomial is given by

$$\Delta(s) = (Ms^2 + Ds)(1 + sK_3T'_{do}) + K_1(1 + sK_3T'_{do})\omega_o - K_2K_3K_4\omega_o \qquad (3.21)$$

3.4- *Damper windings representation* :-

This transfer function block diagram model Fig. 3.4, first developed by Hefferon and Philips [48] and popularised by DeMello and Concordia [11], has, for many years, provided the basis for the explanation of fundamental generator dynamic characteristics and control requirements. The model, while giving a good insight into basic dynamic behaviour, does not account for the generator damper windings; only the direct-axis parameters were considered on the basis that short circuits produce currents of low power factor (quaderature currents predominate). This assumption may not be acceptable for disturbances considered in stability analysis. Therefore, additional synchronous machine parameters are required to more accurately model the behaviour. Quadrature-axis reactances and open circuit constants are defined for that purpose. The 3rd order model may be improved one step

by taking account of the variation of the direct-axis transient reactance, x'_d, with time from its initial value to a steady state value of X_d. The variation will be an exponential described by T'_{do} (transient, open circuit time constant). Another improvement will involve adding the effect of dampers which predominate during fast changing conditions, that is, the subtransient state. This, in effect, extends the 3-rd order model of the synchronous machine to a 5-th order model. To represent those additions, an extended transfer function block diagram model is presented by Saidy and Hughes [53] which takes into account the damper windings on both the d- and q- axes. The block diagram is shown in Fig. 3.6 below

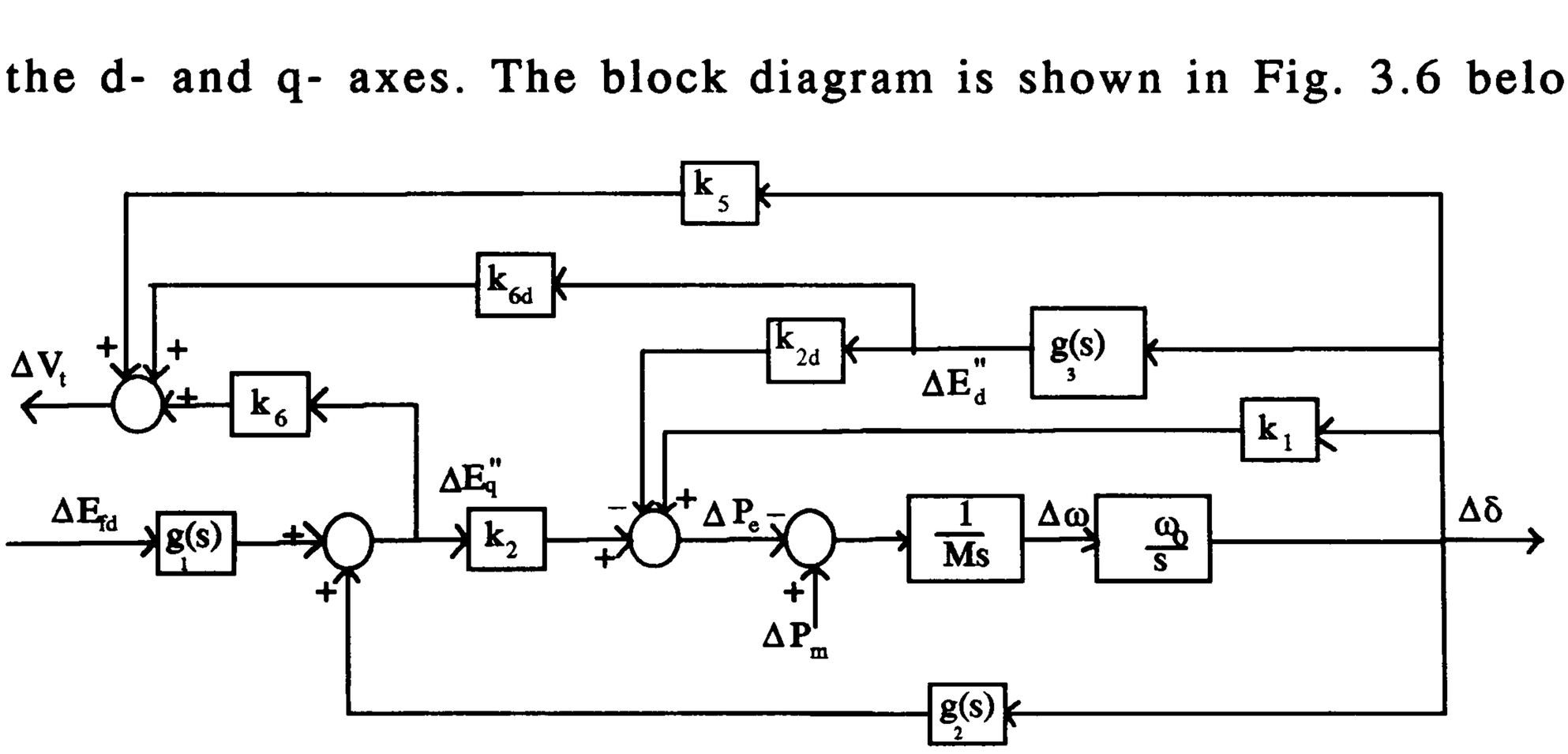

Fig. 3.6 Fifth-order linear model of synchronous machine with damper windings

From which the numerator polynomials of the 5-th order model of the synchronous machine are given by :-

$$g'_{11}(s) = s \tag{3.22}$$

$$g'_{12}(s) = -sk_2 g_1(s) \tag{3.23}$$

$$g'_{21}(s) = \omega_o\left(k_5 - k_6 g_2(s) + k_{6d} g_3(s)\right) \tag{3.24}$$

$$g'_{22}(s) = g_1(s)\left[k_6 M s^2 + \omega_o\left(k_1 k_6 - k_2 k_5\right) - \omega_o g_3(s)\left(k_2 k_{6d} + k_6 k_{2d}\right)\right] \tag{3.25}$$

and open - loop system charateristic polynomial is given by

$$\Delta'(s) = Ms^2 + \omega_o\left(k_1 - k_2 g_2(s) - k_{2d} g_3(s)\right) \tag{3.26}$$

where

$$g_1 = \frac{a\left(1 + T''_{do}s\right)k_3}{\left(1 + aT''_{do}s\right)\left(1 + k_3 T'_{do}s\right)} \tag{3.27}$$

$$g_2 = -k_{4d}\frac{\left(1 + cT'_{do}s\right)}{\left(1 + aT''_{do}s\right)\left(1 + k_3 T'_{do}s\right)} \tag{3.28}$$

$$g_3 = k_{4q}\frac{1}{\left(1 + bT''_{qo}s\right)} \tag{3.29}$$

When $g_3 = 0$, for no damper windings, and so k_{2d} and $k_{6d} = 0$

$$\text{and } g_1(s) = \frac{k_3}{\left(1 + k_3 T'_{do}s\right)} \tag{3.30}$$

$$g_2(s) = \frac{k_4}{\left(1 + k_3 T'_{do}s\right)} \tag{3.31}$$

we end up with the third-order model of Hefferon and Philips model [48] .(T''_{do} and T''_{qo} are the sub-transient open circuit time constants)

3.5- *Exciter and voltage regulator models*

The original function of the exciter and voltage regulator is to provide an adequate excitation to the synchronous machine field winding; in addition, the excitation system performs control and protective functions essential to the satisfactory performance of the power system by controlling the field voltage and thereby the field current. The control functions include the control of voltage and reactive power flow and the enhancement of system stability. The protective functions ensure that the capability limits of the synchronous machine, excitation system, and other equipment are not exceeded. [54]. The IEEE has standardised 12 model structures in block diagram form for representing the wide variety of excitation systems currently in use [55]. These are intended for use in transient stability and small-signal studies. The one used in this study is the IEEE type ST1A model which has the following configuration

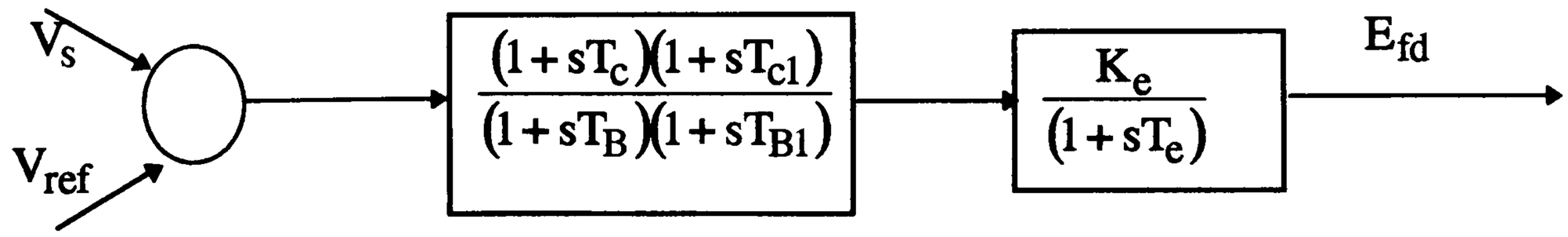

Fig.3.7 IEEE type ST1A Excitation system model

which in a small-signal study can be represented simply by

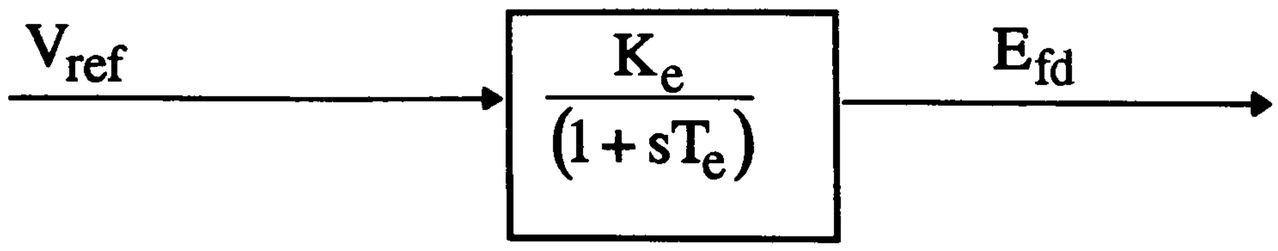

Fig.3.8 IEEE type ST1A Excitation system model (simplified)

3.6- *Governor and turbine models*

Power delivered by a generator is controlled by controlling the mechanical power of a "prime mover" such as steam, water or gas turbines or diesel engine. This is usually done by opening or closing valves regulating steam or water flow. The prime movers convert sources of electrical energy (kinetic energy of water, thermal energy derived from fossil fuels and nuclear fission) into mechanical energy that is, in turn, converted to electrical energy by synchronous machines.

Since the load of a power system is always changing, at least one generator in the system must respond to this change in order to maintain power balance. The way we sense this power imbalance is through its effect on generator speed and/or frequency. If there is excess generation, the generator sets will tend to speed up and the frequency will rise; on the other hand, if there is a deficiency of generation, the generator speed and

frequency will drop. These deviations from nominal speed and/or frequency are used as control signals to cause appropriate valve action automatically. This is done by a speed *governor*, a device which senses the deviation and converts it into appropriate valve action [56]. For speed governors, as with exciters, a composite model which can be reduced to any desired level is the most satisfactory. The Governor/Turbine model used in this study [57], is shown in Fig. 3.9 below

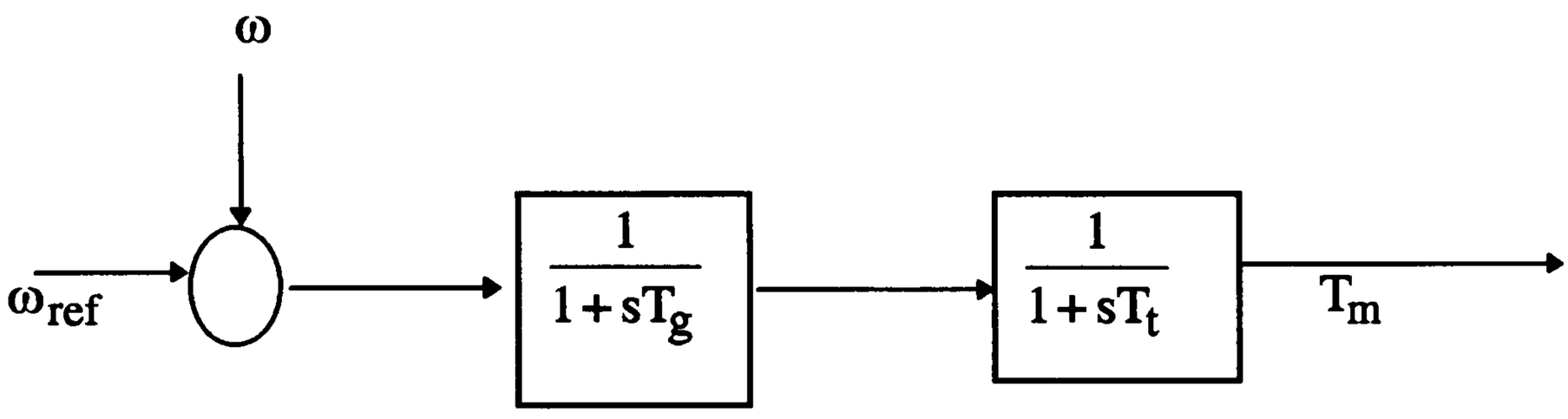

Fig. 3.9 Governor/Turbine Linear Model

3.7- *Analysis of turbogenerator system using ICAD technique*

In block diagram, the turbo generator system is represented by Fig. 3.10 below

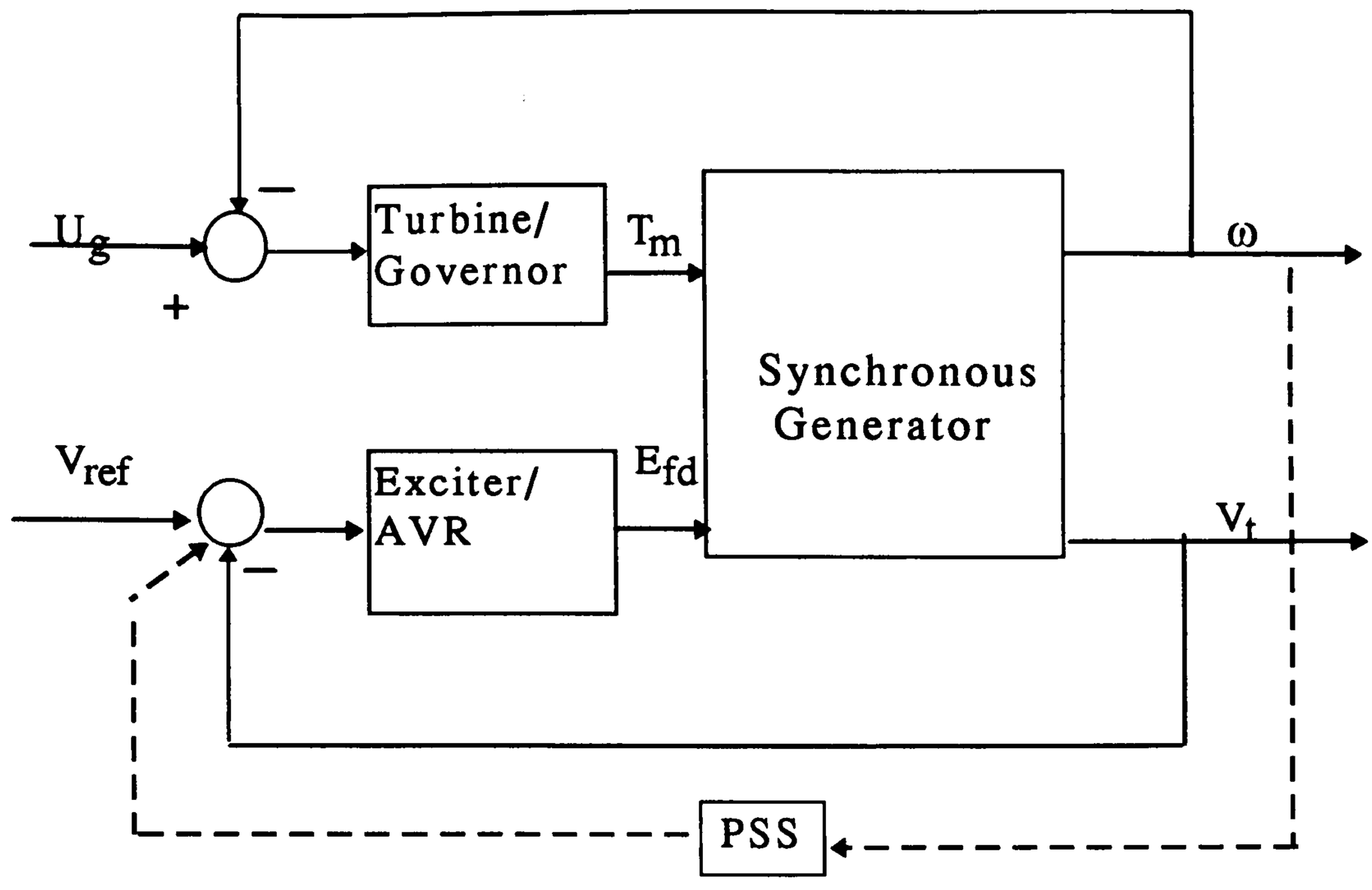

Fig.3.10 Turbogenerator system

The synchronous machine -as said before- could be modelled as a 3rd or higher order model, and a cross-coupling loop between the rotor speed (ω) output, and the exciter input (E_{ref}), in the form of a so-called Power System Stabiliser (PSS) may or may not exist. Neglecting the presence of the PSS for the moment, the governor/turbine and exciter/AVR dynamics, lying as they do on the principal feedback loops; don't affect the multivariable structure function γ(s) of equation (2.2) which is simply that of the synchronous machine model. Under the physical analysis of the synchronous machine, we need to answer two questions :

(1) what types of system configuration and loading conditions are likely to encounter dynamic instability ?. (2) under what situations

can the synchronous machine itself, without control effects, produce negative damping ?

Embarking now on a multivariable analysis of the turbogenerator control system depicted in Fig. 3.11 along the lines of O'Reilly and Leithead [33] and the review of Chapter 2; we consider first the forward signal transmission from the governor reference (ΔU_g) to its associated turbogenerator speed output ($\Delta\omega$) in Fig. 3.11.

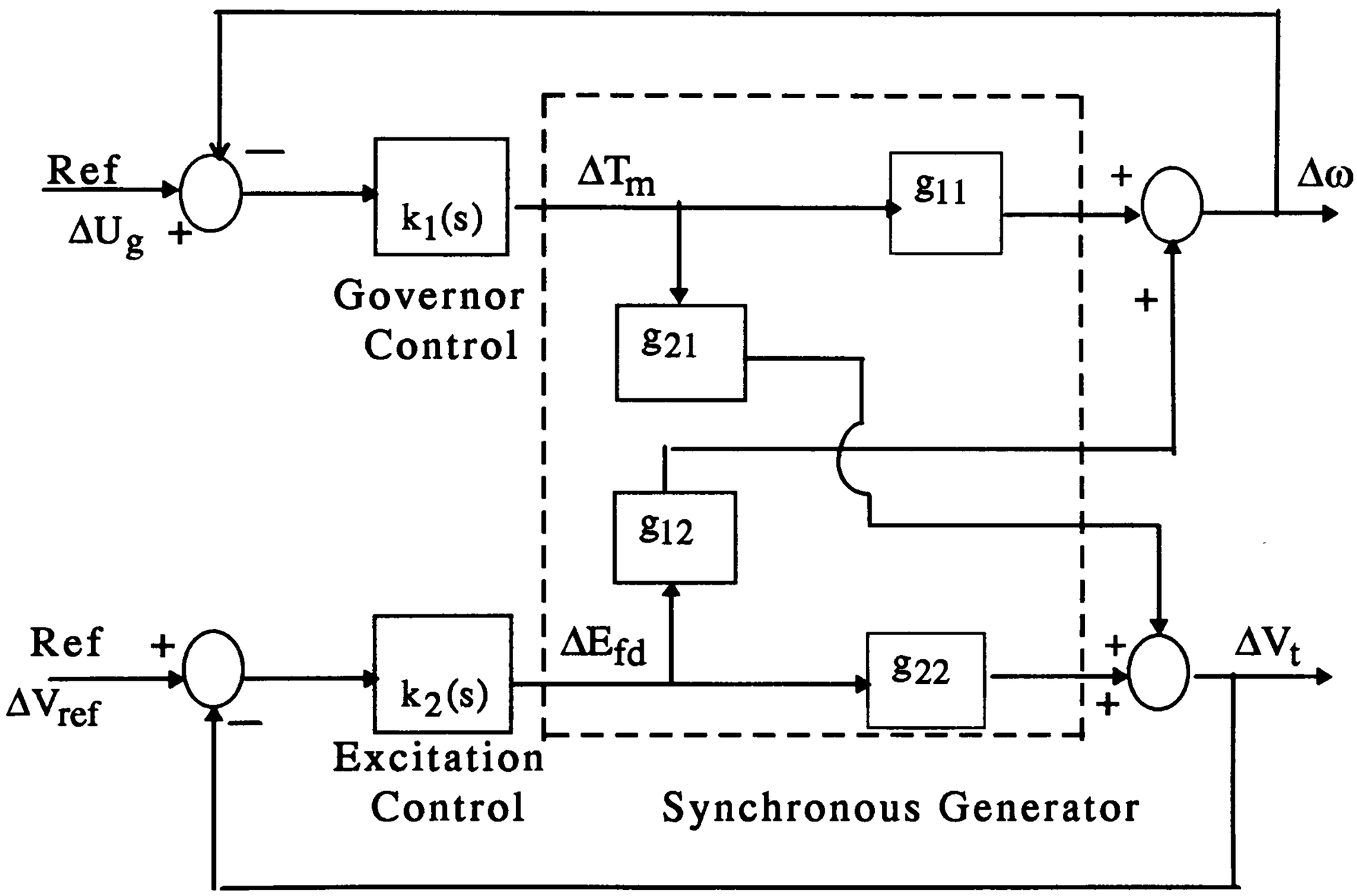

Fig. 3.11 Block diagram of a 2-input 2-output turbogenerator for control system analysis

This forward signal transmission follows two parallel paths: one directly through $g_{11}(s)$; the other via $g_{21}(s)$, the bottom exciter feedback subsystem and $g_{12}(s)$. We observe also in Fig. 3.11 that the forward cross-signal transmission from the generator terminal voltage reference (ΔV_{ref}) to the turbogenerator speed output ($\Delta\omega$) is via the bottom exciter feedback subsystem and $g_{12}(s)$. These signal transmissions from ΔU_g to $\Delta\omega$ and from ΔV_{ref} to $\Delta\omega$ can, after a little block algebra, the details of which are described in [33], be represented as in Fig. 3.12.

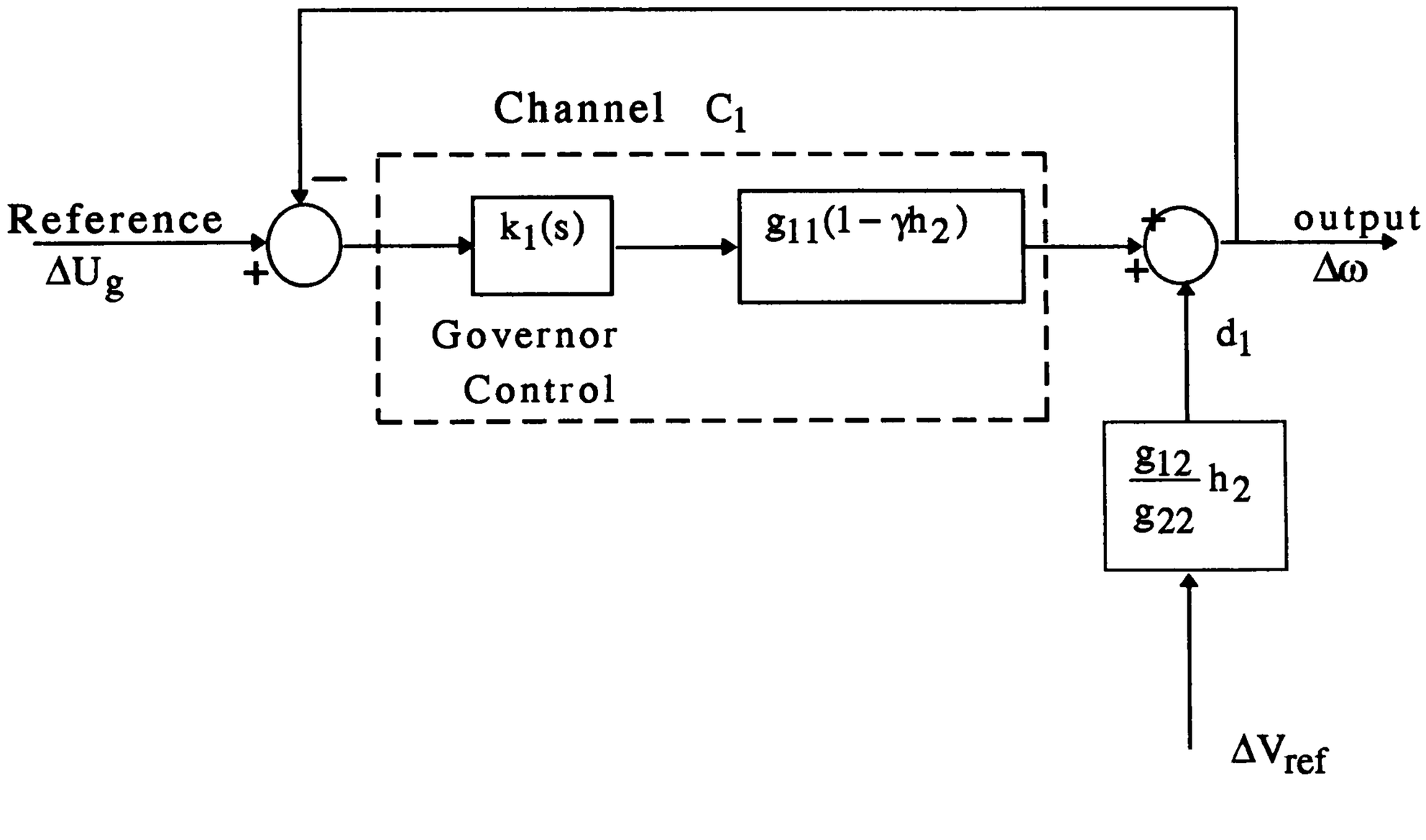

Fig. 3.12 Individual channel design structure : governor/speed channel

In other words, Fig. 3.12 depicts the individual signal transmission Channel C_1 between governor reference (ΔU_g) and its associated generator speed output ($\Delta\omega$) together with the additive cross-reference 'disturbance' signal $g_{12}g_{22}^{-1}h_2\Delta V_{ref}$ at the generator speed output ($\Delta\omega$). Likewise, by symmetry of the topological structure of Fig.3.11, Channel C_2 between the generator terminal voltage reference (ΔV_{ref}) and its associated terminal voltage output (ΔV_t), together with a unity negative feedback excitation control loop and a cross-reference 'disturbance' signal $g_{21}g_{11}^{-1}h_1\Delta U_g$ is represented by Fig. 3.13.

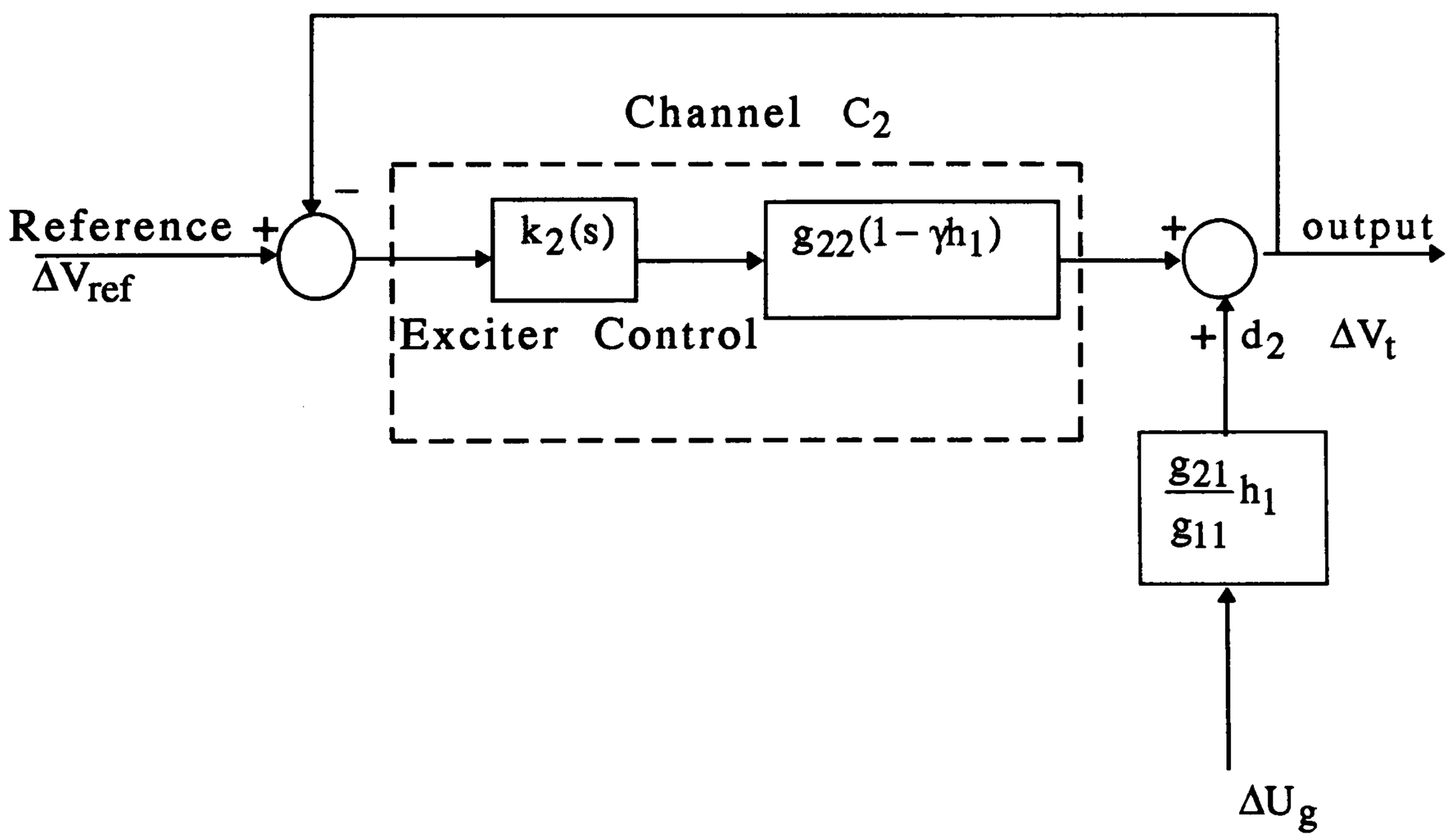

Fig. 3.13 Individual channel design structure : exciter/voltage channel

Thus, we have established [33] that the two individual channel feedback control problems of Fig. 3.12 and Fig. 3.13, are together structurally equivalent to the original 2-input 2-output turbogenerator feedback control problem of Fig. 3.11; all signal interactions via $g_{12}(s)$ and $g_{21}(s)$ are retained and no structural information is lost. From Fig. 3.12, Channel C_1 has the forward path single-input single-output (SISO) transfer function

$$C_1 = k_1 g_{11}(1 - \gamma h_2) \tag{3.32}$$

Similarly, from Fig. 3.13, Channel C_2 has the forward path SISO transfer function

$$C_2 = k_2 g_{22}(1 - \gamma h_1) \tag{3.33}$$

From equations (3.22) to (3.26), the multivariable structure function $\gamma(s)$ of this 2-input 2-output parameterised 3rd-order model assumes the explicit parameterised form given by

$$\gamma(s) = \frac{-K_2\left[K_5(1+sK_3T'_{do}) - K_3K_4K_6\right]\omega_o}{(1+sK_3T'_{do})\left[K_6(Ms+D)s + (K_1K_6 - K_2K_5)\omega_o\right]} \tag{3.34}$$

or, when using the extended model with the damper windings represented (5-th order model) :

$$\gamma'(s) = \frac{-k_2(k_5 + k_6 g_2 + k_{6d} g_3)\omega_o}{k_6 M s^2 + \omega_o(k_1 k_6 - k_2 k_5) + \omega_o(k_2 k_{6d} + k_6 k_{2d})} \tag{3.35}$$

This explicit parameterised form for the multivariable structure function $\gamma(s)$ is extremely useful in analysing the effects of any change in system parameters on the performance of the system; for instance, K_1 related to the natural frequency of oscillation, K_5 related to the system damping and K_6 related to the phase lag contributed by the exciter, [4],[58].

3.8- *Analysis of parameters affecting model performance* :-

(i) Model complexity :-

In state-space form the synchronous machine models are represented by the following equation

$$\dot{x} = Ax + Bu$$
$$y = Cx \qquad (3.36)$$

<u>The 3rd order model</u> :-

With amortisseurs (dampers) winding neglected, the equivalent circuits relating the machine flux linkages and currents are as shown in Fig. 3.14 below

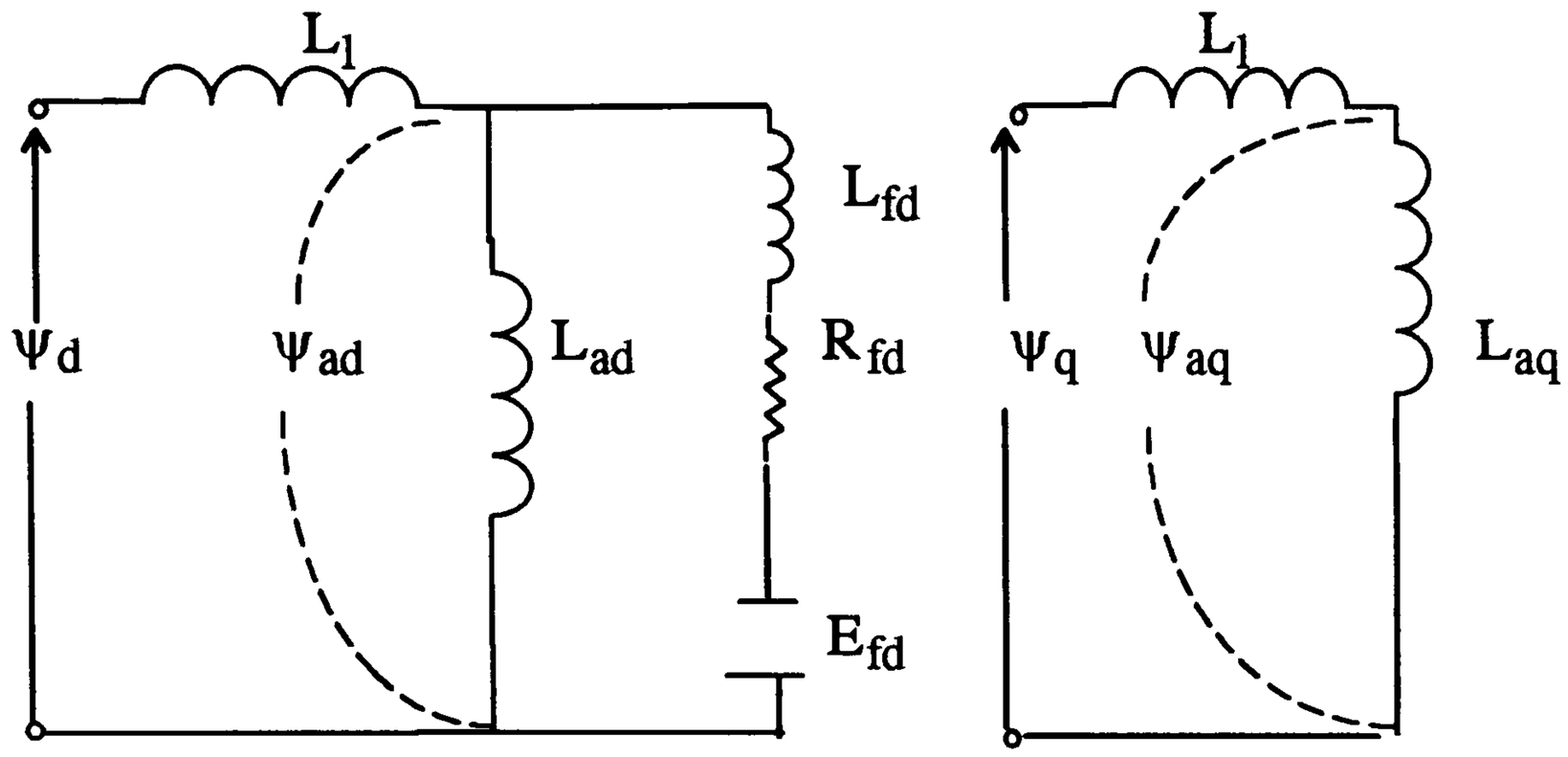

Fig. 3.14 Synchronous machine equivalent circuit : 3rd-order model

Using equation (3.36), the states of the 3rd order model, [x], are [rotor angle, speed, voltage proportional to direct axis]. And in a matrix form :

$$x = \begin{bmatrix} \Delta\delta \\ \Delta\omega \\ \Delta E'_q \end{bmatrix} \quad , \; u = \begin{bmatrix} \Delta T_m \\ \Delta E_{fd} \end{bmatrix} \quad \text{and } y = \begin{bmatrix} \Delta\delta & \Delta e_t \end{bmatrix}$$

where

$$A = \begin{bmatrix} 0 & \omega_o & 0 \\ a_{21} & a_{22} & a_{23} \\ a_{31} & 0 & a_{33} \end{bmatrix} \quad , \; B = \begin{bmatrix} 0 & 0 \\ b_{21} & 0 \\ 0 & b_{32} \end{bmatrix} \quad \text{and } C = \begin{bmatrix} 1 & 0 & 0 \\ c_{21} & 0 & c_{33} \end{bmatrix}$$

(The matrices elements are written in Appendix 5)

<u>The 6th order model :-</u>

When machine amortisseurs (damper) windings are included, (the model now has one d-axis damper and two q-axis damper

windings), the equivalent circuits relating machine linkages and currents is shown in Fig. 3.15 below

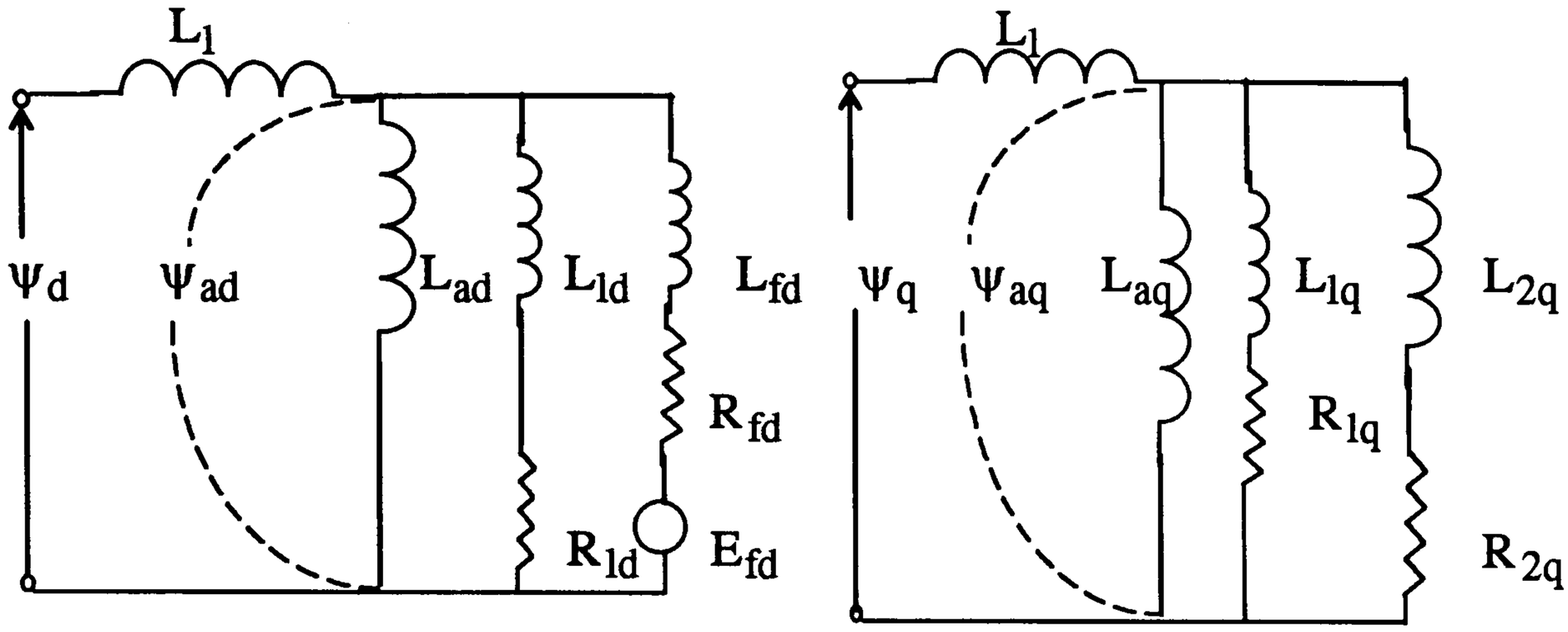

Fig. 3.15 Synchronous machine equivalent circuit : 6th-order model

In equation (3.36), the states of the 6-th order linear model, [x], are [rotor angle, speed, field winding, damper winding in d-direction, first damper winding in q-direction, second damper winding in q-direction]. And in a amtrix form, equation (3.36) for the 6-order model is shown below :

$$x = \begin{bmatrix} \Delta\delta \\ \Delta\omega \\ \Delta\psi_{fd} \\ \Delta\psi_{1d} \\ \Delta\psi_{1q} \\ \Delta\psi_{2q} \end{bmatrix} \quad u = \begin{bmatrix} \Delta T_m \\ \Delta E_{fd} \end{bmatrix} \quad \text{and } y = \begin{bmatrix} \Delta\delta & \Delta e_t \end{bmatrix}$$

where

$$A=\begin{bmatrix} 0 & \omega_o & 0 & 0 & 0 & 0 \\ a_{21} & a_{22} & a_{23} & a_{24} & a_{25} & a_{26} \\ a_{31} & 0 & a_{33} & a_{34} & a_{35} & a_{36} \\ a_{41} & 0 & a_{43} & a_{44} & a_{45} & a_{46} \\ a_{51} & 0 & a_{53} & a_{54} & a_{55} & a_{56} \\ a_{61} & 0 & a_{63} & a_{64} & a_{65} & a_{66} \end{bmatrix}, \qquad B=\begin{bmatrix} 0 & 0 \\ b_{21} & 0 \\ 0 & b_{32} \\ 0 & 0 \\ 0 & 0 \\ 0 & 0 \end{bmatrix}$$

and $$C=\begin{bmatrix} 0 & 1 & 0 & 0 & 0 & 0 \\ c_{21} & 0 & c_{23} & c_{24} & c_{25} & c_{26} \end{bmatrix}$$

(the matrices elements are given in Appendix 5).

Since one of the effective ways of demonstrating the dynamic characteristics of a system is via its frequency response; the influence of the simplifications of third and sixth or any order linear model on dynamic behaviour can be shown using frequency response by comparing the polar plots of the multivariable structure function $\gamma(s)$ for both models. In particular, polar plots of $\gamma(s)$ for these two different model orders described above at a heavy loading condition (P=0.9, Q=0.3, V_t=1) and a typical synchronous reactance (x_d=1.81 pu, x_q=1.76 pu) are shown in Fig. 3.16.

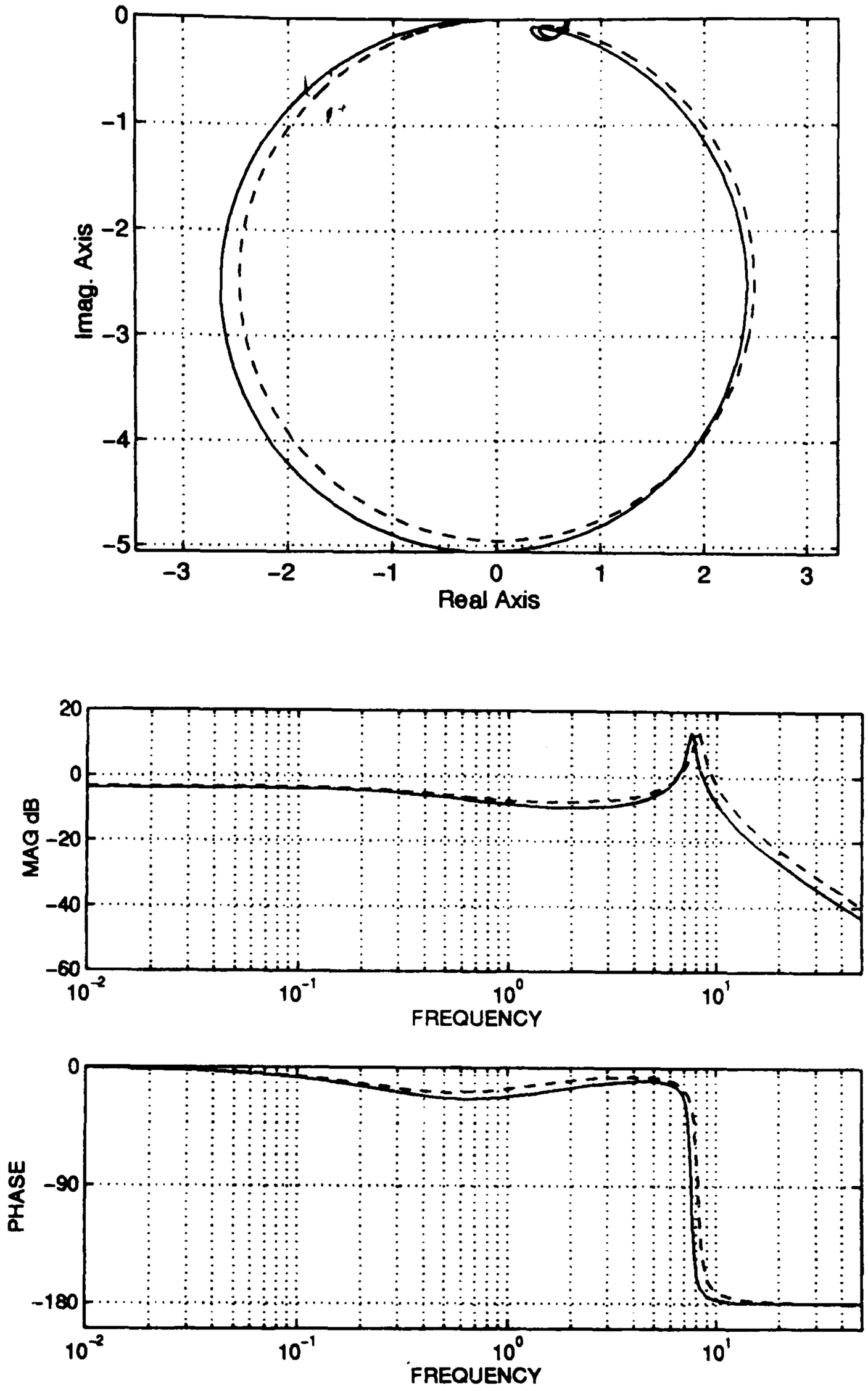

(———) 3rd-order model; (— — —) 6th-order model

Fig. 3.16. Nyquist & Bode plots of $\gamma(s)$ for third and sixth order models

These polar plots are not significantly different, and this provides further justification for the very common use [59],[60]

[61],[62], of the 3-rd order model of the synchronous machine shown in Fig. 3.4.

(ii) *Changes in loading conditions*:

Secondly, the effect of changes in loading conditions (real and reactive power) on the multivariable structure function $\gamma(s)$ for a fixed synchronous reactance (x_d=1.445 pu, x_q=0.959 pu) is considered. Three different loading conditions, lagging power factor (P=0.736, Q=0.752), unity power factor (P=0.812, Q=0.16), and leading power factor (P=0.912, Q=0.392) are chosen as in Hughes and Saidy [53]. The initial rotor angle of the machine changes from 29.85^o to 41.72^o to 58.85^o for the three loading conditions respectively. The machine is connected to a tie-line of reactance x_e=0.2 pu. While K_3 does not change at all (impedance factor), the rest of the parameters change as follows: K_1 increases with the increase in real power, so does K_2 and K_4; while K_5 and K_6 decreases (sometimes K_5 changes sign). Polar plots of $\gamma(s)$ for these different loading conditions are shown in Fig. 3.17, where it is observed that $\gamma(s)$ moves towards the (1,0) point for increasing real power (loading condition), and although the interaction start to decrease at 1 rad/sec, it increases again in the important frequency range (4-10) rad/sec. (see Chapter 4) From Result 2.3 of

Chapter 2, this indicates a decrease in stability robustness to model uncertainties for increasing real power.

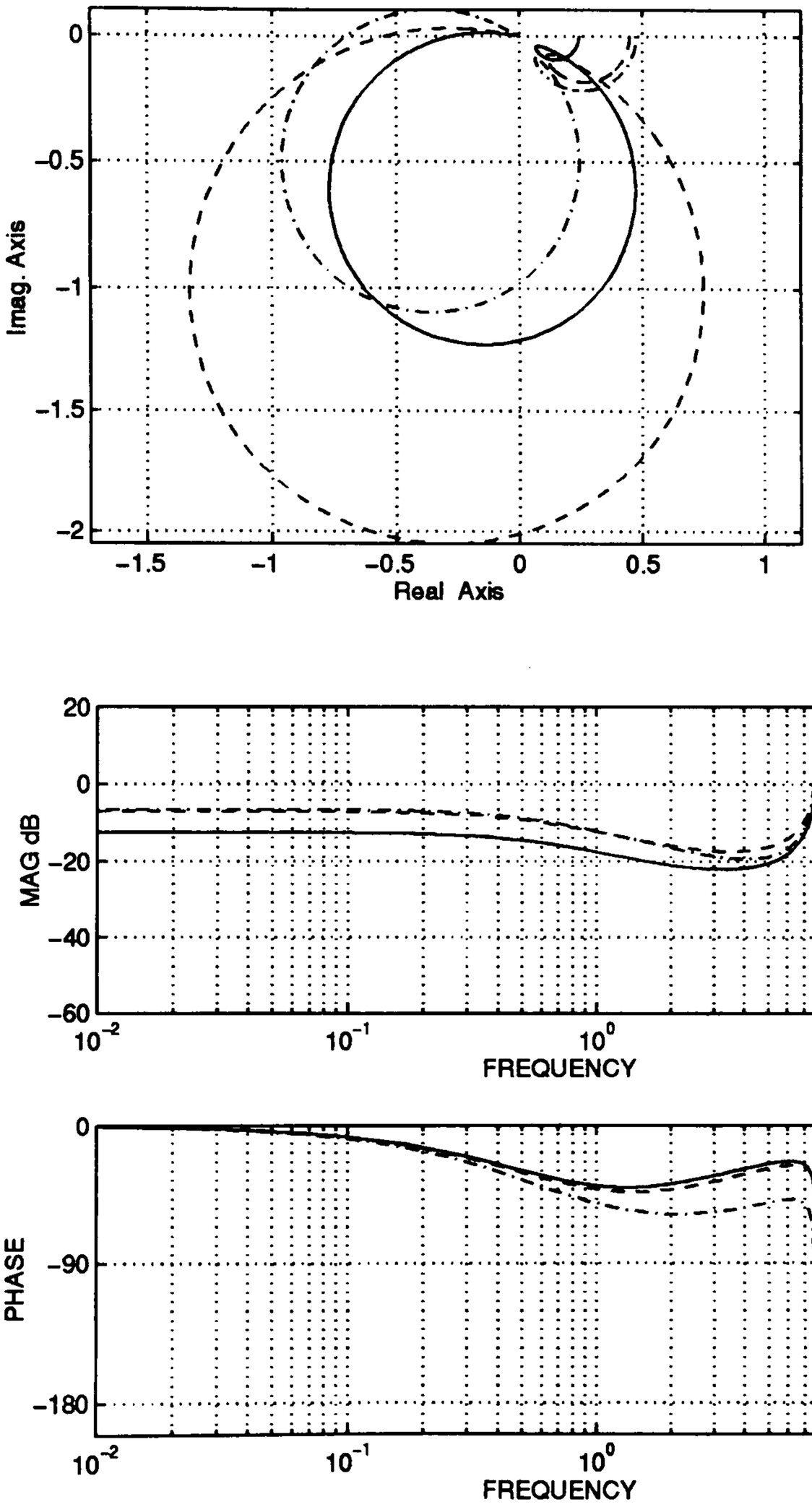

(——) low ,(–·–·–·) medium, and (– – – –) high

Fig. 3.17 Nyquist and Bode plots of $\gamma(s)$ for third order models at different operating conditions

(iii) *Changes in synchronous reactance:*

Consider next the effect of different choices of a particular model synchronous reactance at a fixed loading condition (P=0.9, Q=0.3). Three different values of synchronous reactance are considered; namely synchronous reactance $x_d=x_q=1.6$ pu [63], synchronous reactance $x_d=x_q=2.0$ pu [64], and synchronous reactance $x_d=x_q=2.6$ pu[65]. Polar plots of the multivariable structure function $\gamma(s)$ are shown in Fig. 3.18 where it is observed that $\gamma(s)$ moves towards the (1,0) point for increasing model synchronous reactance. Again from Result 2.3 of Chapter 2, this indicates a decrease in stability robustness to model uncertainties for increasing model synchronous reactance. On the other hand, higher values of synchronous reactance are desirable from the point of view of more power generation [66]. Typical values of synchronous reactance used in practice [67], however, are always less than 2.0 pu for which our multivariable analysis shows that there is no stability robustness problem ($\gamma(s)$ nowhere near the (1,0) point).

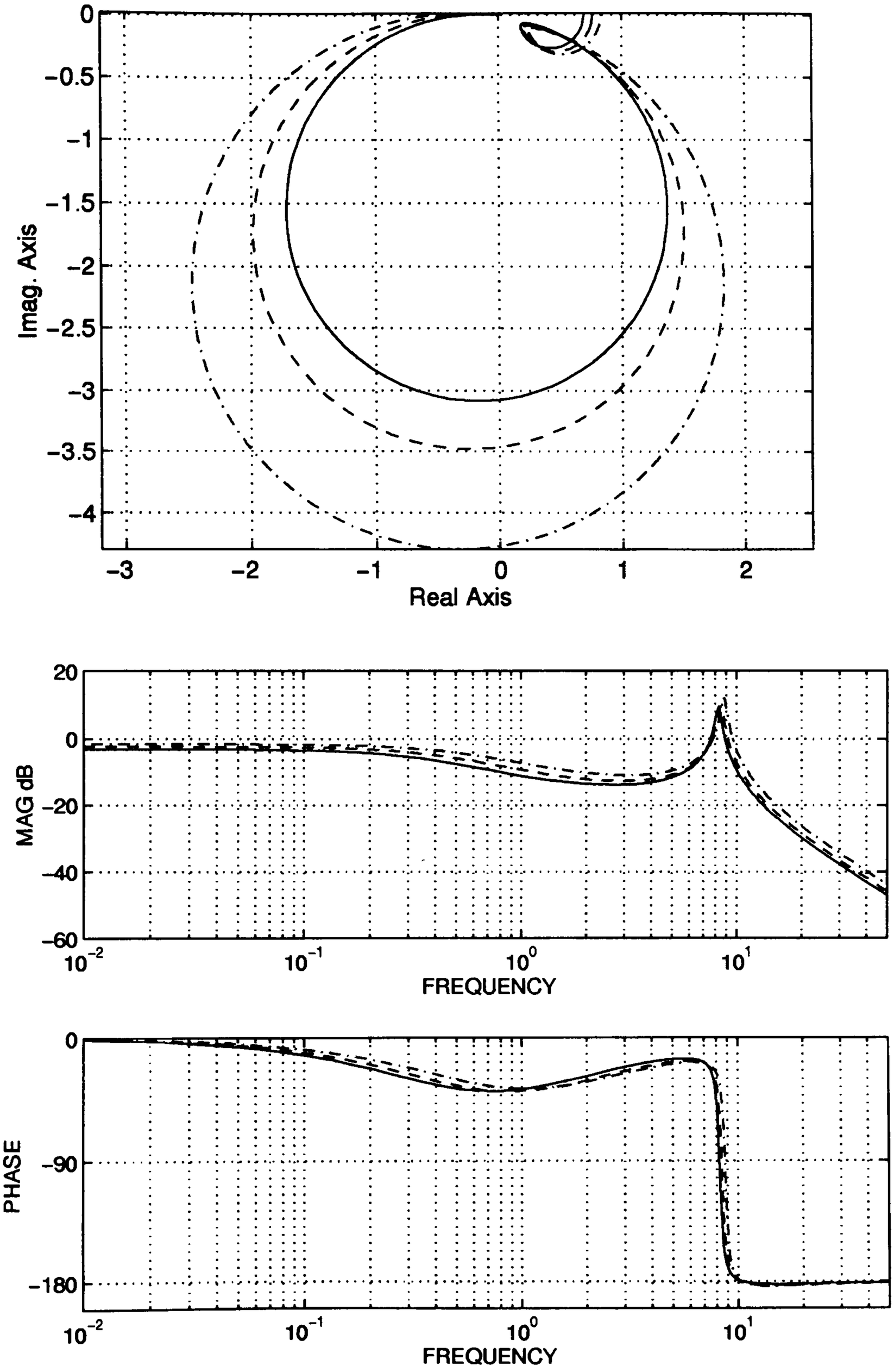

(_ . _ . _ . _ . _ . _) high reactance, (– – – – ·) medium, (———) low

Fig. 3.18 Nyquist and Bode plots of γ(s) for third order models with different synchronous reactance

(iv) *changes in tie-line reactances*

Taking now the effect of tie-line variation on the performance of the generator; the tie-line reactance x_e is changed from 0.2 pu, (strong transmission line), to 0.4 pu (medium) and 0.8 pu (weak transmission line). The generator is operated under lagging power factor ,light loading conditions. The infinite-bus voltage and current flowing into the grid system are considered constant. The synchronous reactance of the generator is x_d=1.445 pu, x_q=0.959 pu; and the terminal voltage V_t=1.0 pu. Polar plots of the multivariable structure function $\gamma(s)$ are shown in Fig. 3.19.

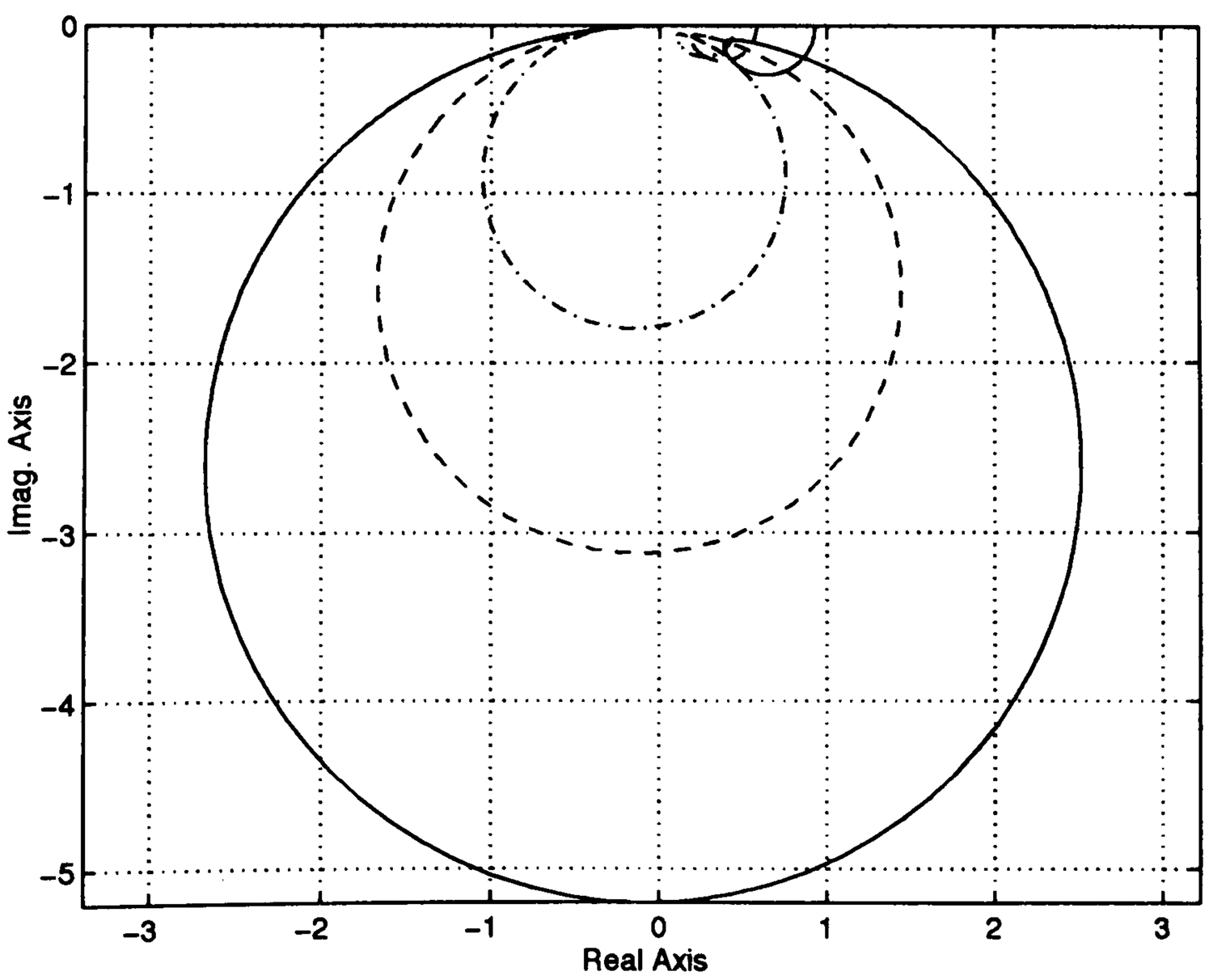

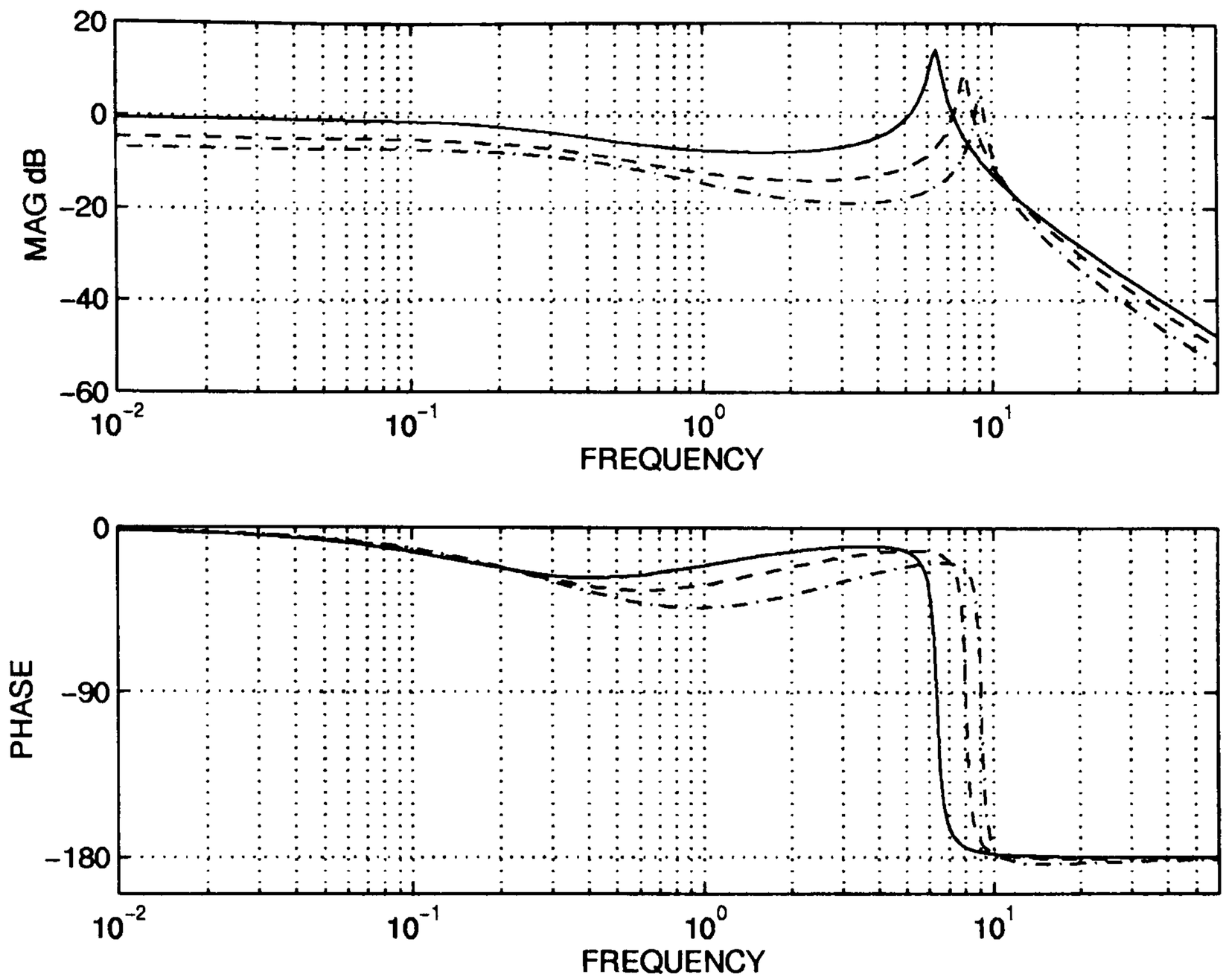

(– · – · – · – · –) strong (– – – – –) medium (————) weak trans. line

Fig. 3.19 Nyquist and Bode plots of $\gamma(s)$ for third order models connected to 3 different transmission lines.

It is observed that $\gamma(s)$ moves towards the (1,0) point for increasing model tie-line (weaker transmission lines) reactance throughout the frequency range (0-4) read/sec, and start to increase even more after 4 rad/sec as the transmission line becomes weaker. Again from Result 2.3 of Chapter 2, this indicates a decrease in stability robustness to model uncertainties for increasing model tie-line reactance.

(v) *Effect of the damping constant*

Here, the effect of damping constant variation on the performance of the generator is considered. The machine is at a heavy loading condition (P=0.9, Q=0.3, V_t=1) and a typical synchronous reactance (x_d=1.81 pu, x_q=1.76 pu) and an inertia constant of M=7. The damping constant is changed from D=3 pu, to D=6 pu, and to D=10 pu. Polar plots of the multivariable structure function $\gamma(s)$ are shown in Fig. 3.20.

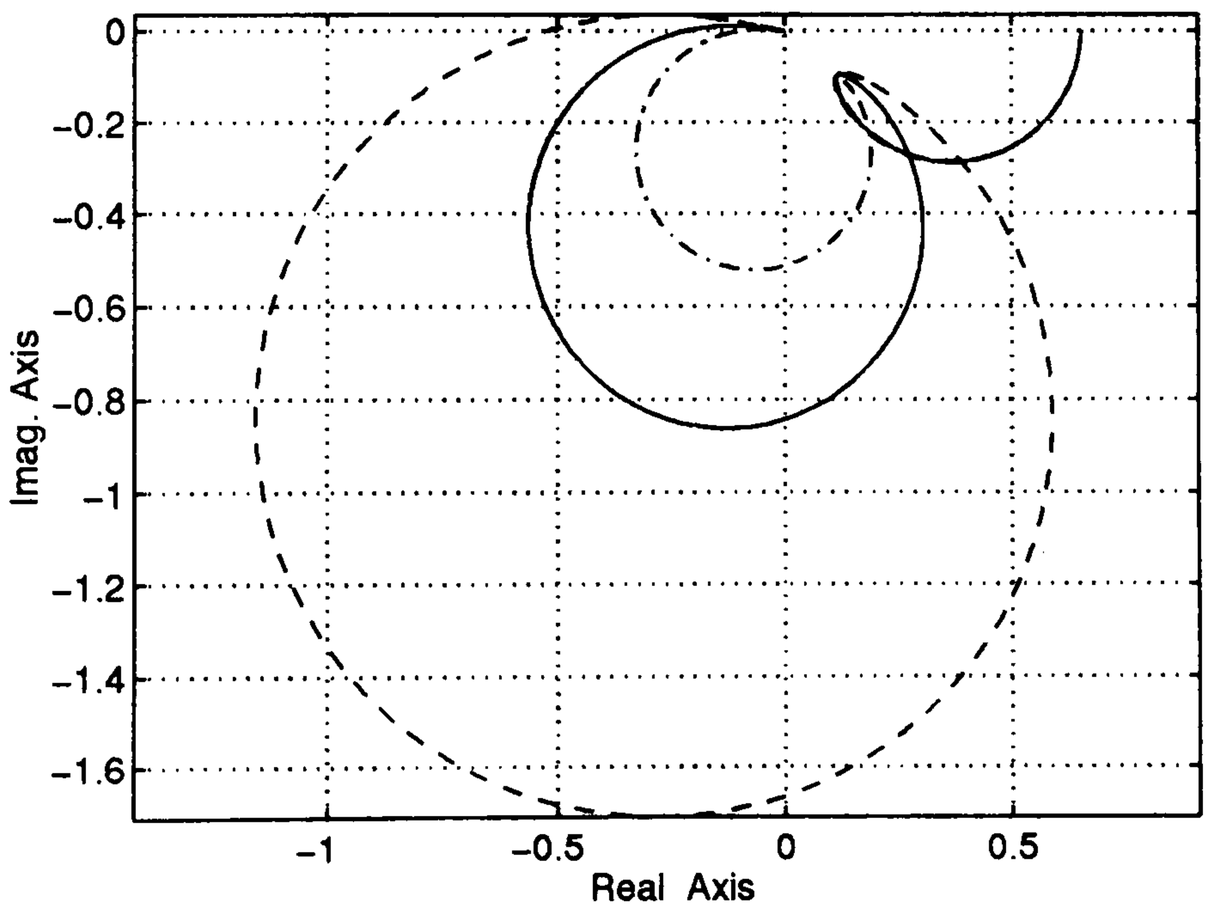

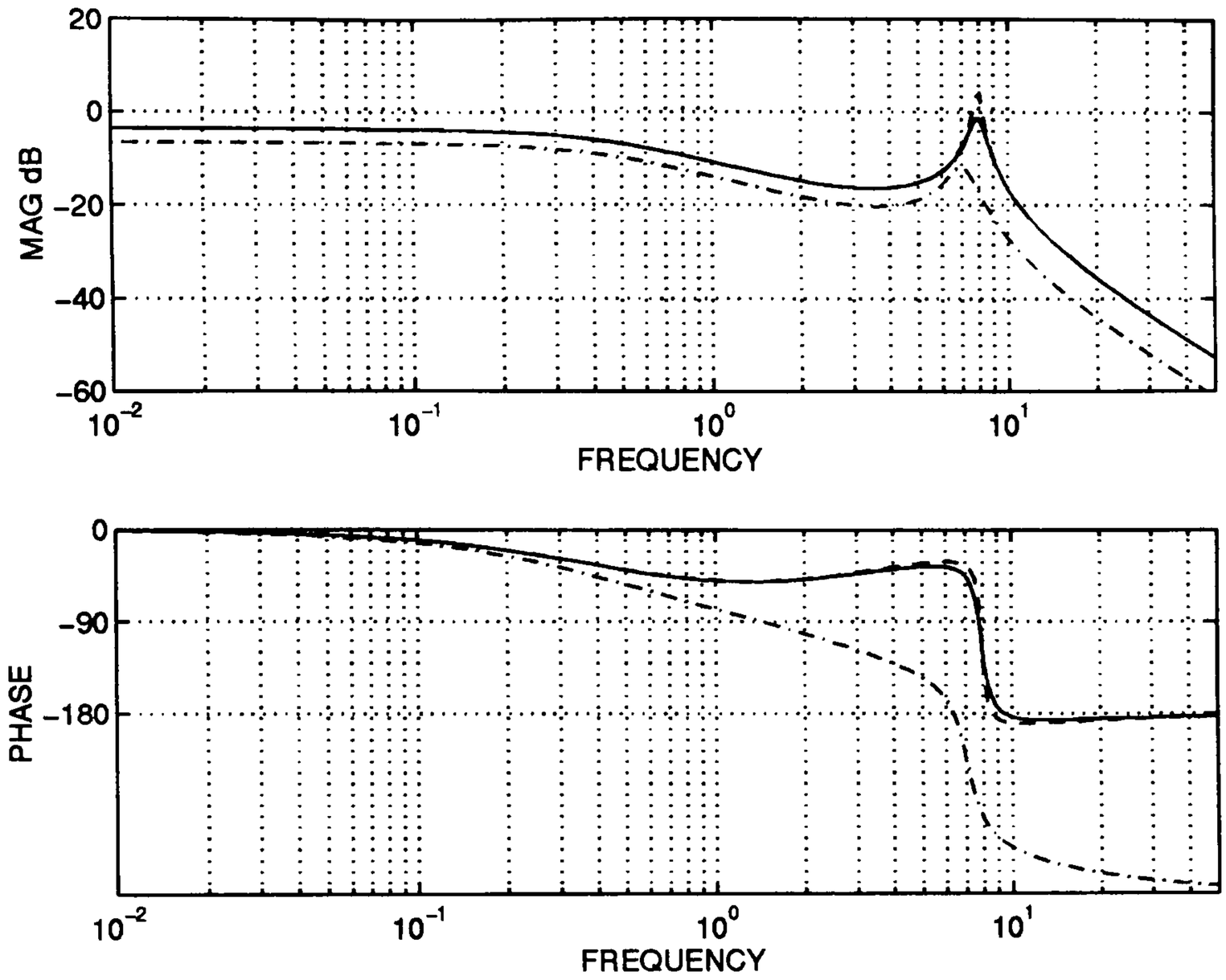

(– – – – – –) low, (————) medium, (– · – · – · –) high damping

Fig. 3.20 Nyquist and Bode plots of $\gamma(s)$ for third order models with 3 different damping constant value

As it is clear that the gain of $\gamma(s)$ (the interaction idicator) increases for decreasing model damping constant espacially at the important frequency range (5-15) rad/sec. (see Chpater 4). Again from Result 2.3 of Chapter 2, this indicates a decrease in stability robustness to model uncertainties for decreasing model damping constant.

(vi) *Effect of changing inertia constant*

Finally, the effect of inertia constant variation on the performance of the generator is considered. The machine is at a

heavy loading condition (P=0.9, Q=0.3, V_t=1) and a typical synchronous reactance (x_d=1.81 pu, x_q=1.76 pu). The damping constant is D=3 pu. The inertia constant is changed from M=3 to M=7 pu, and to M=10 pu. Polar plots of the multivariable structure function $\gamma(s)$ are shown in Fig. 3.21

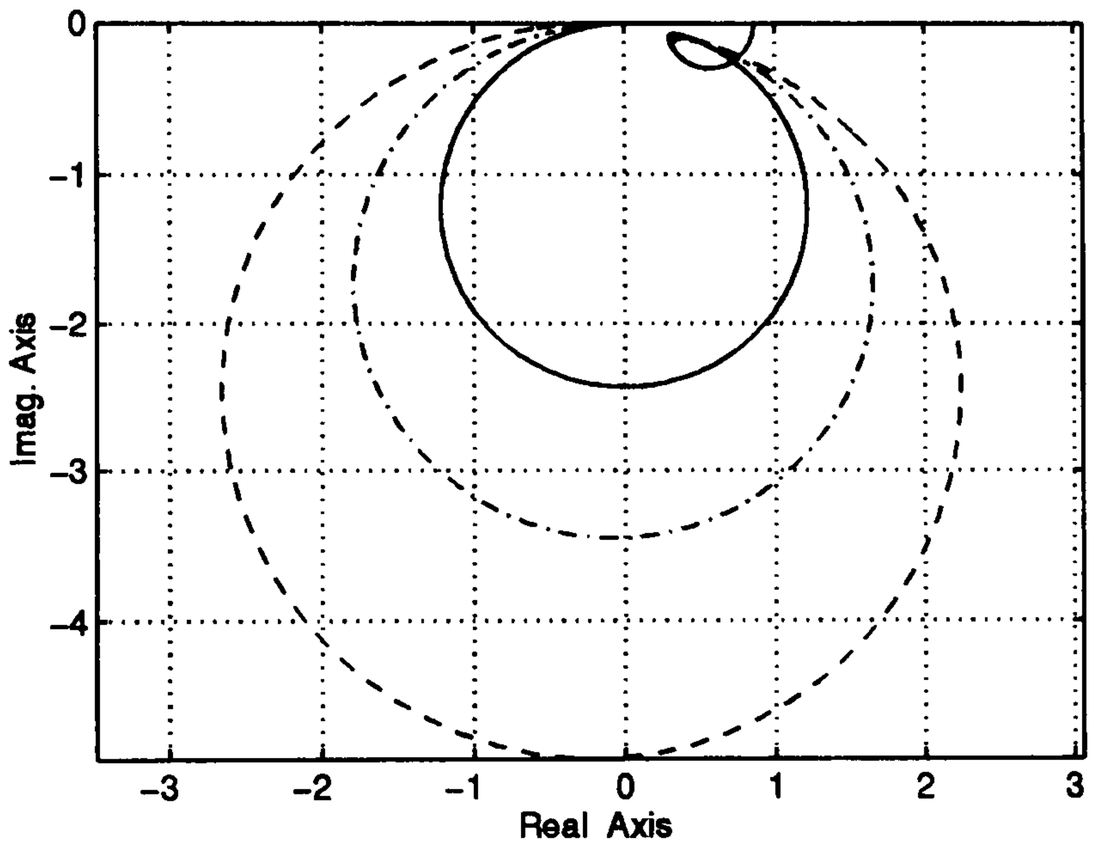

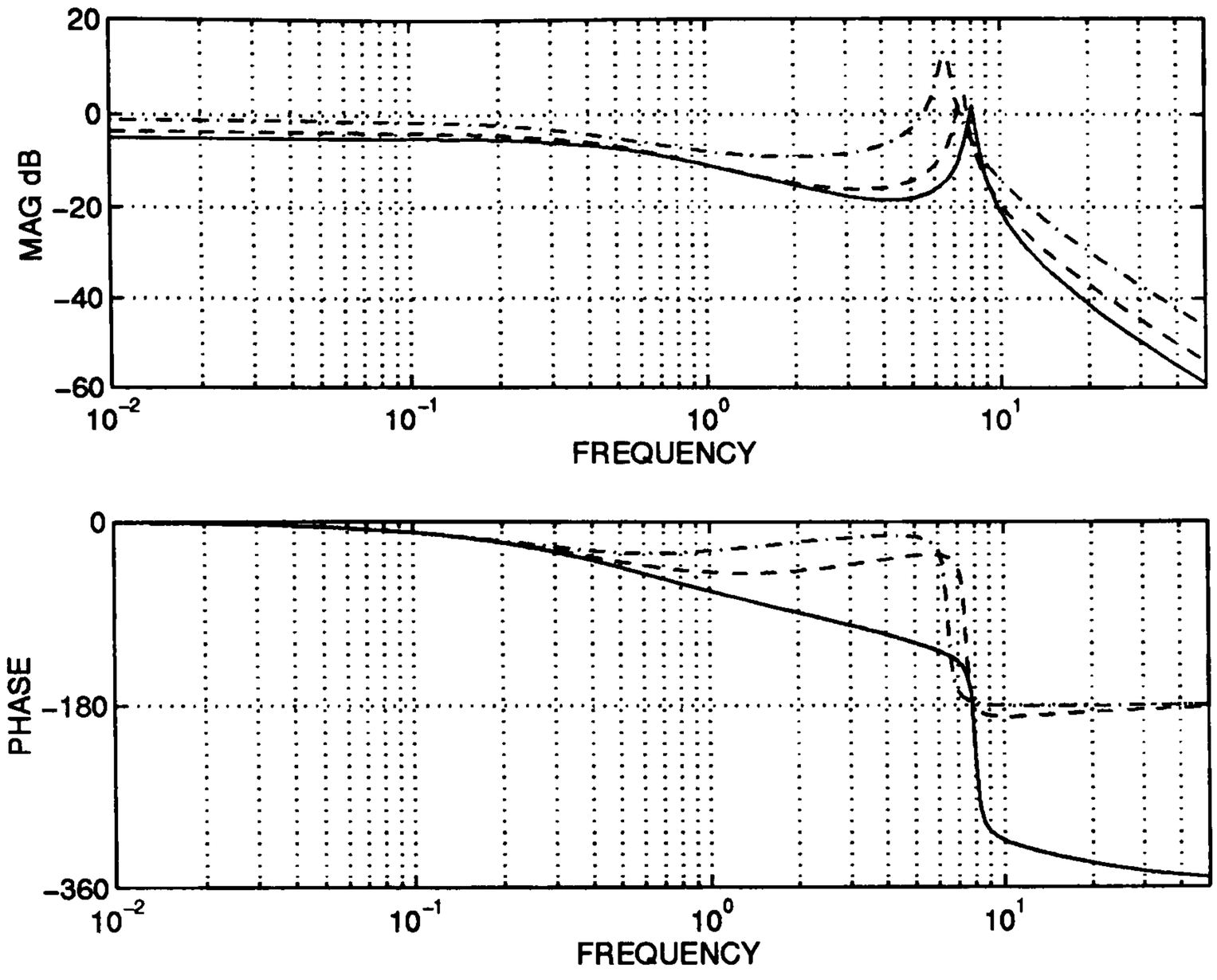

(−·−·−·−·) high, (− − − − −) medium, (————) low

Fig. 3.21 Nyquist and Bode plots of $\gamma(s)$ for third order models with 3 different value of inertia constant

It is observed that the highest value of the inertia constant increase the gain of $\gamma(s)$ at a lower frequency than smaller values. This indicates a decrease in stability robustness to model uncertainties forincreasing model inertia constant.

Final remark: The effect of changes of some parameters of synchronous machine models on the stability robustness of the turbogenerator to model uncertainties are summarised in Table 3.1 below

Parameter	Effect on stability robustness
Loading conditions	decrease with the increase of real power
Synchronous reactance	decrease with the increase of reactances
Damping constant	increase with the increase of damping
Inertia constant	decrease with the increase of inertia
Tie-line reactance	decrease with the increase of reactance

Table 3.1 Effect of parameters change on the stability

Chapter 4 : Control Options Available to Turbogenerator Systems

4.1- *Introduction*

Traditionally, the problem of power systems control is split into the two separate problems of excitation control and governor control; the design of excitation control systems and governor control systems are carried out independently. The turbine governor is designed assuming constant flux linkage, and is used to achieve set point regulation of the shaft speed, as in Fig. 4.1.

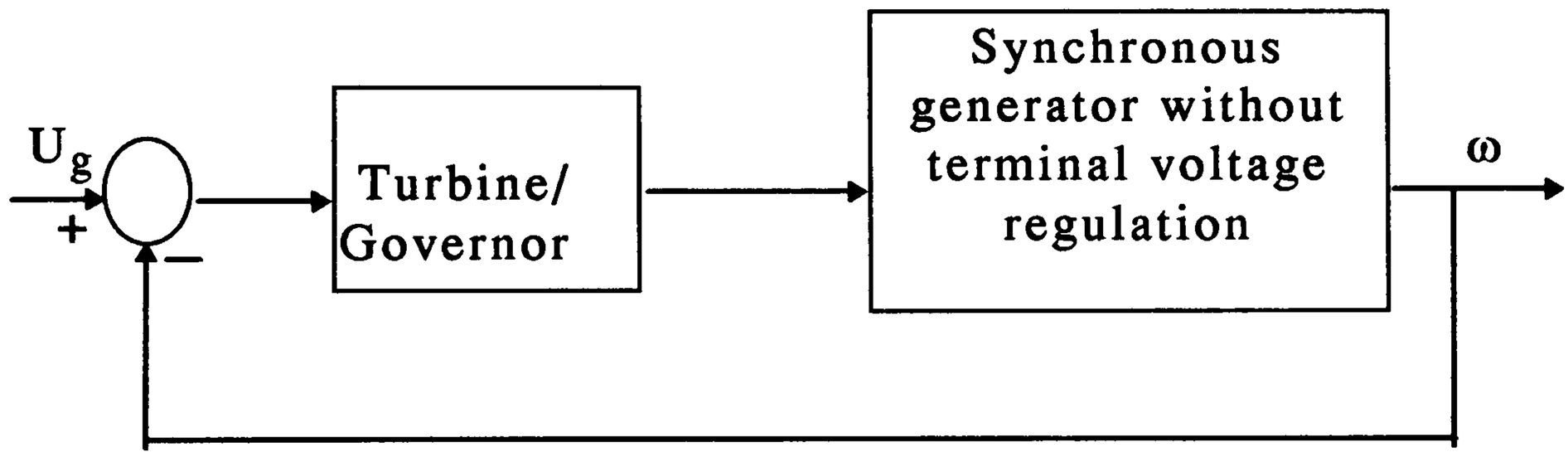

Fig.4.1 machine speed regulation

Subsequently, the excitation/AVR is designed, assuming constant mechanical torque input, and is used to achieve set point regulation of the generator terminal voltage, as in Fig. 4.2.

ω

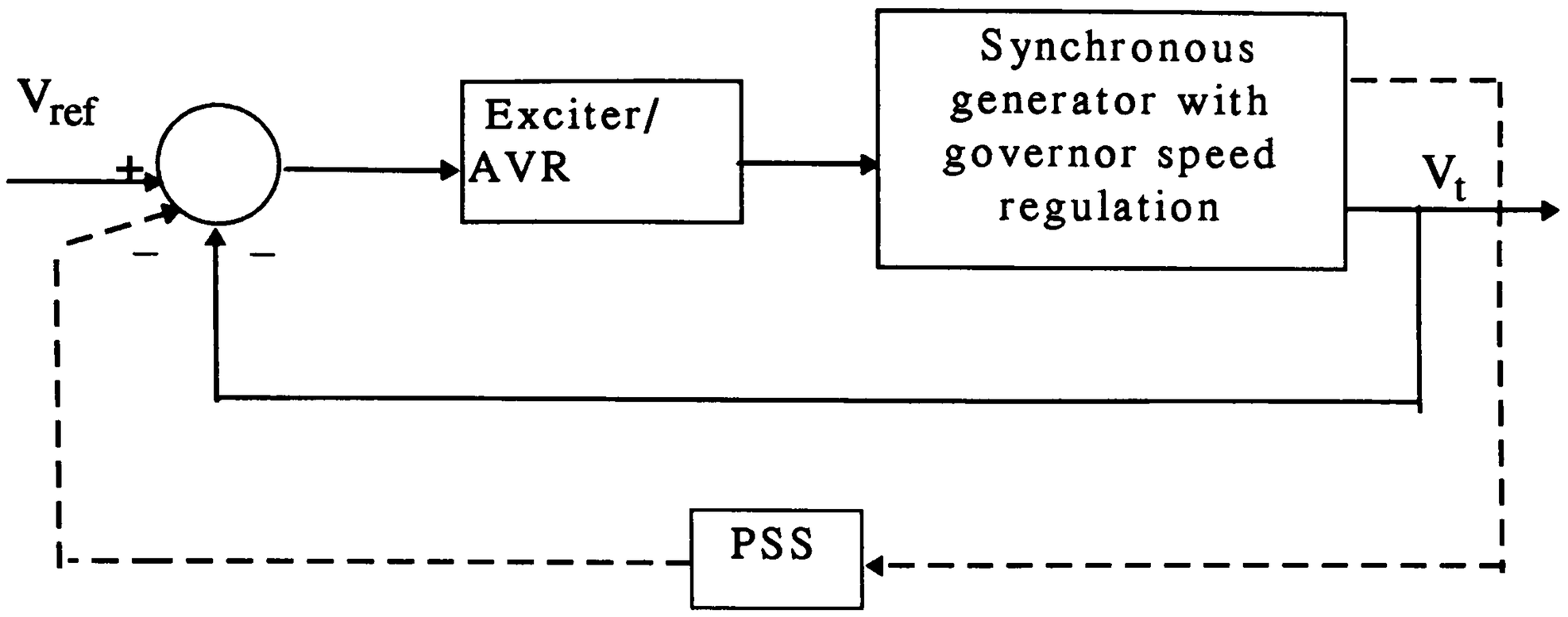

Fig.4.2 terminal voltage regulation

In other words, turbogenerator regulation is considered to consist of two single-input, single-output feedback systems. Speed regulation is typically required to be effective over a frequency range 0 to 1 rad/sec, avoiding subjection of the governor to higher-frequency signals. Voltage regulation is typically required to be effective over a frequency range 0 to 10 rad/sec, providing adequate voltage disturbance rejection.

However, an alternative interpretation is possible; specifically, turbogenerator regulation can be considered to consist of a single two-input, two-output feedback system where the overall structure of a one-machine turbogenerator system, connected to an infinite bus and incorporating excitation/AVR control, turbine/governor control together with a supplementary speed power system stabiliser (PSS), is as depicted in Fig. 3.10. (Nomenclature is as defined in Appendix 2). In the latter multivariable context,

three questions immediately arise: (a) to what extent is the single-loop regulation approach appropriate ; (b) what is the role of the PSS ; (c) are there other more suitable approaches to the regulation ? These questions are answered in the discussions of Options 1, 2 and 3 respectively in this Chapter.

4.2- *Multivariable analysis of turbogenerator regulation*

The 3-rd order model [24] is chosen at the operating point (P=0.9, Q=0.3) with a typical synchronous reactance of $\left(x_d = 1.81\,\text{pu},\ x_q = 1.76\,\text{pu and } x'_d = 0.3\,\text{pu}\right)$ with $x_e = 0.65\,\text{pu}$.

Substituting the values K1=0.7643, K2=0.8649, K3=0.323, K4=1.4187, K5=-0.1463, K6=0.4168 of [24] into Appendix (4), the 2-input 2-output machine transfer-function matrix of Fig. 3.11, at these conditions, is given by

$$\begin{bmatrix} g_{11} & g_{12} \\ g_{21} & g_{22} \end{bmatrix} = \begin{bmatrix} 974.168s + 377 & -1053.2 \\ -142.520s - 127.16 & 0.942s^2 + 0.424s + 54.2 \end{bmatrix} \qquad (4.1)$$

$$\Delta(s) = 18.088s^3 + 14.7452s^2 + 747.5566s + 138.724$$

The governor control, k_1 , of Fig. 3.11 is given by

$$k_1(s) = \frac{k_g}{s\left(1 + sT_g\right)\left(1 + sT_t\right)} \qquad (4.2)$$

where T_g is the governor value actuator time constant (0.2 sec), T_t is the steam turbine time constant (0.3 sec), and k_g is the governor loop gain (1). The excitation control, k_2, in Fig. 3.11 is provided by the fast response thyristor excitation system with the transfer function

$$k_2(s) = \frac{k_e}{(1+sT_e)} \tag{4.3}$$

where k_e is the regulator system gain (200) and T_e is the excitation system time constant (0.01 sec).

The governor control $k_1(s)$ of equation (4.2) is applied to regulate the machine speed, fig. 4.1; that is, the loop is closed round the turbine/governor subsystem $k_1 g_{11}(s)$ to yield the closed-loop subsystem $h_1(s)$ defined by equation (2.5).

Subsequent application of the exciter $k_2(s)$ of equation (4.3) to regulate the machine terminal voltage is examined through the frequency response of the excitation channel C_2 of equation (3.33) shown in Fig. 4.3. A simple approximation of the channel C_2 of equation (2.4) is however as follows. Since the turbine/governor channel is relatively slow with a bandwidth of about 1 rad/sec, the frequency response of the turbine/governor subsystem $h_1(s)$ of

equation (2.5) will have rolled off in the frequency of interest to the faster excitation channel C_2 in equation (2.4); that is, the excitation channel C_2 in equation (2.4) can be approximated by $k_2 g_{22}$ in the typical excitation channel frequency range of 1 to 10 rad/sec as shown in Fig. 4.3.

In effect, this is a formal confirmation of the observed fact that the slow governor loop has little effect on the faster exciter loop response and so the performance of the overall turbogenerator system is largely determined by that of the electrical subsystem transfer function $g_{22}(s)$ with input field voltage and output terminal voltage.

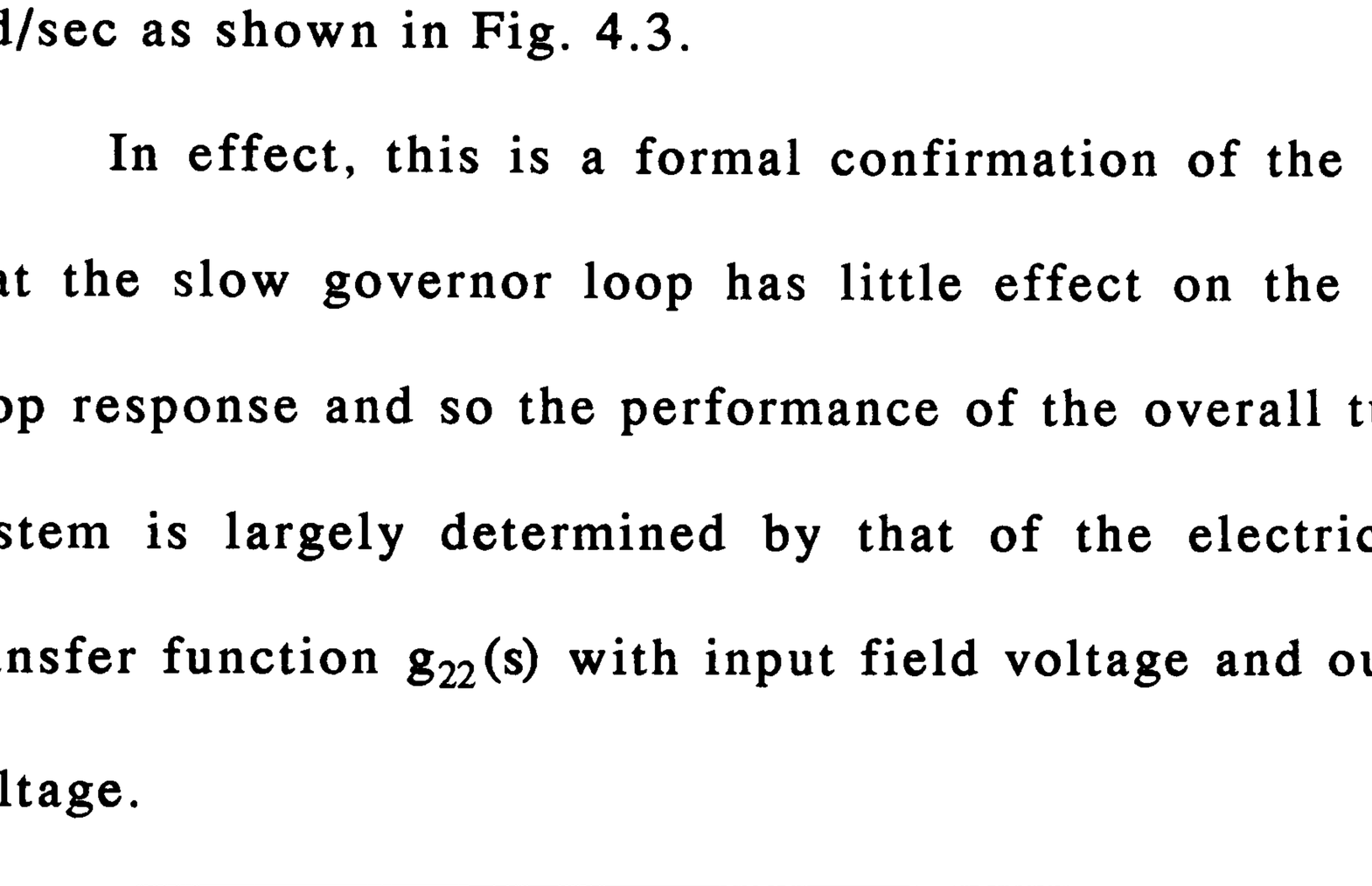

Fig.4.3 Bode plots of excitation channel (———) and the excitation channel approximation (— — — —)

Focusing therefore on the electrical subsystem $g_{22}(s)$, it is observed in Fig. 4.3 that its frequency response possesses the extremely awkward switch-back characteristic round 7 rad/sec of a resonance (lightly damped left-hand plane pole pair -0.31+j6.41) at 6.42 rad/sec closely followed by an anti-resonance (lightly damped left-hand plane zero pair -0.21+j7.58) at 7.58 rad/sec.

This is the fundamental problem that besets the control of a turbogenerator set; not the presence of the lightly damped left-hand plane (LHP) pole pair or lack of system damping [22] *per se* but the close proximity to these poles of the lightly damped LHP zero pair; an interesting similar conclusion is also arrived at by Hamdan and Hughes [28] using pole-zero analysis. Any attempt to apply direct control, active over a frequency range including 7 rad/sec to the electrical subsystem $g_{22}(s)$ would be problematic because of the LHP zero pair closely following the LHP pole pair implies a need for unrealistically precise knowledge of the dynamics (recall the variation with choice of model observed in Figs.3.14-3.19). Indeed, the closed-loop response for either k_2g_{22} or $k_2g_{22}(1-\gamma h_1)$ would be unstable as may be observed from Fig. 4.3. Furthermore, the frequencies of these pole-zero pairs change with the loading condition, choice of reactances .....etc., (see

Figs. 4.5, 4.6, 4.7), making direct control that might cater for more than one loading condition impossible.

Taking the adverse switch-back characteristic of the electrical subsystem frequency response in Fig. 4.3 into account, among the various control options that may be considered, two options that demand scrutiny from the point of view of past and present power engineering practice are excitation/governor control without PSS and excitation/governor control with PSS. For completeness, a new third option is also considered, excitation/governor control only with swapped input/output pairings.

Before examining the first two options, observe that, since the high-frequency limit of $\gamma(s)$, shown in Fig. 4.4 is less than one, Result 4.3 of [68] establishes the existence of stable minimum phase stabilising controllers for the two channels. Also, when as here, see Chapter 2, there is a separation of bandwidths between excitation channel and governor channel, the controller, $k_2(s)$, for the higher bandwidth channel, namely the excitation channel, is determined essentially by $g_{22}(s)$.

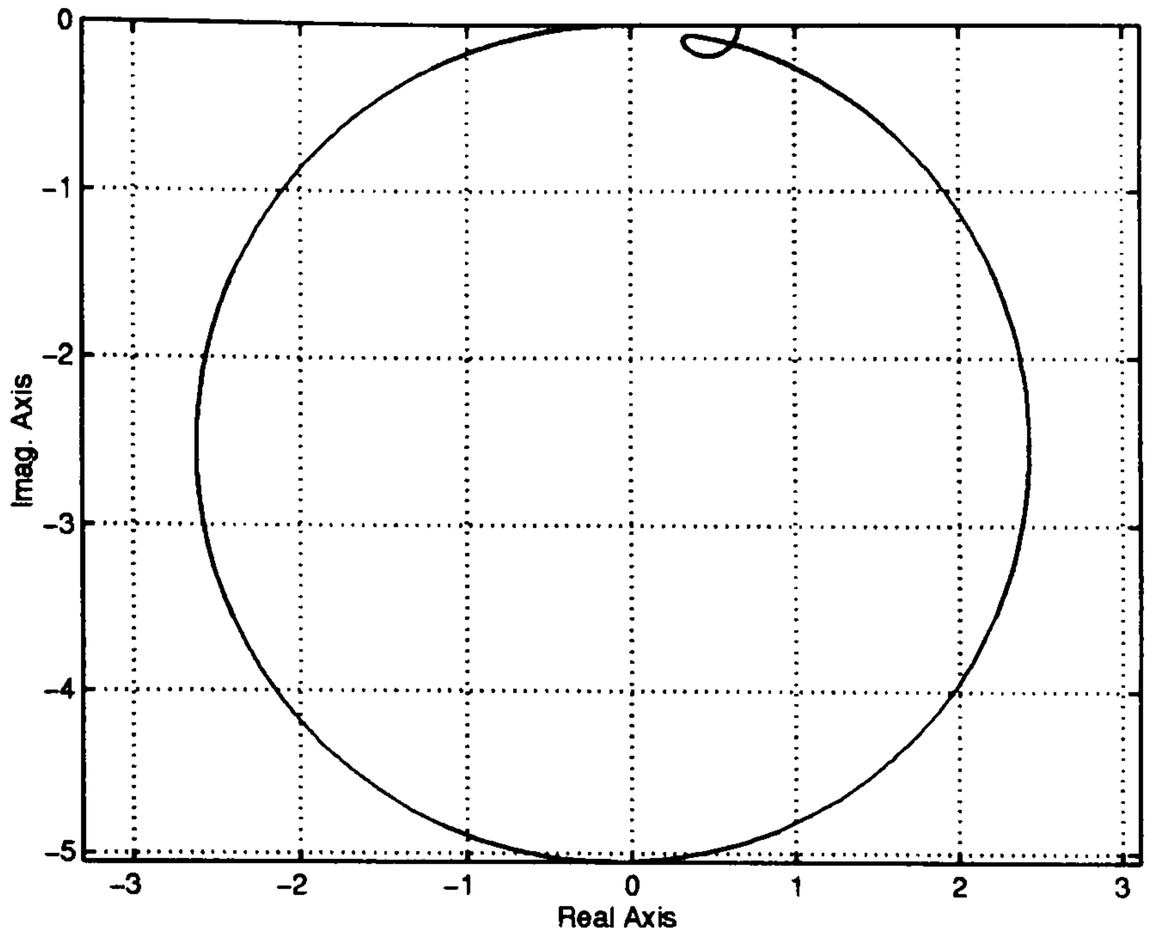

Fig. 4.4 Nyquist plot of $\gamma(s)$ of the model of equation (4.1)

4.3- *Factors affecting the switch-back characteristics*

(i) Loading conditions :

Two different loading conditions, low (P=0.6, Q=0.4), and high (P=0.9, Q=0.4) are chosen as in Ahson and Nicholson [69]. The machine has a synchronous reactance x_d=1.6 pu, and x_q=1.55 pu.

Polar plots of the electrical subsystem $g_{22}(s)$ for these different loading conditions are shown in Fig. 4.5 where it is observed that a switch-back characteristic is created with increasing real power (loading condition).

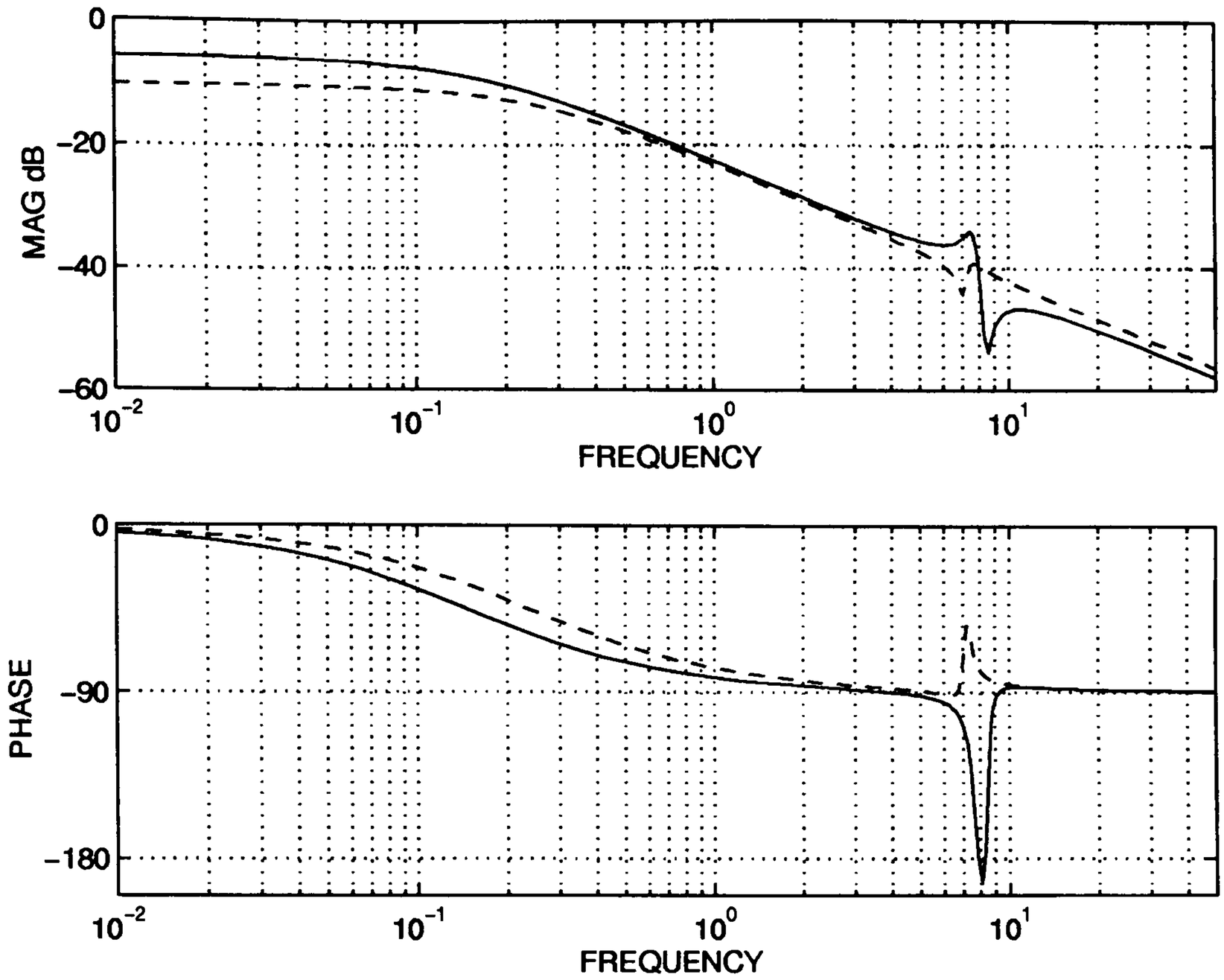

Fig. 4.5 Bode plot of electrical subsystem $g_{22}(s)$ transfer function for different loading conditions, low (- - - - -), and high (————)

(ii) Synchronous reactance :

Two different values of synchronous reactance are considered; namely synchronous reactance x_d=1.6 pu, and x_q=1.55 pu [69], and synchronous reactance x_d=2.6 pu, and x_q=2.6 pu [28]. The machine has a low operating conditions and is connected to a strong transmission line.

Polar plots of the electrical subsystem $g_{22}(s)$ are shown in Fig. 4.6 where it is observed that the switch-back characteristic gets

worse for increasing model synchronous reactance, in the sense that higher gain and phase advance are required to overcome its effect.

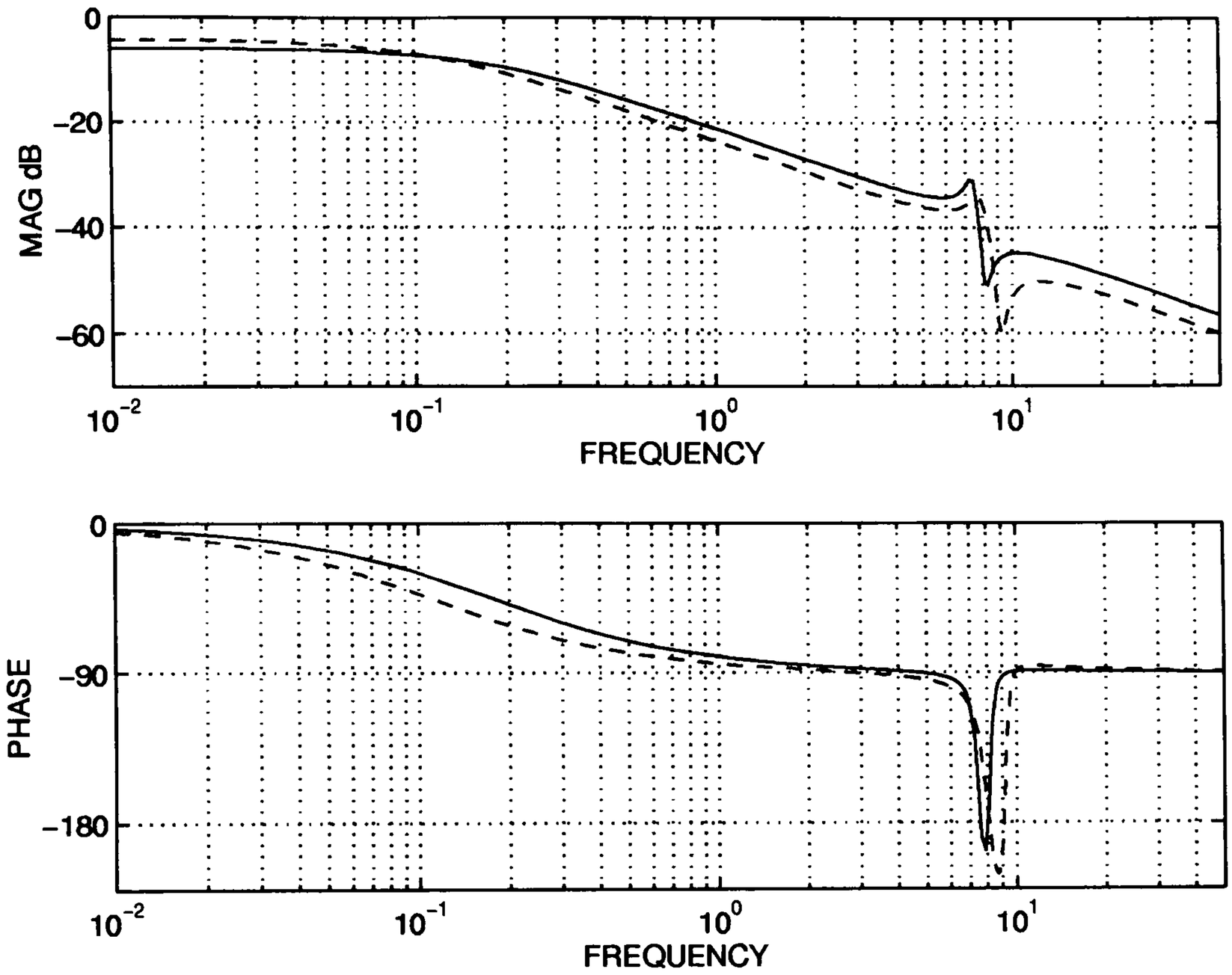

Fig. 4.6 Bode plot of electrical subsystem $g_{22}(s)$ transfer function for different synchronous reactance, (——) small, and (– – –) large

(iii) Tie-line reactance:

Finally, the tie-line reactance x_e is changed from 0.2 pu, to 0.8 pu [51]. The generator is operated under lagging power factor, light loading conditions. The infinite-bus voltage and current flowing into the grid system are considered constant. The synchronous reactance of the generator is x_d=1.445 pu, x_q=0.959 pu; and the terminal voltage V_t=1.0 pu, with a damper winding

D=3 pu. Polar plots of the electrical subsystem $g_{22}(s)$ for these two different values of tie-line reactance are shown in Fig. 4.7 where it is observed that the switch-back characteristic occurs at lower frequency in the weak tie-line case with more gain and phase advance required to overcome its effect.

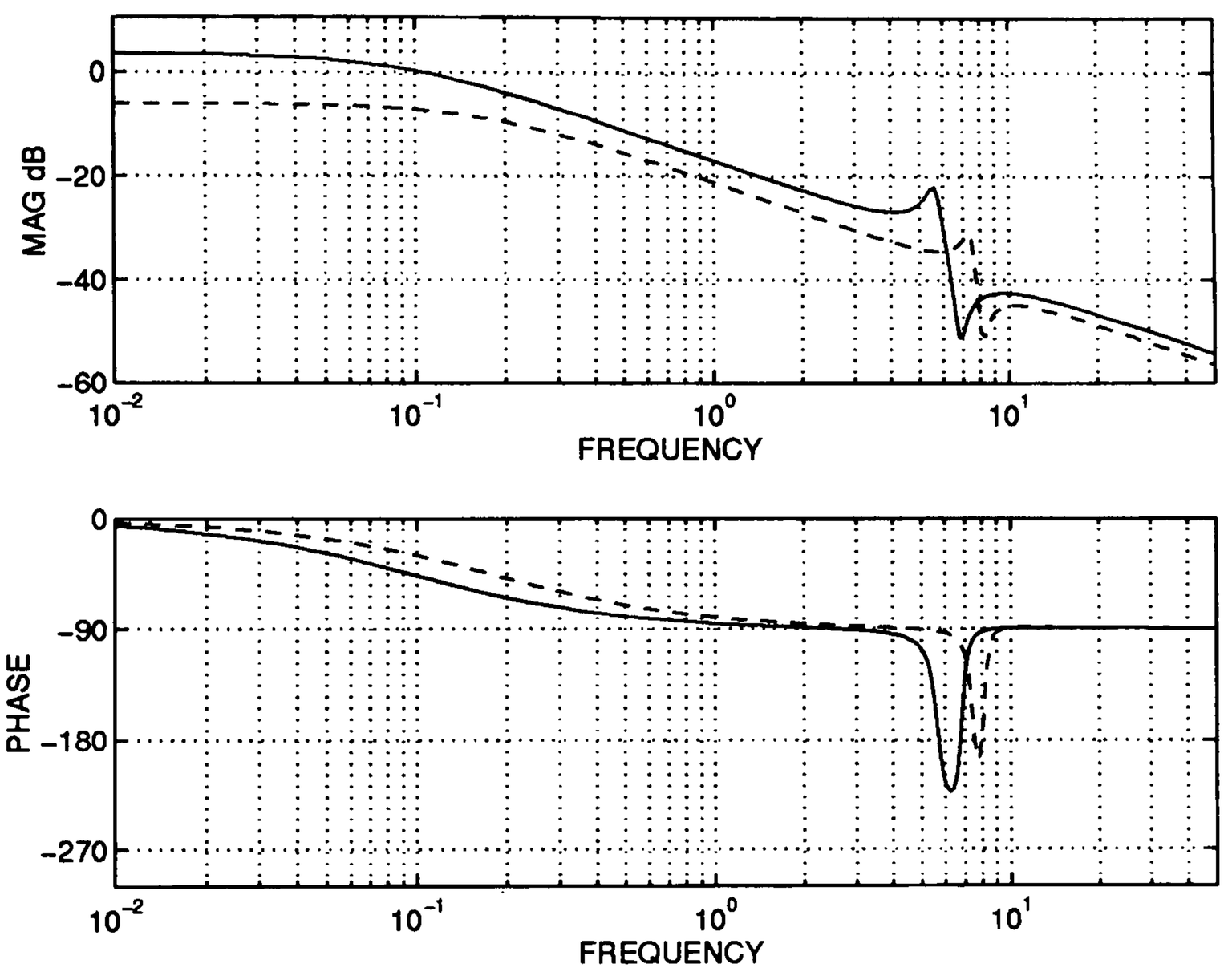

(————————) weak, (– – – – – – –·) strong

Fig. 4.7 Bode plot of electrical subsystem $g_{22}(s)$ transfer function for 2 different tie line connections

Like the decrease in stability robustness to model uncertainties, the switch-back characteristic worsen with machines having higher synchronous reactances, and small number of damper windings, working at higher operating conditions (high real power),

while connected to weak transmission lines. Taking this adverse switch-back characteristic of the electrical subsystem frequency response into account, and using the model in (4.1) and the governor control and excitation control of (4.2) and (4.3) respectively; the control options available to turbogenerator systems are described below .

4.4- *Control option 1 : Excitation/governor control without PSS*

One way of avoiding the problematic switch-back characteristic of the electrical subsystem frequency response at 7 rad/sec is to restrict the bandwidth (open-loop gain crossover frequency) of the excitation channel to be relatively low, say 3 rad/sec. This is achieved by using a slower response excitation system $k_2(s)$ defined by the transfer function of equation, (4.3) where $k_e = 200$ and $T_e = 0.01$, in cascade with the transient gain reduction [11] given by $m(1+sT_1)/(1+sT_2)$ where m=0.06533, T_1=0.7542 and T_2=0.3367. The governor control $k_1(s)$ of equation (4.2) is as before. The resulting frequency responses of the turbine/governor channel C_1, given by equation (2.1), and the

excitation channel C_2, given by equation (2.4), are shown in Fig. 4.8 and Fig. 4.9 respectively.

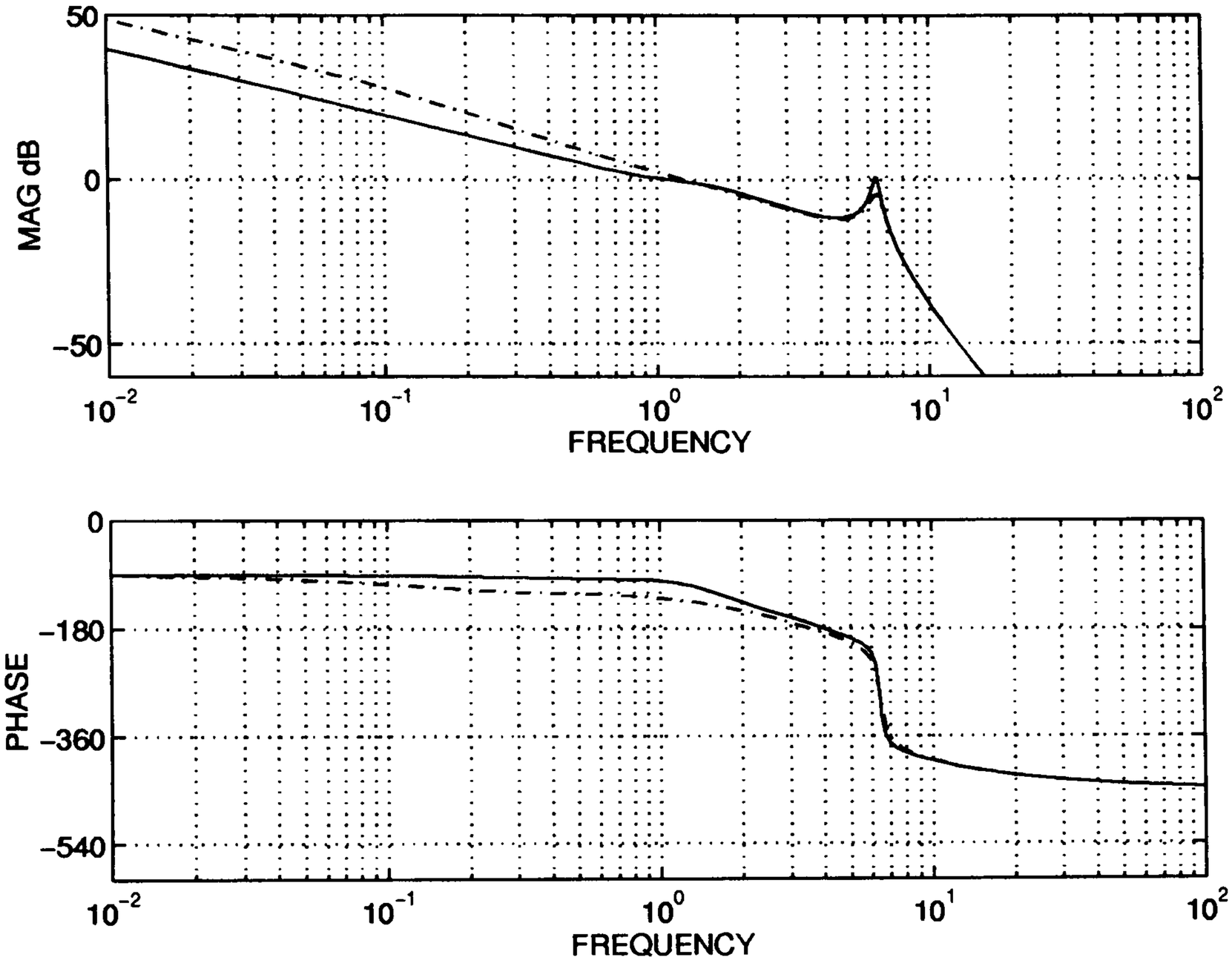

(————) $C_1 = k_1 g_{11}(1 - \gamma h_2)$

(– · – · – ·) $k_1 g_{11}$

Fig. 4.8 Bode plots of the turbine/governor channel without PSS (Option 1).

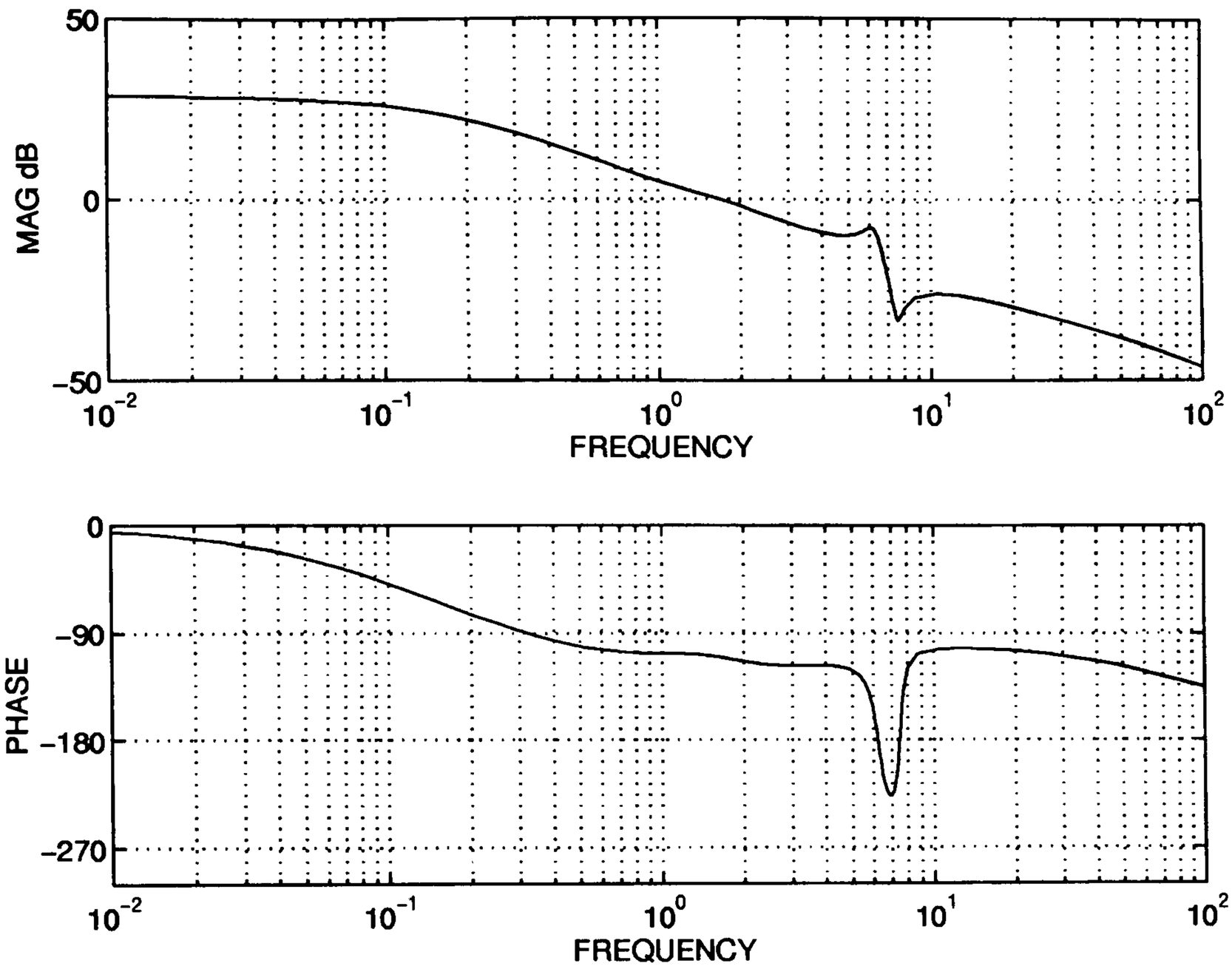

Fig. 4.9 Bode plots of the exciter channel without PSS (Option1)

Comparison of the frequency response of the turbine/governor open-loop channel C_1, given by equation (2.1), with that of the turbine/governor open-loop subsystem $k_1 g_{11}(s)$ in Fig. 4.8 (dashed-lines) show them not to be significantly different over the frequency range of interest (0 to 1 rad/sec).

This, together with the discussion immediately prior to Section 4.3, justifies the original approach of considering the turbogenerator system to consist of two single-input single-output feedback systems, see Section 4.2. The corresponding step

responses of speed and terminal voltage are shown in (Figs. 4.10, 4.11) and are quite satisfactory.

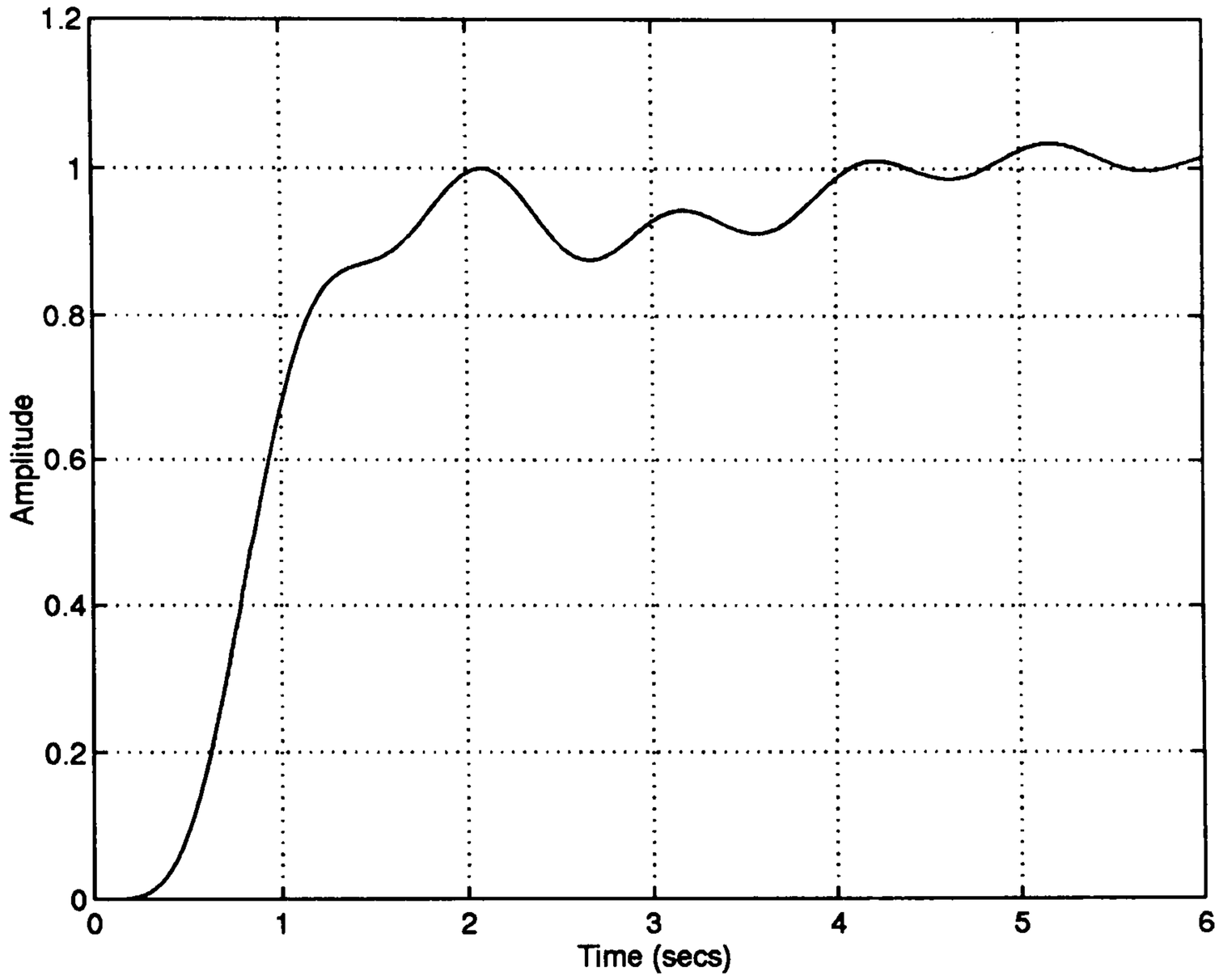

Fig. 4.10 Step response of the system without PSS : speed output (Option 1)

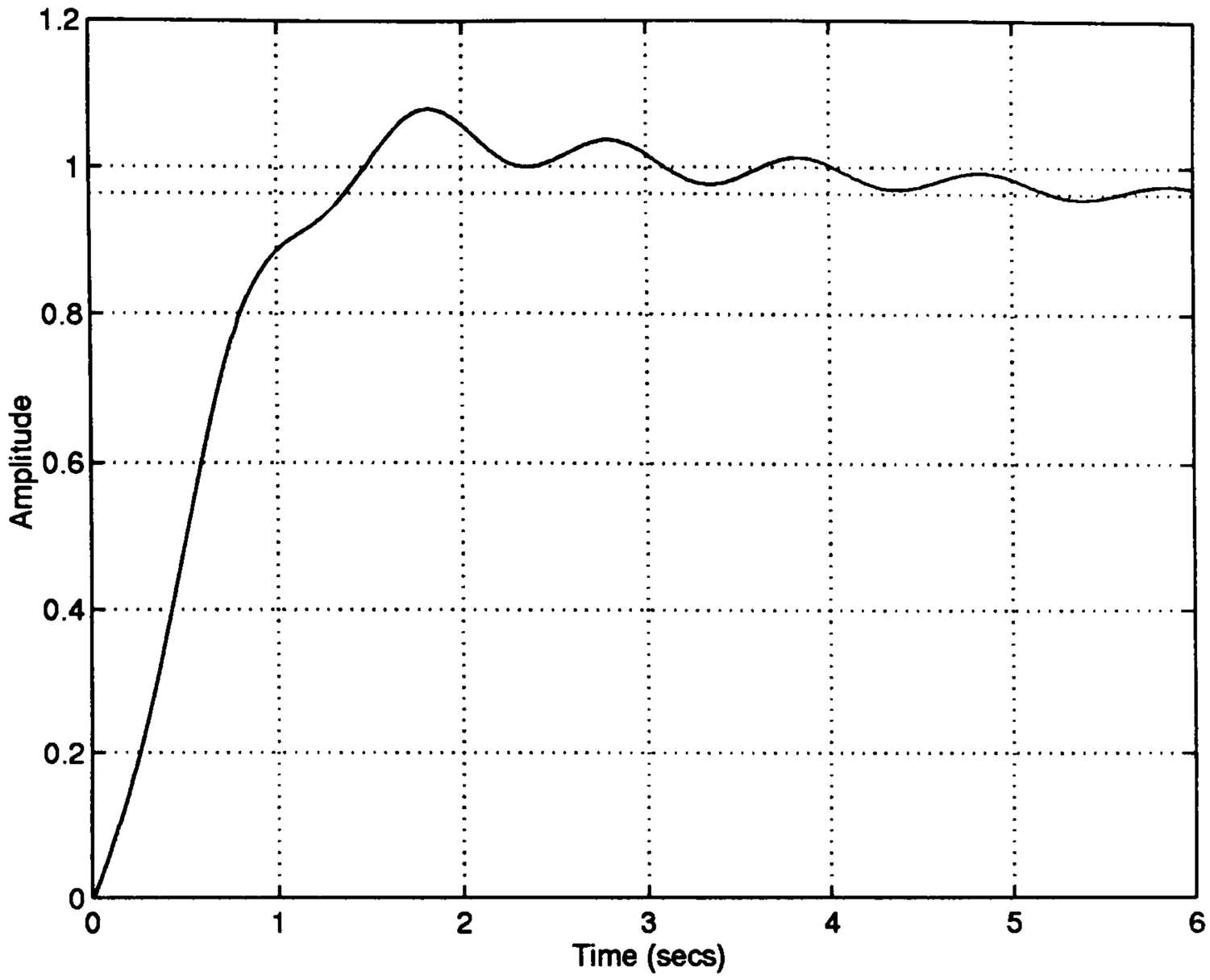

Fig. 4.11 Step response of the system without PSS: terminal voltage output. (Option 1)

Thus, if set point regulation of the shaft speed (channel C_1) and terminal voltage (channel C_2) are the only control requirements, then the relatively low channel C_2 bandwidth of 3 rad/sec suffices, without need of a PSS. This first control option was the option taken with smaller machines and smaller per unit synchronous reactance before the introduction of the PSS in the early 1960's [70].

Control option 1 does however have a major disadvantage highlighted by the terminal voltage output response to 10% voltage disturbance in Fig. 4.12.

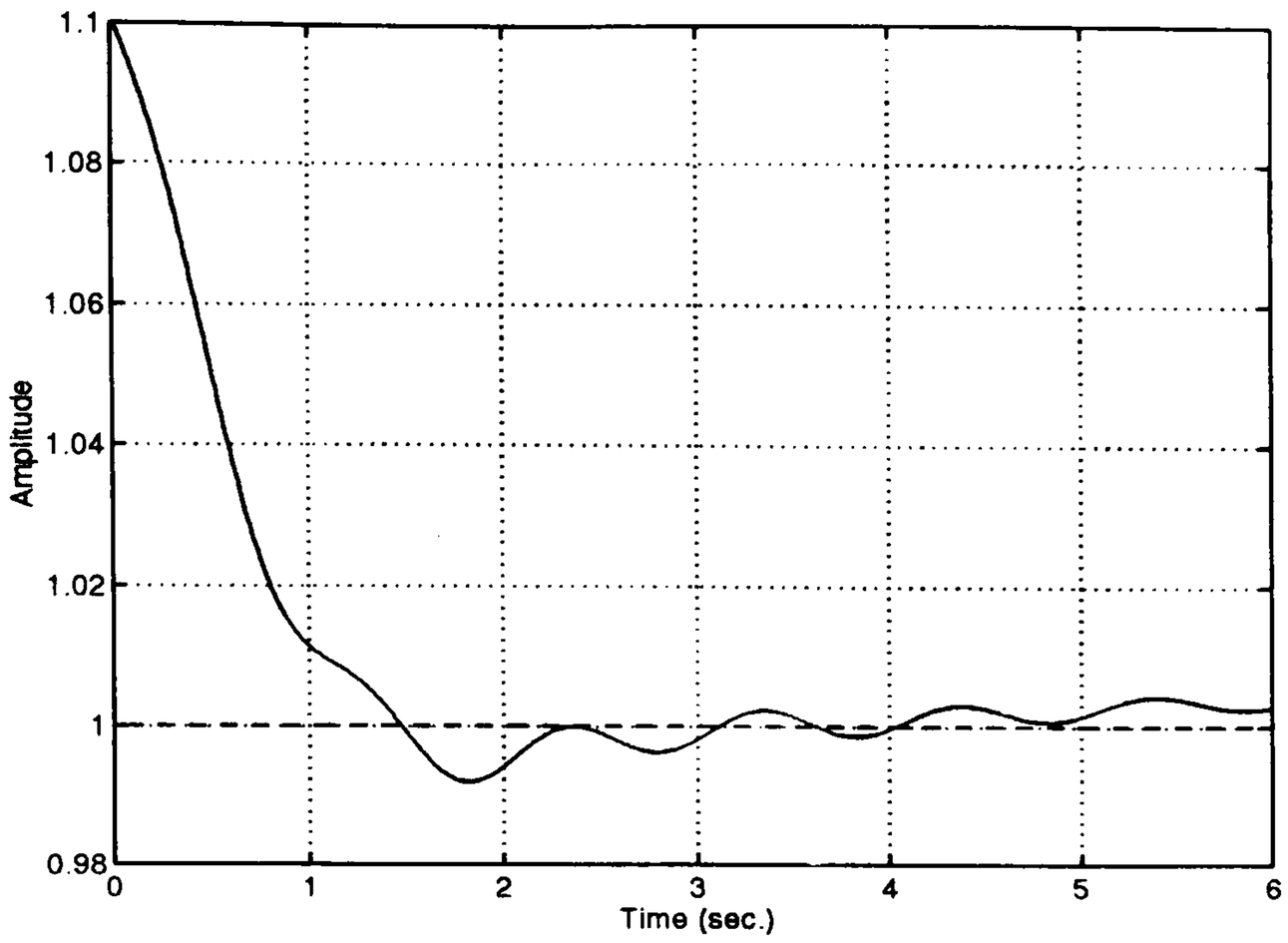

Fig. 4.12 Terminal voltage output response to 10% voltage disturbance (Option 1).

This is corroborated by the Bode diagram of the sensitivity function $1/(1+C_2)$ of the excitation channel shown in Fig. 4.13.

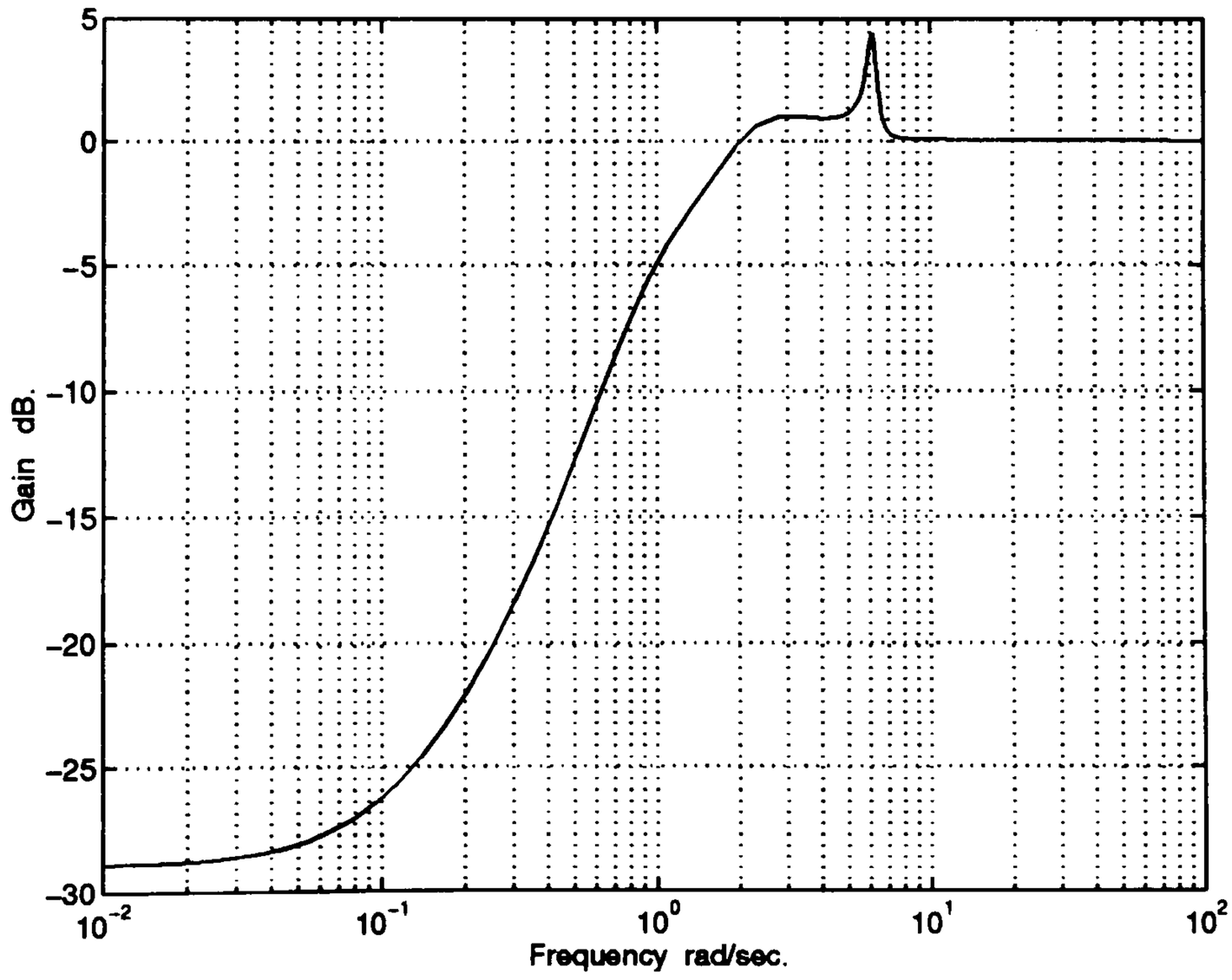

Fig. 4.13 Bode plot of the sensitivity element $\frac{1}{1+C_2}$ without PSS. (Option 1).

This disadvantage of Control option 1 lies in the relatively poor sensitivity disturbance rejection properties of the closed-loop excitation channel over the latter part of the frequency range 0 to 10 rad/sec.

4.5- *Control option 2: Excitation/governor control with PSS*

The second control option is to seek an excitation channel C_2 bandwidth of roughly 10 rad/sec. Unlike Control option 1, this specification is compatible with a control requirement to provide strong voltage disturbance rejection over the frequency range 0 to 10 rad/sec. However, the presence of the lightly damped LHP zero pair near 7 rad/sec, shown in the frequency response of Fig. 4.3, prevents the use of such a high-bandwidth excitation channel as discussed under Control option 1.

Let us now explore how the additional use of the PSS in Fig. 4.2 might alleviate these two seemingly irreconcilable control features : the high bandwidth for disturbance rejection and the presence of the switch-back frequency response characteristic round 7 rad/sec. From Fig. 4.2, it is observed that the PSS acts as a post-compensator on the speed output, so that taking Fig. 3.11 or

equation (4.2) into account, the system with PSS assumes the post-compensated form

$$G'(s) = P(s)G(s)$$
$$= \begin{bmatrix} 1 & 0 \\ p & 1 \end{bmatrix} \begin{bmatrix} g_{11} & g_{12} \\ g_{21} & g_{22} \end{bmatrix} \qquad (4.4)$$
$$= \begin{bmatrix} g_{11} & g_{12} \\ g_{21}+pg_{11} & g_{22}+pg_{12} \end{bmatrix} = \begin{bmatrix} g'_{11} & g'_{12} \\ g'_{21} & g'_{22} \end{bmatrix}$$

where, in the post-compensator matrix P(s), the cross-coupling element p(s) denotes the transfer-function of the PSS given by [22]

$$p(s) = k_s \frac{sT_w}{1+sT_w}\left[\frac{1+sT_3}{1+sT_4}\right] \qquad (4.5)$$

where $sT_w/(1+sT_w)$ denotes a washout filter (T_w=1.4) and $\left[(1+sT_3)/(1+sT_4)\right]$ denotes a phase advance compensator (T_3=0.145, T_4=0.03) and k_s =9.5 denotes the stabiliser gain. The governor control $k_1(s)$ and the excitation system control $k_2(s)$ are as defined as before in equations (4.2) and (4.3).

In equation (4.4), the PSS transfer function p(s) multiplies the benign $g_{12}(s)$ subsystem transfer function which contains no lightly damped LHP zeros, so causing the electrical subsystem transfer function $g_{22}(s)$ to be amended to $g_{22}+pg_{12}$. Comparing the frequency responses of $g_{22}+pg_{12}$ to those of $g_{22}(s)$, in Fig. 4.14, it is observed that the effect of the inverted notch characteristic of

the PSS, p(s), in equation (4.5), multiplied by the benign system dynamics, $g_{12}(s)$, is to dominate the problematic switch-back characteristic of $g_{22}(s)$ at 7 rad/sec. It should be noted that this approach is effective for different loading conditions, see Fig. 4.15, because the dynamics of the turbogenerator itself are exploited.

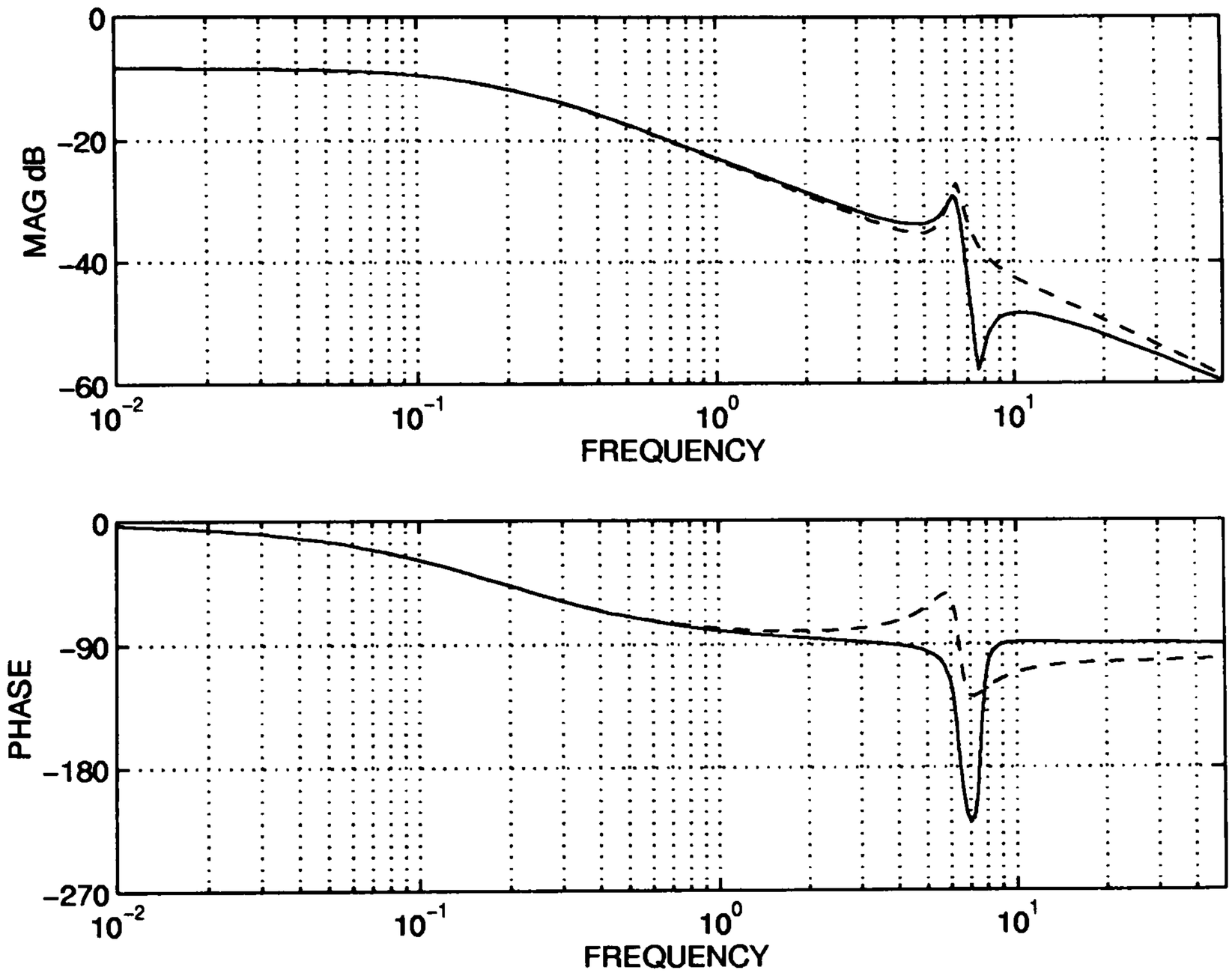

Fig. 4.14 Bode plot of $g_{22}+pg_{12}$ and $g_{22}(s)$

Working with the amended electrical subsystem $g_{22}+pg_{12}$ instead of the original electrical subsystem $g_{22}(s)$, the PSS thereby facilitates in a most ingenious way the use of a high-bandwidth excitation channel. Essentially, an artificial system output is created which is the weighted sum of the terminal voltage and the

shaft speed output. At low and high frequency, the artificial output is essentially the terminal voltage as desired; at frequencies close to that of the LHP pole-zero pairs of $g_{22}(s)$ at 7 rad/sec, the artificial output is dominated by the speed output.

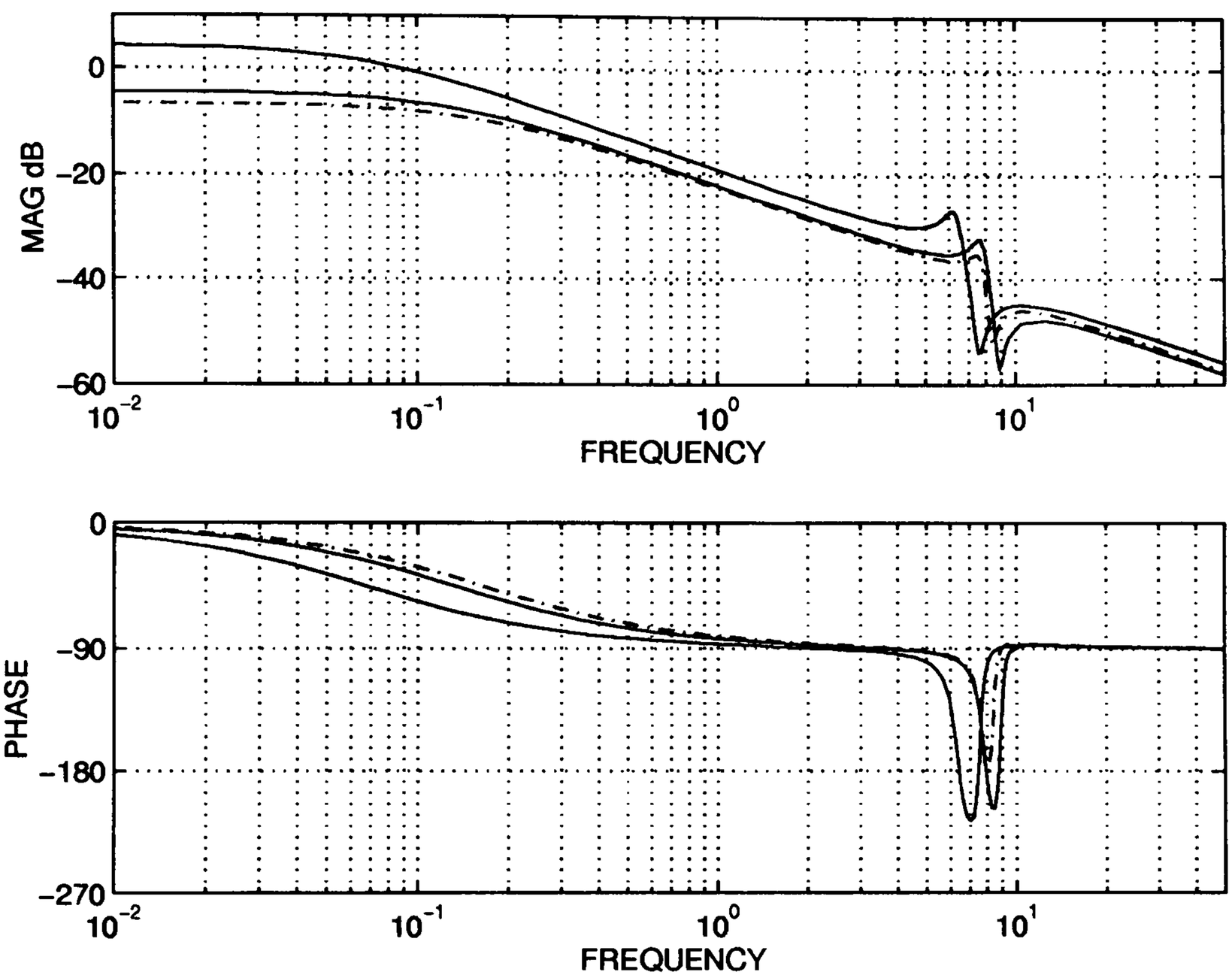

Fig. 4.15a Bode plots of the electrical subsystem g_{22} for three different loading conditions

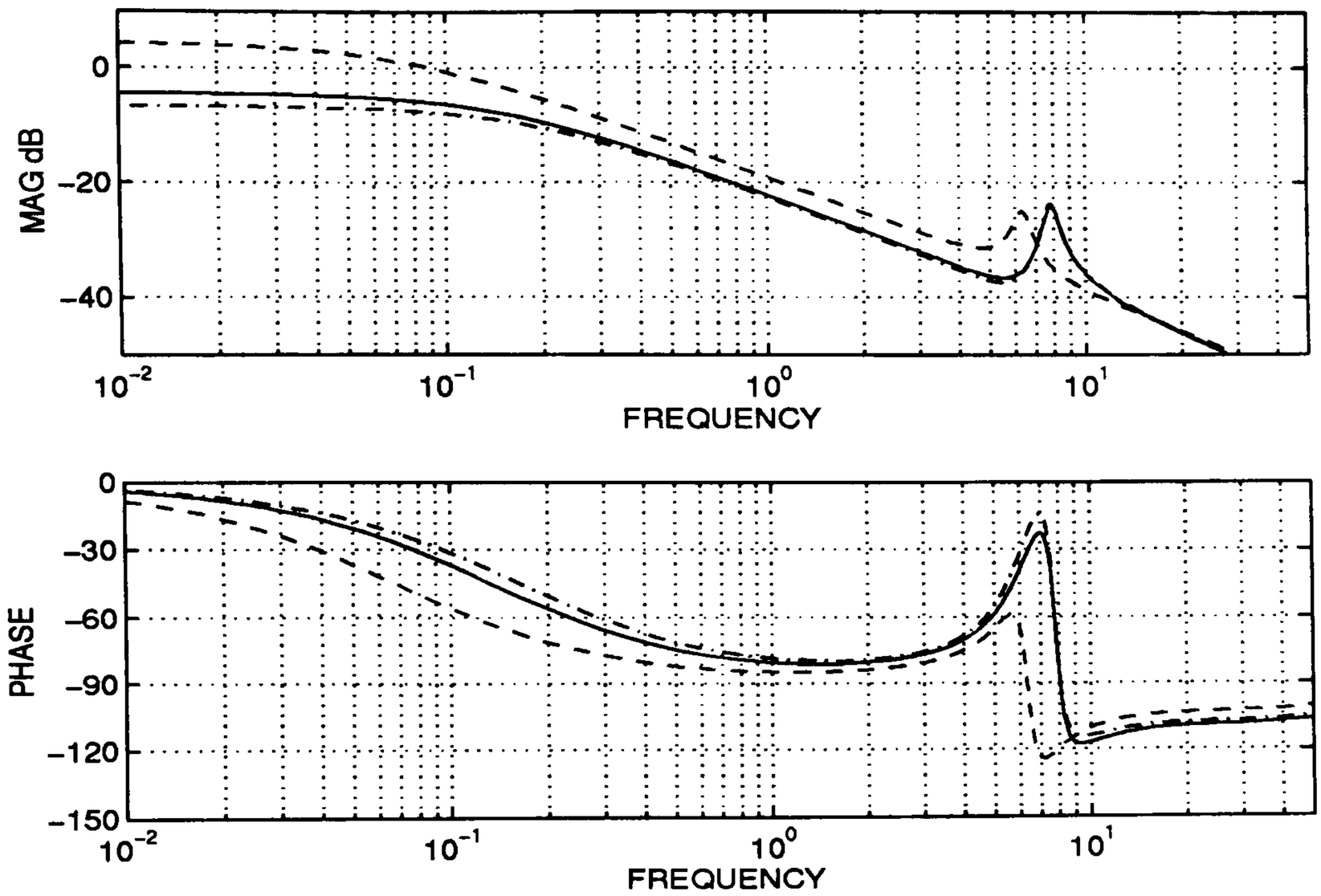

Fig. 4.15b Bode plots of the electrical subsystem $g_{22} + pg_{12}$, for different loading conditions.

The resulting frequency responses of the turbine/governor channel C_1 and excitation channel C_2 with PSS are shown in Fig. 4.16 where they may be compared to those of the lower frequency channel C_1 and C_2 without PSS in Fig. 4.9-10. The step responses of the terminal voltage and shaft speed are seen in Fig. 4.17 to be quite satisfactory with little detrimental effect on the terminal voltage step response caused by the creation of the artificial speed output near 7 rad/sec in the frequency response.

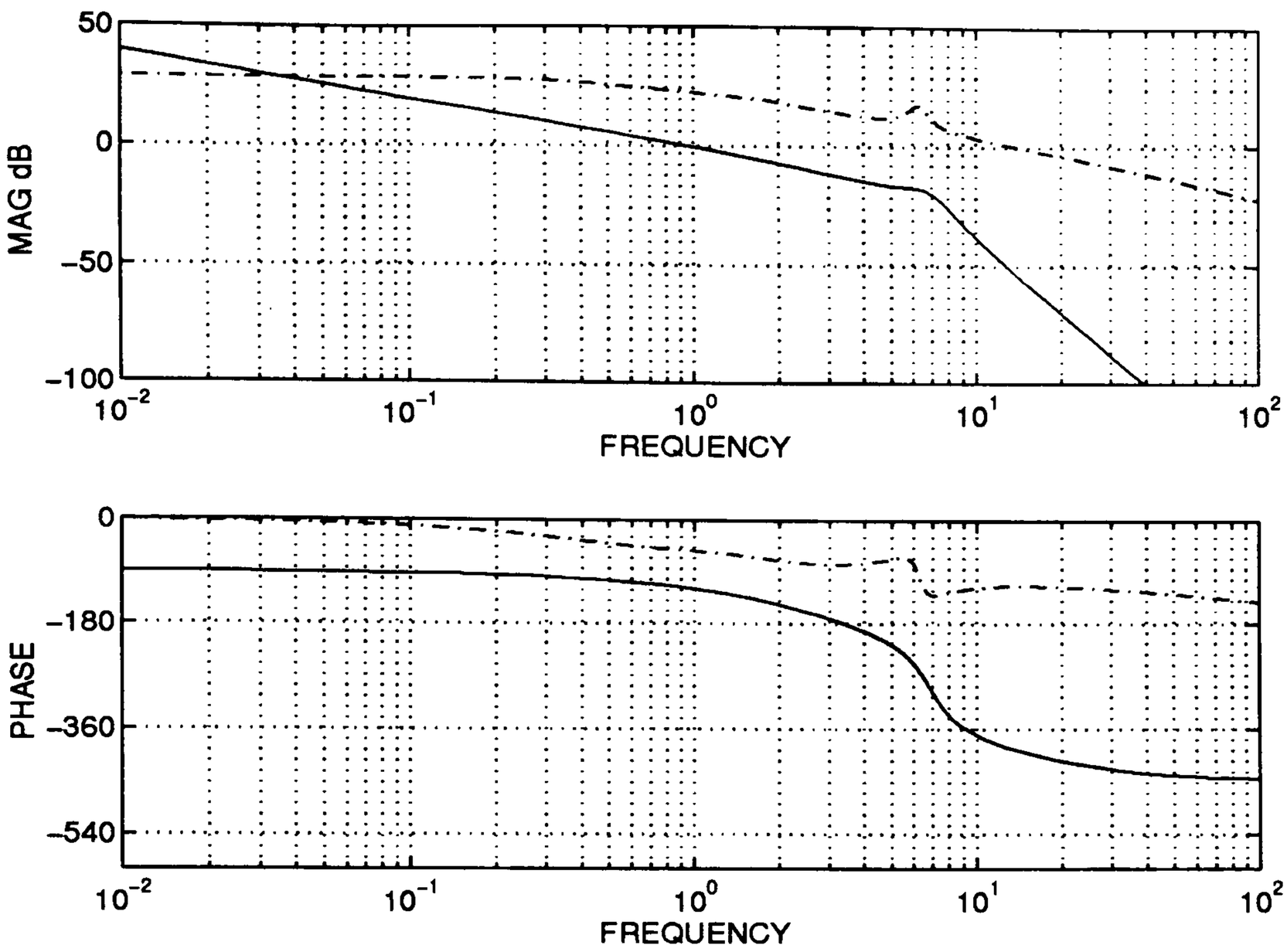

Fig. 4.16 Bode plots of the turbine/governor channel C_1 (———), and the exciter channel C_2 (– · – · – · –) with PSS (Option 2).

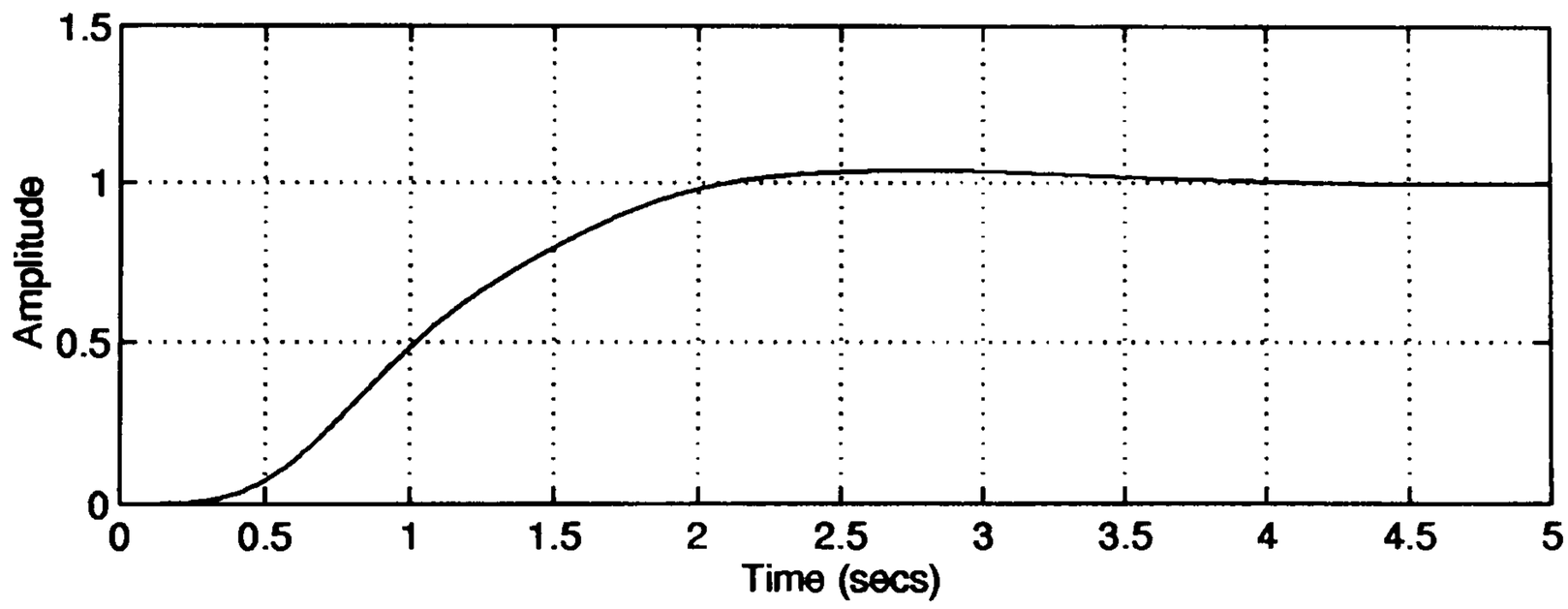

Fig. 4.17 Step response of the system with PSS , (a) speed output, (b) terminal voltage output.(Option 2).

It is observed in Fig. 4.17 that the step response of the excitation channel C_2 with PSS is still somewhat oscillatory. This is not due to lack of damping in the closed-loop system since in Fig. 4.16, the phase margin of the open-loop channel C_2 is observed to be above 60^o; rather, the oscillation is due to the residual effects of the open-loop system poles. The terminal voltage output response to 10% voltage disturbance, in Fig. 4.18, is observed to be much superior to that of Fig. 4.12 without PSS as is the Bode diagram of the sensitivity function $1/(1+C_2)$ of Fig. 4.19.

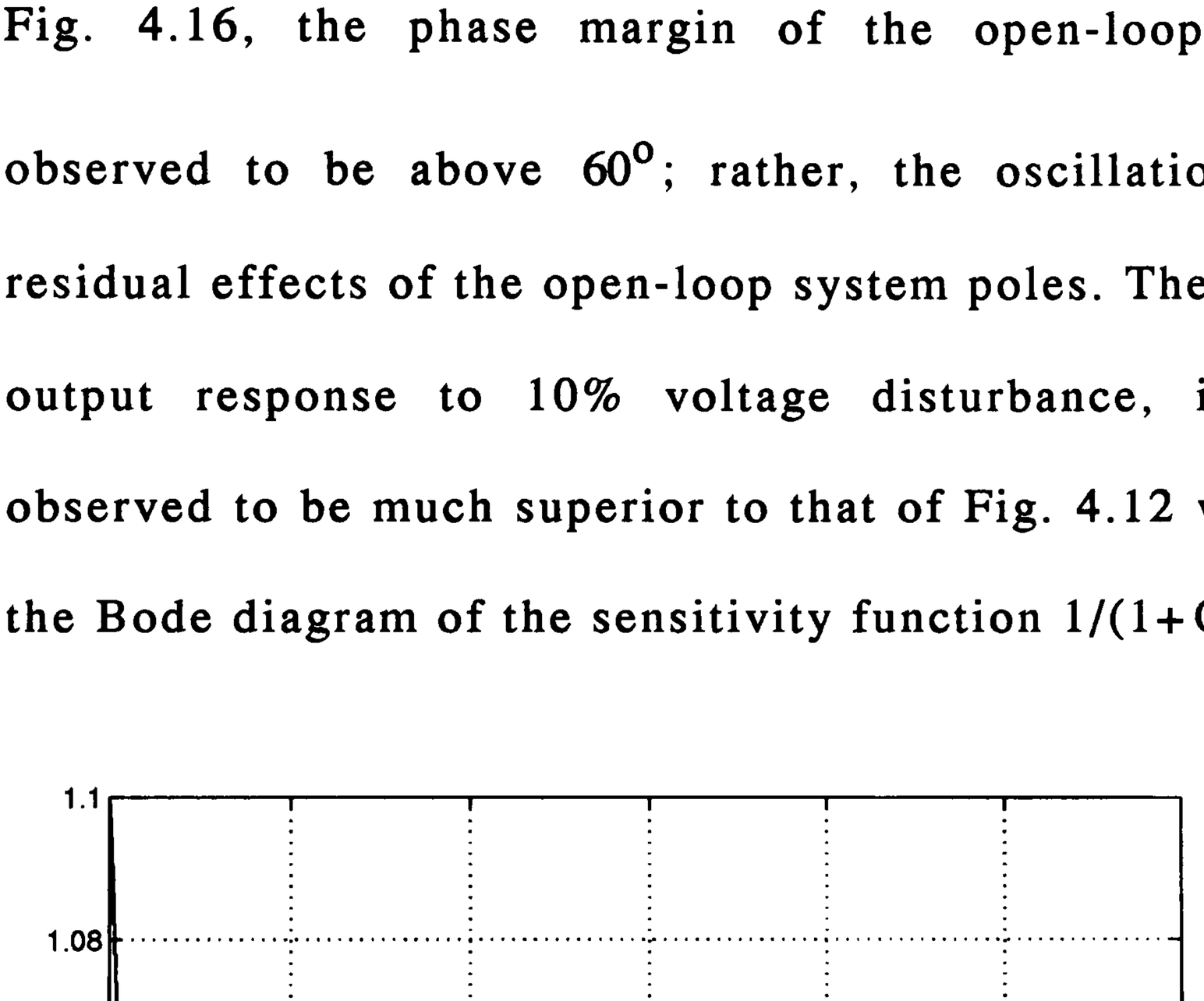

Fig. 4.18 Terminal voltage output response to 10% voltage disturbance (Option 2)

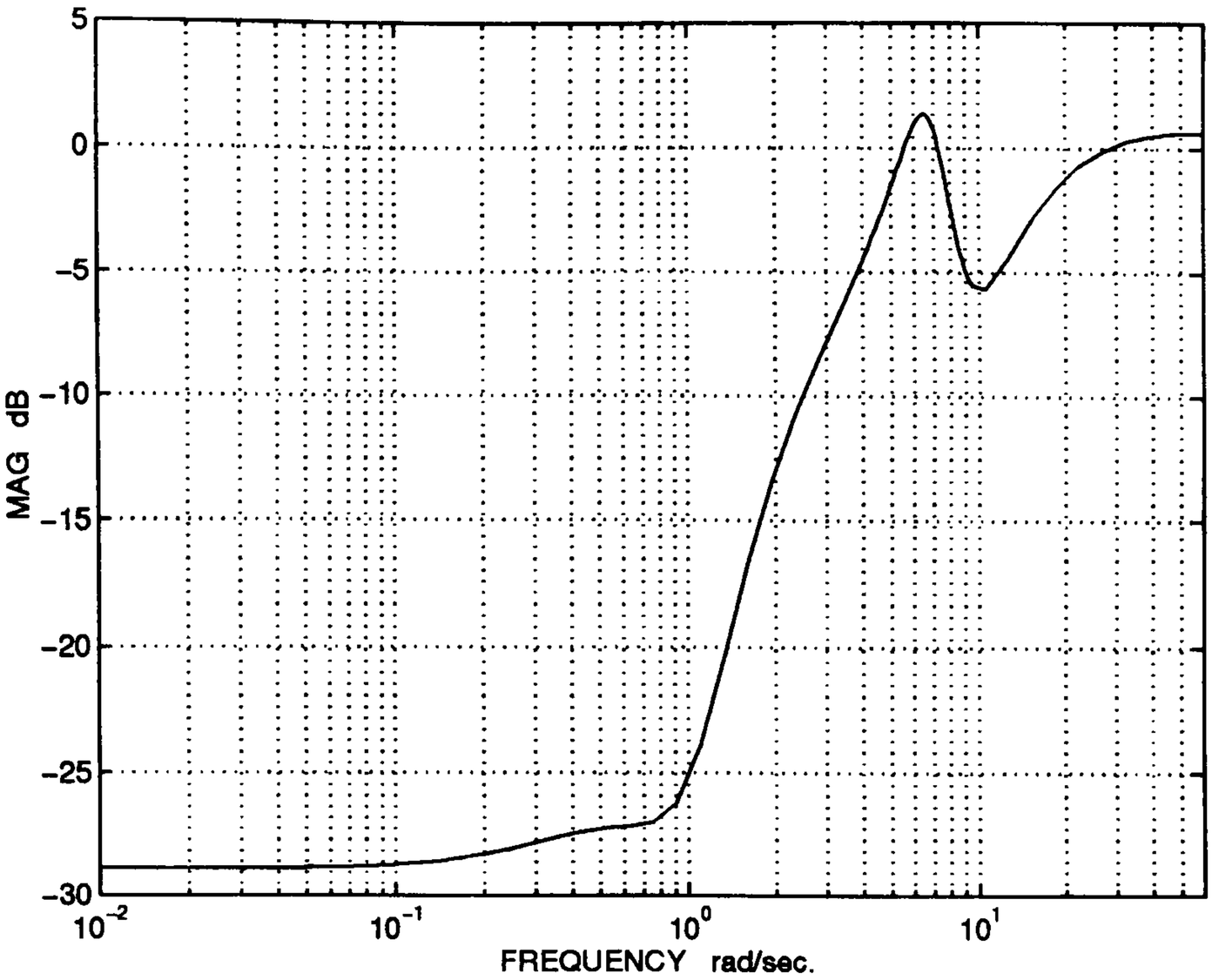

Fig. 4.19 Bode plot of the sensitivity element of the voltage channel with PSS. (Option 2).

4.6- *Robustness of turbogenerator system with PSS*

The PSS of equations (4.4) and (4.5) take the form of a non-diagonal system post-compensation. In general, it is shown in Leithead and O'Reilly [36] that the relative error (uncertainty) for any individual system transfer-function element $g'_{ij}(s)$ of equation (4.4) is increased by system post-compensation compared to the relative error (uncertainty) of the transfer-function element $g_{ij}(s)$ of the original system equation (4.1). Specifically, the relative uncertainty $\Delta g'_{ij} / g'_{ij}$ (i,j=1,2) of the elements of the post-compensated system transfer-function $G'(s)=P(s)G(s)$ of equation (4.4) is related to the relative uncertainty $\Delta g_{ij} / g_{ij}$ of the elements of

the un-compensated system transfer-function matrix G(s) of equation (4.1) as follows [36]

$$\frac{\Delta g'_{11}}{g'_{11}} = \frac{1}{1-\gamma}\left[(1-A_1)\frac{\Delta g_{11}}{g_{11}} + (A_1-\gamma)\frac{\Delta g_{21}}{g_{21}}\right] \tag{4.6}$$

$$\frac{\Delta g'_{12}}{g'_{12}} = \frac{1}{1-\gamma}\left[(B_1-\gamma)\frac{\Delta g_{12}}{g_{12}} + (1-B_1)\frac{\Delta g_{22}}{g_{22}}\right] \tag{4.7}$$

$$\frac{\Delta g'_{21}}{g'_{21}} = \frac{1}{1-\gamma}\left[(B_2-\gamma)\frac{\Delta g_{21}}{g_{21}} + (1-B_2)\frac{\Delta g_{11}}{g_{11}}\right] \tag{4.8}$$

$$\frac{\Delta g'_{22}}{g'_{22}} = \frac{1}{1-\gamma}\left[(1-A_2)\frac{\Delta g_{22}}{g_{22}} + (A_2-\gamma)\frac{\Delta g_{12}}{g_{12}}\right] \tag{4.9}$$

where

$$A_1 = \frac{g'_{12}g_{21}}{g'_{11}g_{22}} \quad ; \quad A_2 = \frac{g_{12}g'_{21}}{g_{11}g'_{22}} \tag{4.10}$$

$$B_1 = \frac{g'_{11}g_{12}}{g_{11}g'_{12}} \quad ; \quad B_2 = \frac{g_{21}g'_{22}}{g'_{21}g_{22}} \tag{4.11}$$

Thus, the price paid for the use of PSS (post-compensation) is that relative uncertainty in the post-compensated system, compared with that of the original system without PSS, is multiplied by the factor $1/(1-\gamma)$. Since in the frequency range of interest (0 to 10 rad/sec.), the polar plot of $\gamma(s)$ is nowhere near the point (1,0), the factor $1/(1-\gamma)$ is not very large and the *PSS (post-compensation) does not significantly reduce robustness* to system uncertainty.

4.7- *Control Option 3 :Excitation/governor control only with swapped input-output pairings*

A third option, to avoid the problematic switch-back characteristic of the electrical subsystem frequency response at 7 rad/sec yet retain high excitation channel bandwidth, at least of theoretical interest, is to use non-diagonal precompensation (non-diagonal control). One particular simple form of system precompensation is to swap the assignment of system inputs to outputs so that the output speed $\Delta\omega$ is paired with the field voltage input ΔE_{fd} and the output terminal voltage ΔV_t is paired with the mechanical torque input ΔT_m. The effect of this swapping of the assignment of system inputs to outputs is to pre-compensate the system in Fig. 3.5 such that the amended pre-compensated system is given by

$$G^*(s) = G(s)P(s) = \begin{bmatrix} g_{11} & g_{12} \\ g_{21} & g_{22} \end{bmatrix} \begin{bmatrix} 0 & 1 \\ 1 & 0 \end{bmatrix} = \begin{bmatrix} g_{12} & g_{11} \\ g_{22} & g_{21} \end{bmatrix} \tag{4.12}$$

The governor control $k_1(s)$ of Fig. 3.11 is given by

$$k_1 = \frac{30}{s(s+10)} \tag{4.13}$$

The excitation control $k_2(s)$ of Fig. 3.11 is given by

$$k_2 = -\frac{100(s+3.686)(s+0.288)\left(s^2+5.779s+23.892\right)}{s(s+63.9584)(s+0.47)\left(s^2+0.955s+1.365\right)} \qquad (4.14)$$

Just as before the high-frequency limit of the multivariable structure function $\gamma(s)$ of equation (4.1) was less than one, $\gamma^*(s) = 1/\gamma(s)$ for the amended system (4.12) is greater than one. Also, it is observed in equation (4.12) that the problem of the electrical subsystem $g_{22}(s)$ possessing lightly damped LHP zeros is removed to the off-diagonal element.

As a consequence, advantages of this third control option are firstly that a high bandwidth for the excitation channel C_2 can now be used (20 rad/sec) and secondly the actual outputs are directly controlled unlike Control Option 2 with the PSS. Performance is also robust to plant uncertainty. The good performance is confirmed by channel frequency responses, step responses and sensitivity plots in Fig. 4.20 to Fig. 4.22.

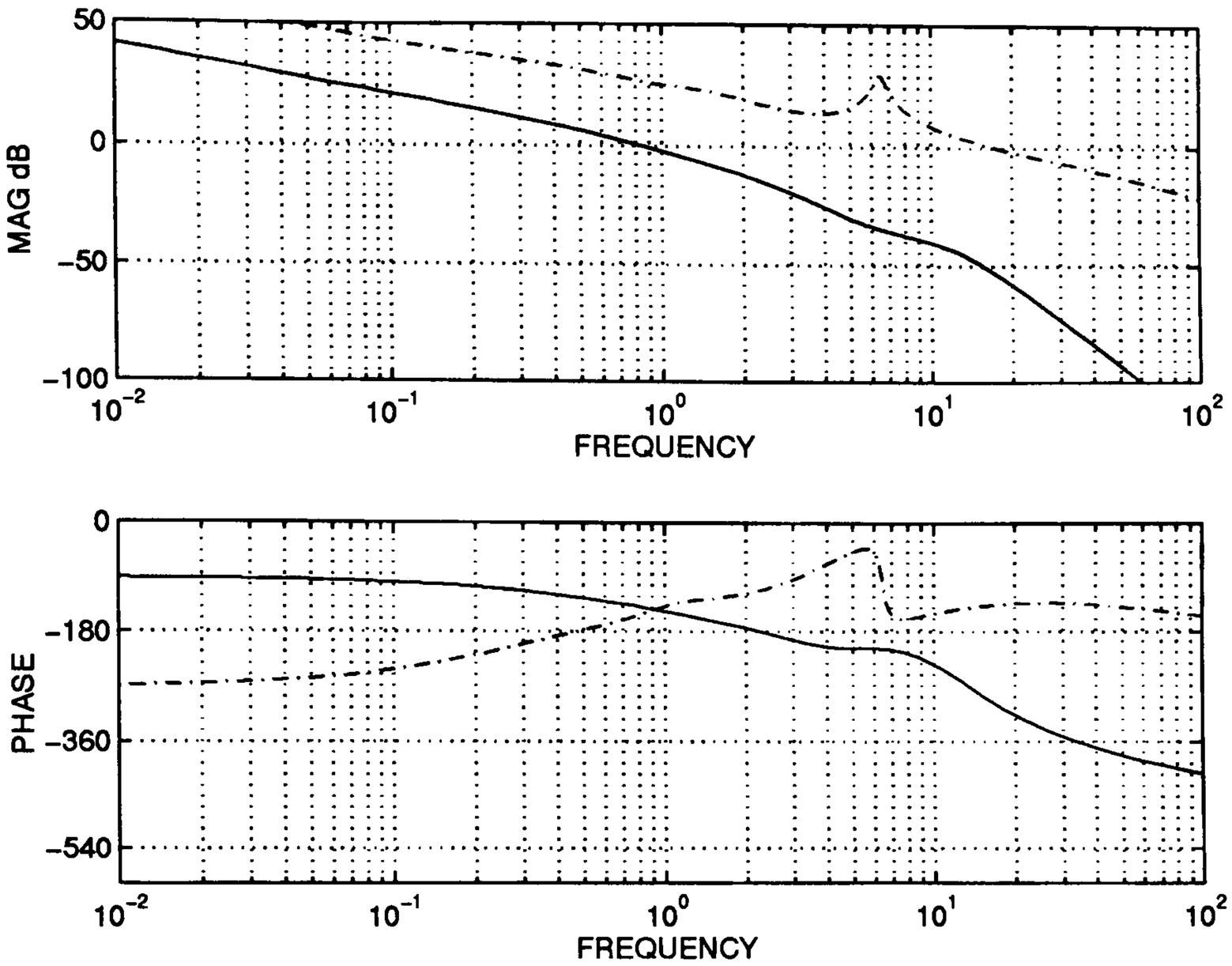

Fig. 4.20 Bode plots of the turbine/governor channel C1 (——) , and the exciter channel C2 (−·−·→ with swapped assignment of system inputs to outputs of equation 4.12 (Option 3).

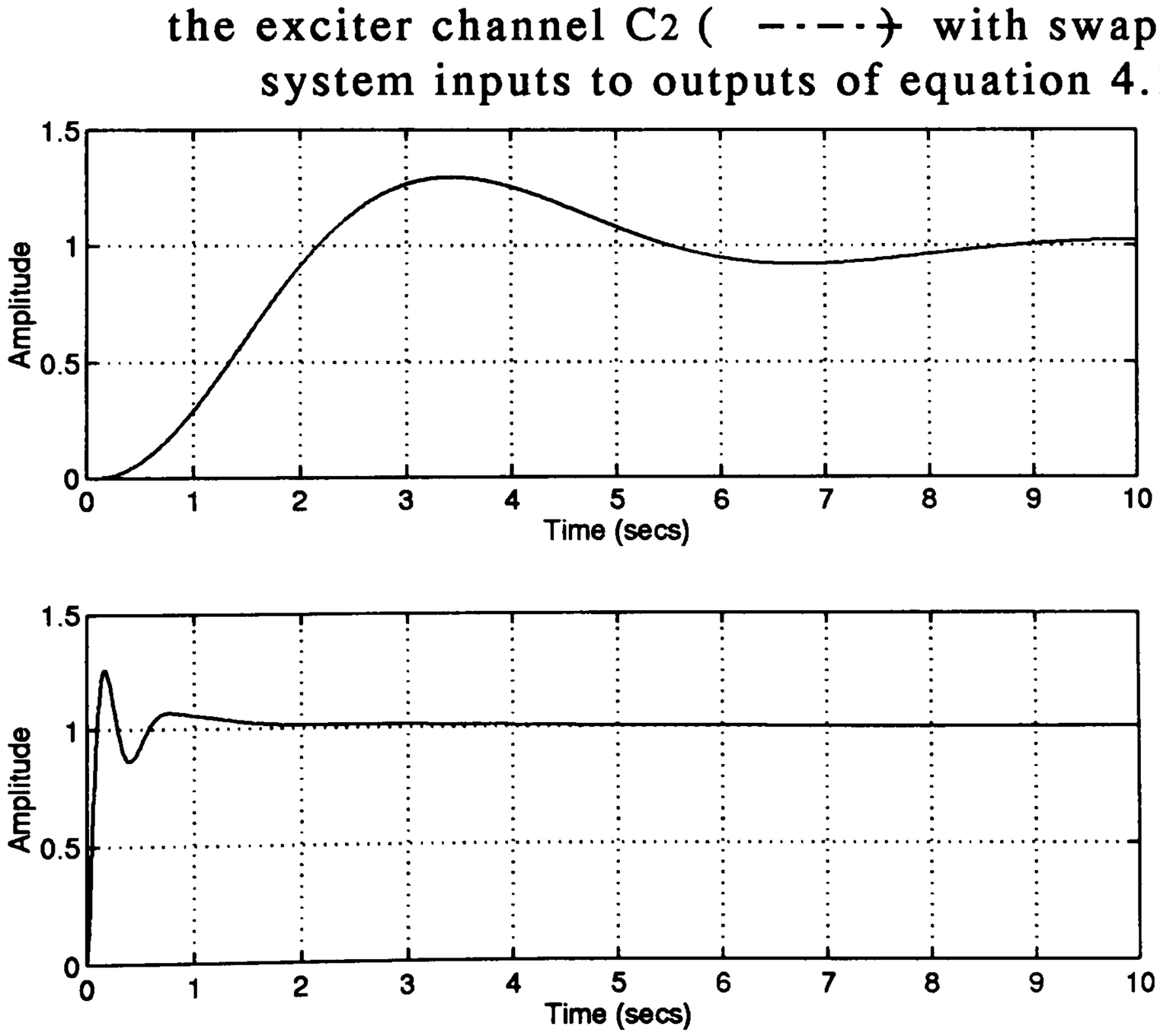

Fig. 4.21 Step response of the system with PSS , (a) speed output, (b) terminal voltage output.(Option 3).

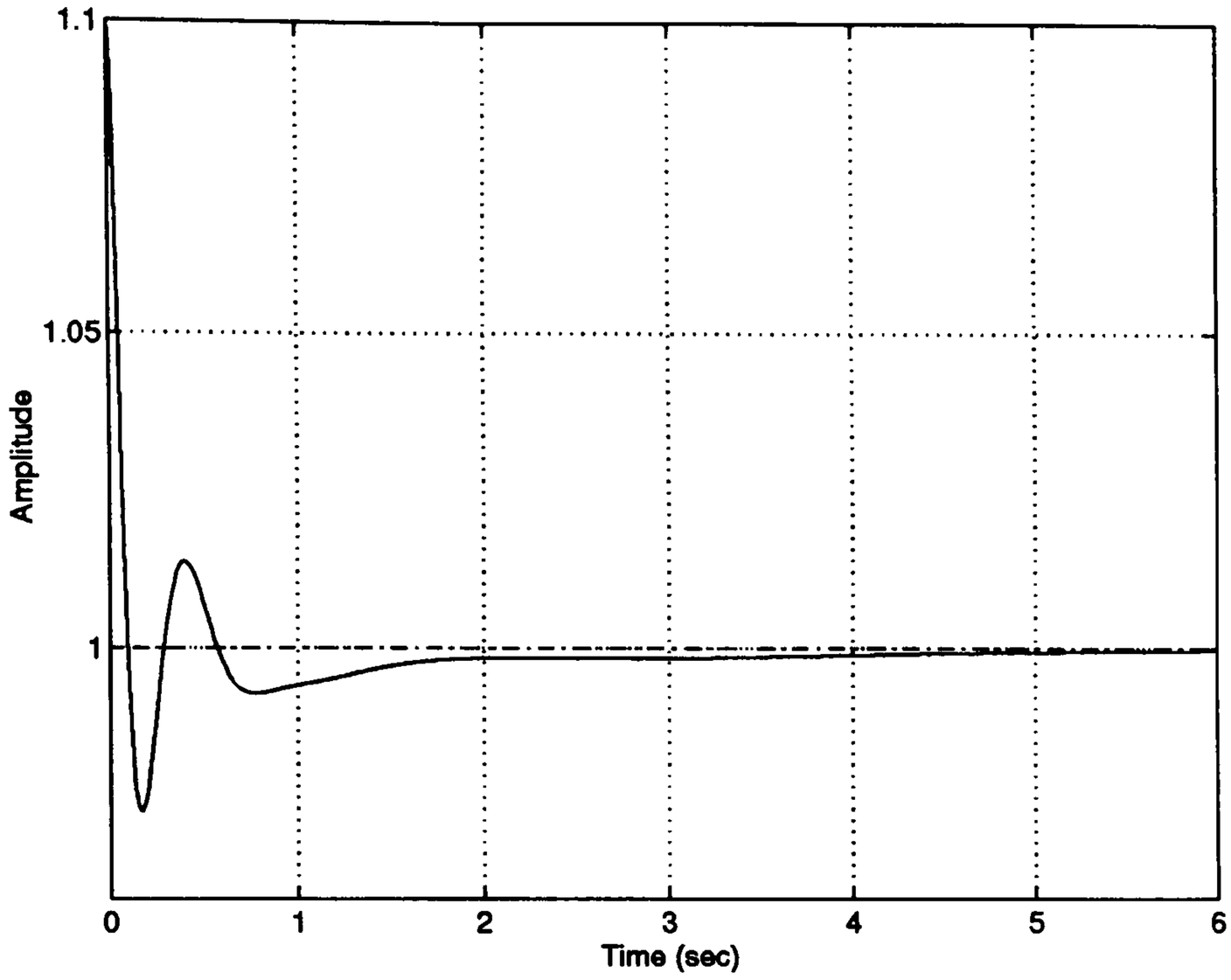

(a)

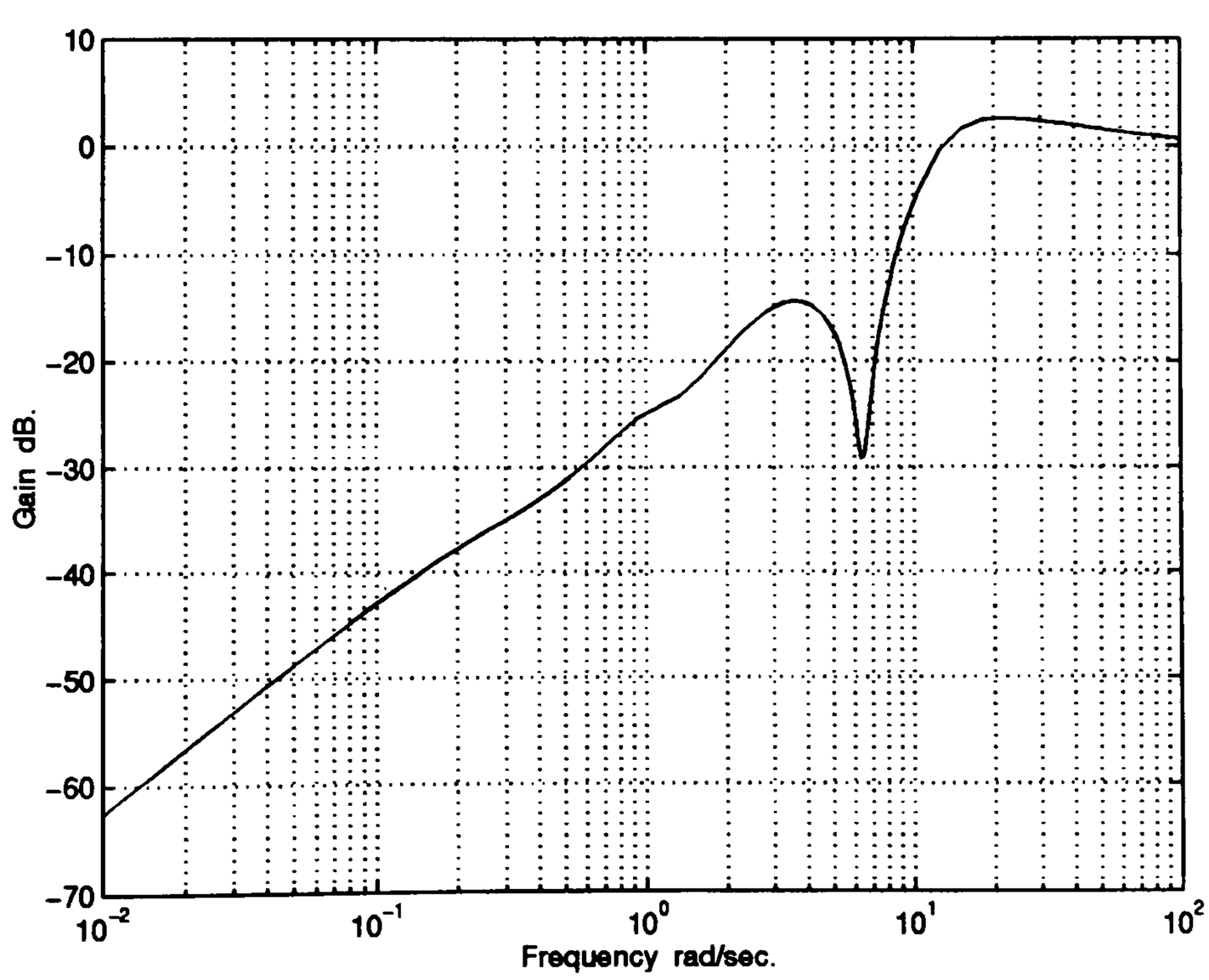

(b)

Fig. 4.22 **(a)** Terminal voltage output response to 10% voltage disturbance, and **(b)** Bode plot of the sensitivity element $\frac{1}{1+C_2}$ without PSS. (Option 3).

There are, however, two practical disadvantages to the use of Control Option 3. The first is that the governor subsystem $h_1(s)$ of equation(2.5) for the amended system (4.12) given by

$$h_1'(s) = \frac{k_1 g_{12}}{1 + k_1 g_{12}} \tag{4.15}$$

is unstable. This causes a system integrity problem; for, should the exciter loop fail, the whole system will go unstable. This is a direct consequence of the multivariable structure function, $\gamma^*(s)$, associated with the amended system (4.12), having a high-frequency limit greater than one and cannot be avoided, see Result 4.1 of [68]. The second practical disadvantage of the swapping of input-output pairing is the subjection of the governor to high frequency signals. In summary, all three control options evaluated above have their advantages and disadvantages in the methods by which they deal with the awkward switch-back frequency characteristic of the electrical subsystem near 7 rad/sec. On balance, the use of the PSS in Control Option 2 remains the most practical option with satisfactory performance.

Table 4.1 below summarises the control options available for the multivariable turbogenerator control system

Control option	Advantages	Disadvantages	Suitable machine
Low band-width Exciter channel	1-more economical “no fast exciters or PSS are required” 2-direct control on outputs	1- low stability margins 2-highly sensitive exciter channel 3- some loss of performance	small machines with smaller per unit synchronous reactance
Power System Stabiliser (PSS)	1- no loss of performance “high bandwidth exciter channel available” 2- no integrity problem “low performance controller on governor channel OK” 3-increased stability margin	1- increase in cost (PSS+fast exciter) 2- no direct control on the second output (effectively it is speed+voltage) 3- some stability problems if the two channels are strongly coupled	all types of machines with high damping

Control option	Advantages	Disadvantages	Suitable machine
swapping assignment of system input-output pairs	1- no loss of performance "high exciter bandwidth OK" 2- actual outputs are directly controlled	1- an integrity problem due to the instability of subsystem h_1 2-needs a very fast governor	all machines and extremely fast governor

Table 4.1 Control options avialable to the turbogenerator

Final remark : The multivariable control analysis of this section provides formal justification of the loop by loop design practice used for turbogenerator control [14], [15] despite being a multivariable (cross-coupled) system. In other words, the multivariable analysis justifies treating the turbogenerator system as a pseudo-SISO system where the governor loop is first closed and the exciter loop is treated as a SISO system for the prime purpose of rejecting voltage disturbances.

Chapter 5 : Analysis of Some Recent Developments in Turbogenerator Control

5.1- *Introduction*

In previous chapters, it was illustrated that oscillatory stability problems generally occur in the presence of a high load operating conditions, high synchronous reactance, and a high-reactance transmission system. Under these conditions, it is known that excitation systems can have a very strong influence on the damping of machine/system oscillations,[71]. In the analysis of oscillatory stability, Power Engineers used to look at the important characteristics of the excitation system ; its effective gain and time constant which is considered to have an effect on machine damping. High response excitation systems generally have a larger effective gain and lower time constant than normal response systems,[72]. Engineers are convinced that the effect of these characteristics on unit oscillatory damping depends upon whether or not added complexity of a PSS is to be applied to supplement the normal voltage control.

But as was demonstrated in Chapter 4, there exist a complex pair of lightly damped zeros in the exciter/voltage loop (the electrical subsystem g_{22} of the synchronous machine) of the turbogenerator

system, which are dangerously close to the complex pair of pole of the system at the mechanical mode of the machine (4-10 rad/sec.) creating a "switch-back" characteristic which gets worse with increasing real power, high synchronous reactance of a synchronous machine and weaker transmission lines. It is undesirable to cancel these zeros as they are lightly damped (very near to the imaginary axis). The presence of these complex zeros in the closed loop (since they cannot be cancelled) limits the achievable closed loop bandwidth ;(see Fig. 4.3 in Chapter 4). If the closed loop bandwidth of the exciter/voltage loop is greater than the natural frequency of these zeros, then

(a) the closed loop system time response will have a very oscillatory characteristics; Fig. 5.1, (b) the system will have a very poor sensitivity function; Fig. 5.2.

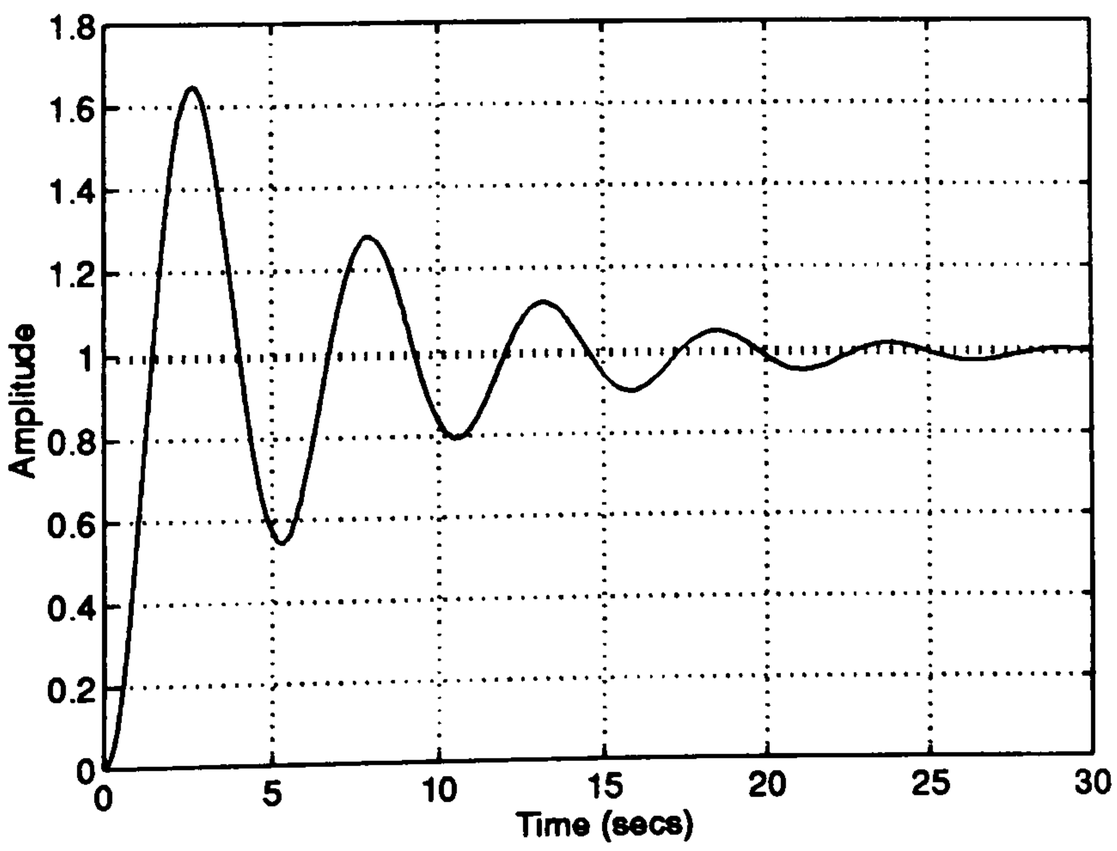

Fig. 5.1 Excitation channel step response

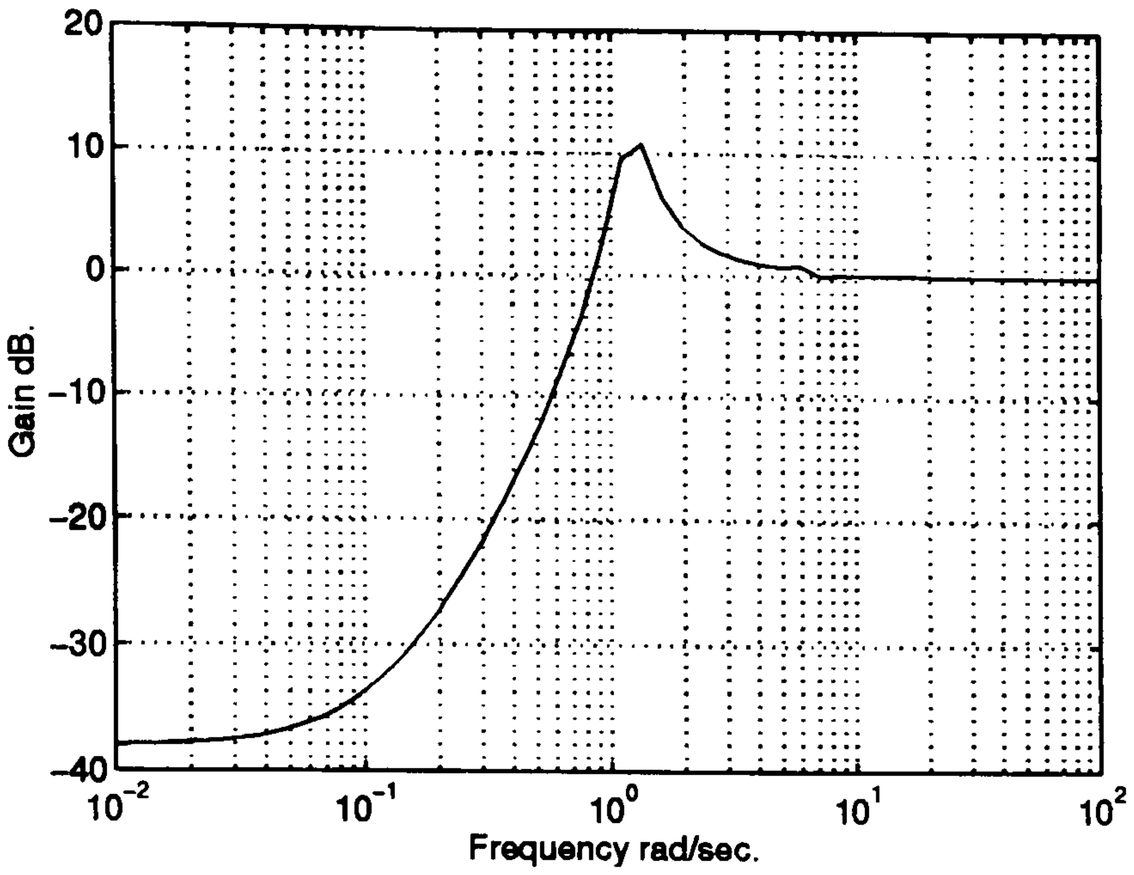

Fig. 5.2 Excitation channel sensitivity

Three options were presented in Chapter 4 for enhancing the machine performance by considering these lightly damped zeros; one is to have a closed loop bandwidth much less than the natural frequency of the mechanical mode of the system, another one is to get rid of these zeros from the electrical subsystem g_{22} to the off-diagonal part of the machine transfer function matrix by swapping the assignment of inputs to outputs of the machine; and the last one is to "bury" the effects of these zeros by crossfeed of the natural dynamics of the system by a way of a PSS.

Unlike the previously believed objective of a designed PSS, which was to get a signal which should force terminal voltage changes that are in phase with speed changes; here, in this study, the main purpose of the PSS is presented as to overcome effects of the

machine lightly damped zeros using the plant natural dynamics. Of the three options discussed, the one involving the PSS is the only one used in practice today. The PSS is comparatively cheap and can maintain a good performance in a wide range of operating conditions.

5.2- *Recent Studies involving the PSS*

Remarkable efforts have been devoted to the design of appropriate PSS; many methods such as root locus, eigenvalue techniques [73], pole placement [74], adaptive control [75], and H_∞ [76]..etc have been used. One of the very recent studies of such methods is the :

Augmented PSS

In 1995 Saidy and Hughes [77], proposed an augmented control scheme to enhance the performance of conventional power system stabiliser (CPSS) under weak tie-line conditions. It is consist simply of an additional loop in parallel with the conventional stabiliser. The design of this additional control loop is based on the inherent generator and excitation system dynamic characteristics. The additional loop seeks to co-ordinate the contributions of the d-axis and the CPSS to damping performance. The benefits of the scheme

were presented as contributing positive damping power in the lower frequency range and contributing positive synchronising power.

But in Chapter 4, it was established that, what the PSS really does is to rid the system of a "switch-back" characteristic which arises from the presence of a lightly-damped pair of zero very near to the natural mechanical mode of the turbogenerator. To see the effects of this scheme on a power system model taken from [77],in the light of Chapter 4's clarification of the PSS objective; the model is first treated with a conventional PSS, of the form

$$CPSS = K_s \frac{(1+sT_1)(1+sT_3)}{(1+sT_2)(1+sT_4)} \frac{sT_w}{(1+sT_w)} \tag{5.2}$$

where

$K_s = 10,\ T_w = 10,\ T_1 = T_3 = 0.3,\ T_2 = T_4 = 0.0595$

and then an augmented PSS is used in parallel with the CPSS. The augmented PSS has the form

$$APSS = K_s \frac{(1+sT_i)}{(1+sT_f)} \frac{K_c}{(1+sT''_{do})} \frac{sT_w}{(1+sT_w)} \tag{5.3}$$

the APSS uses the natural dynamics of the CPSS and the exciter system, these are :

$T_i = K_e * K_f + T_e + T_f$

$$K_s = \frac{K_{4d}}{a * K_3}$$

$$K_c = \left(c * T'_{do} - T''_{do}\right) * \frac{\omega_o}{K_e}$$

where $K_e = 198$, $T_e = 0.03$, $K_f = 0.01$, $T_f = 0.371$, are characteristics of the excitation system, and

K_3, K_{4d}, T'_{do}, T''_{do}, a, and c, are characteristics of the synchronous machine.

The effect of the added APSS to the system with the CPSS was mainly illustrated by analysing the electrical subsystem g_{22} of the synchronous machine.

Form Saidy and Hughes [77], the 5-th order linearised model connected to a strong transmission line is :

$$g_{11} = 0.512s^3 + 35.903s^2 + 539.954s + 314.6$$
$$g_{12} = -0.168s^2 - 9.49s - 124.715$$
$$g_{21} = -0.043s^3 - 3.347s^2 - 12.382s - 49.506$$
$$g_{22} = 0.001s^4 + 0.064s^3 + 0.956s^2 + 4.948s + 36.518$$
$$den = 0.014s^5 + 0.976s^4 + 15.84s^3 + 73.78s^2 + 605.212s + 170.06$$

The same model for the weak tie-line case is :

$$g_{11} = 1.6992s^3 + 90.01s^2 + 855.624s + 314.6$$

$$g_{12} = -0.254s^2 - 12.091s - 107.743$$

$$g_{21} = -0.168s^3 - 12.411s^2 - 93.124s - 112.064$$

$$g_{22} = 0.006s^4 + 0.316s^3 + 3.06s^2 + 10.758s + 80.816$$

$$den = 0.046s^5 + 2.446s^4 + 24.74s^3 + 70.225s^2 + 574.62s + 128.28$$

The nominal plant has a fairly good characteristic in the important range of (1-10) rad/sec; this is expected because the system has a low synchronous reactance and is connected to a strong transmission line. The plant has a small $\gamma(s)$, Fig. 5.3, with a "well-behaved" g_{22}, Fig. 5.4; and so the addition of the PSS (as a non-diagonal feedback control element) will not increase its sensitivity (see Section 4.6 in the last Chapter).

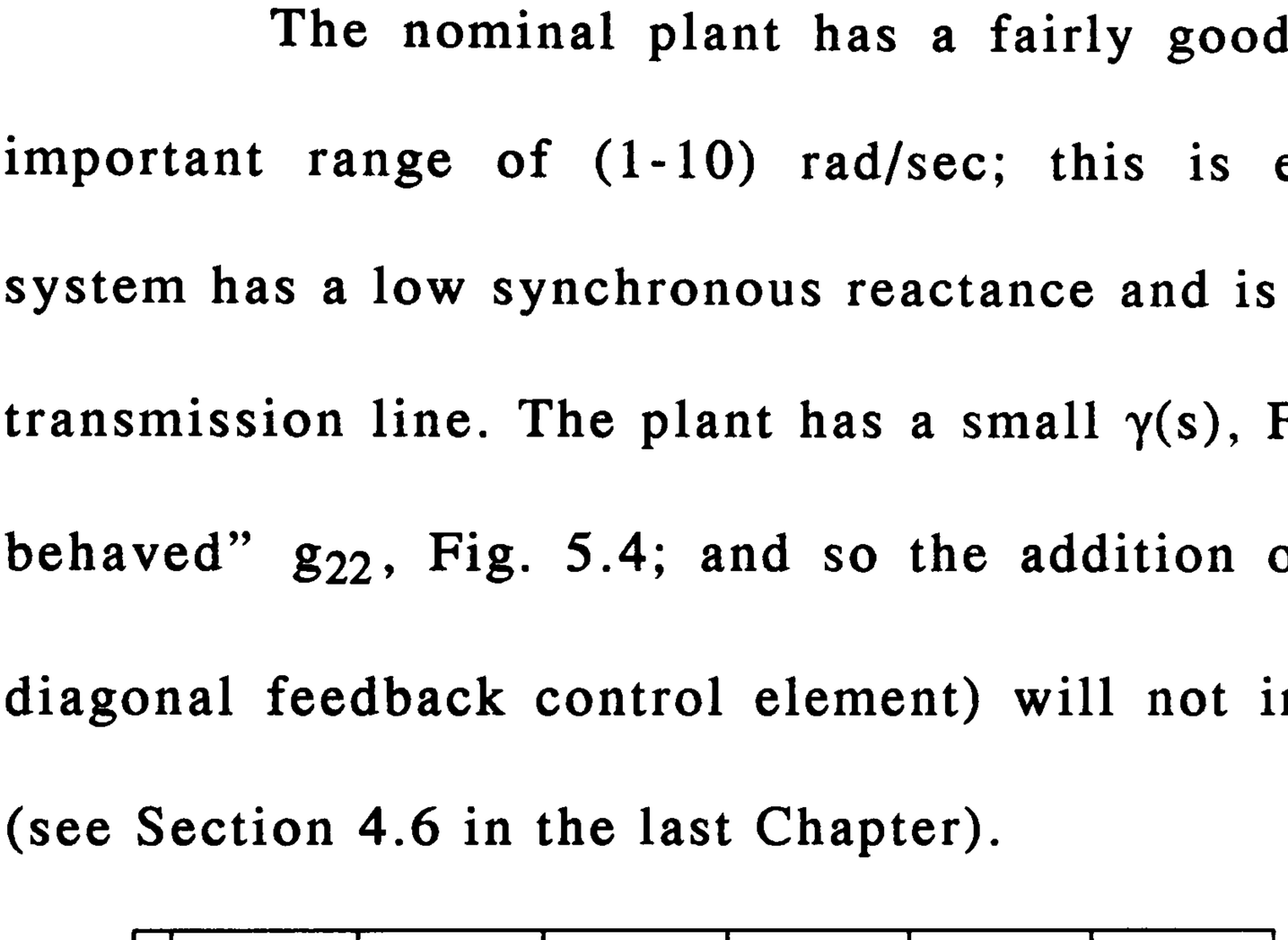

Fig. 5.3 Nyquist plot of $\gamma(s)$ for strong transmission line model

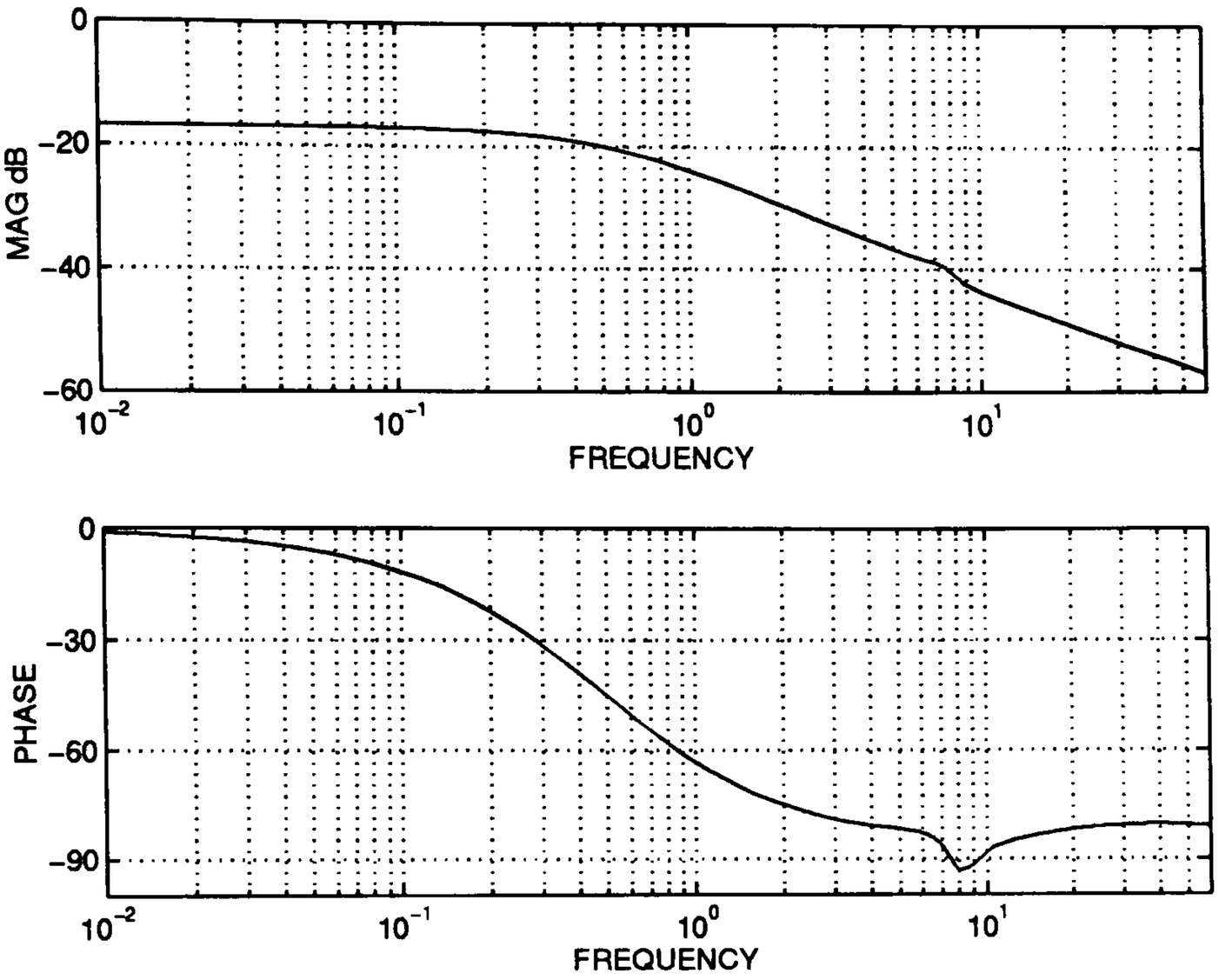

Fig. 5.4 Bode plot of g_{22} for strong transmission line model

For the system connected to the weak transmission line, the $\gamma(s)$ of the plant increases, Fig. 5.5, and a "switch-back" characteristics developed in the electrical subsystem $g_{22}(s)$ in the frequency range (4-6) rad/sec, Fig. 5.6.

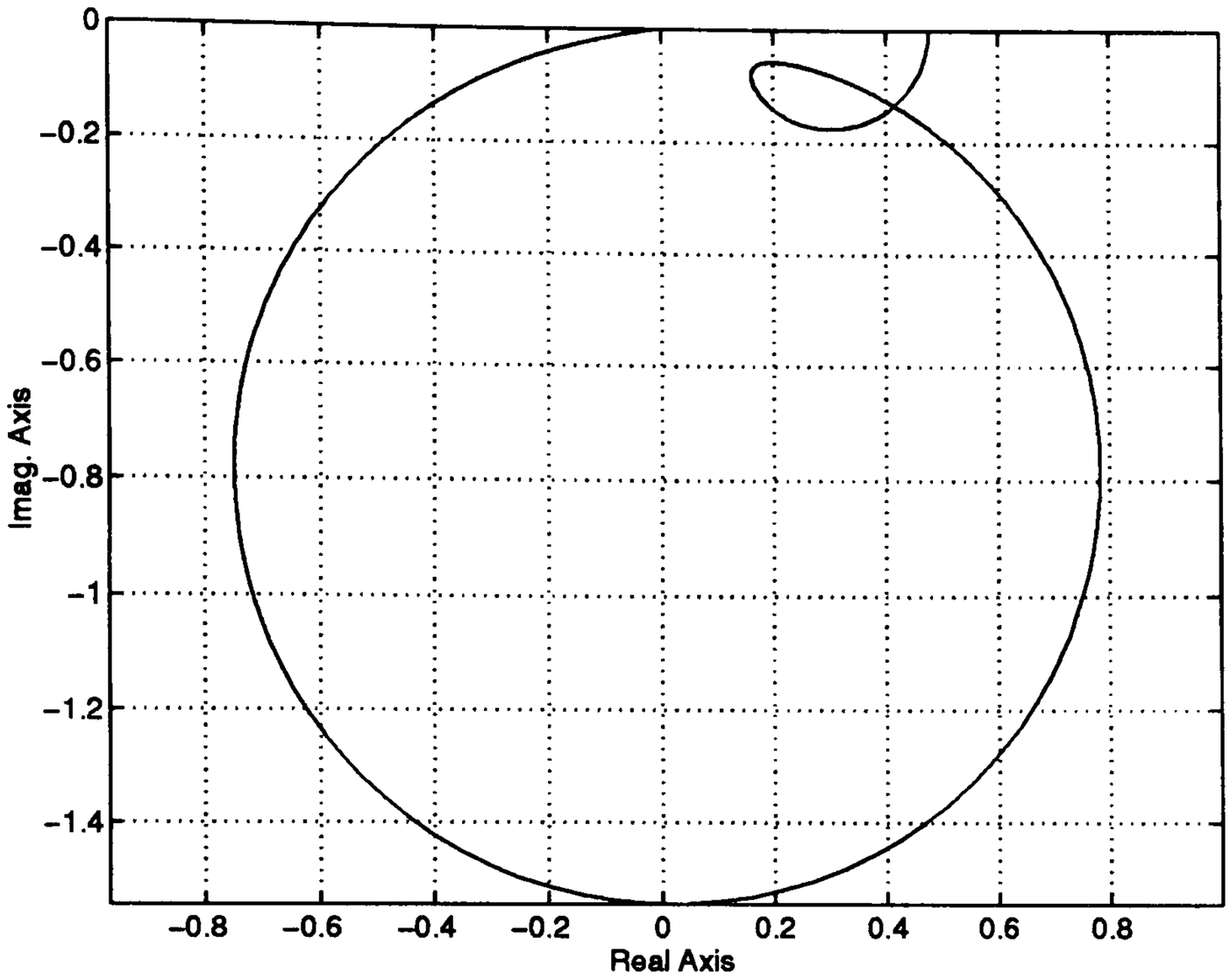

Fig. 5.5 Nyquist plot of $\gamma(s)$ for the weak transmission line model

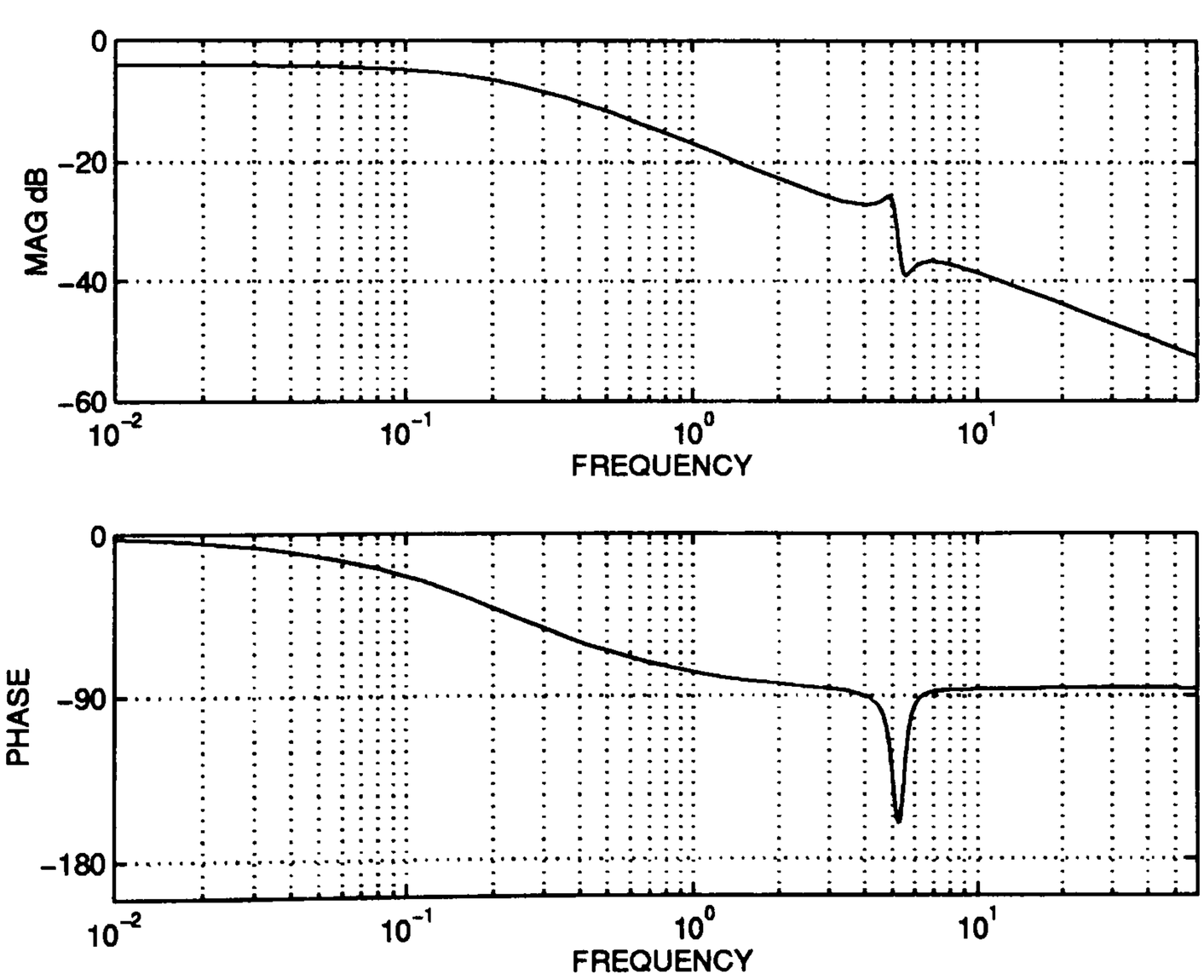

Fig. 5.6 Bode plot of g_{22} for the weak transmission line model

The Bode plot of the electrical subsystem $g_{22}(s)$ for the model with conventional PSS and augmented PSS is shown in Fig. 5.7 (for

the nominal model), and Fig. 5.8 (for the weak transmission line model).

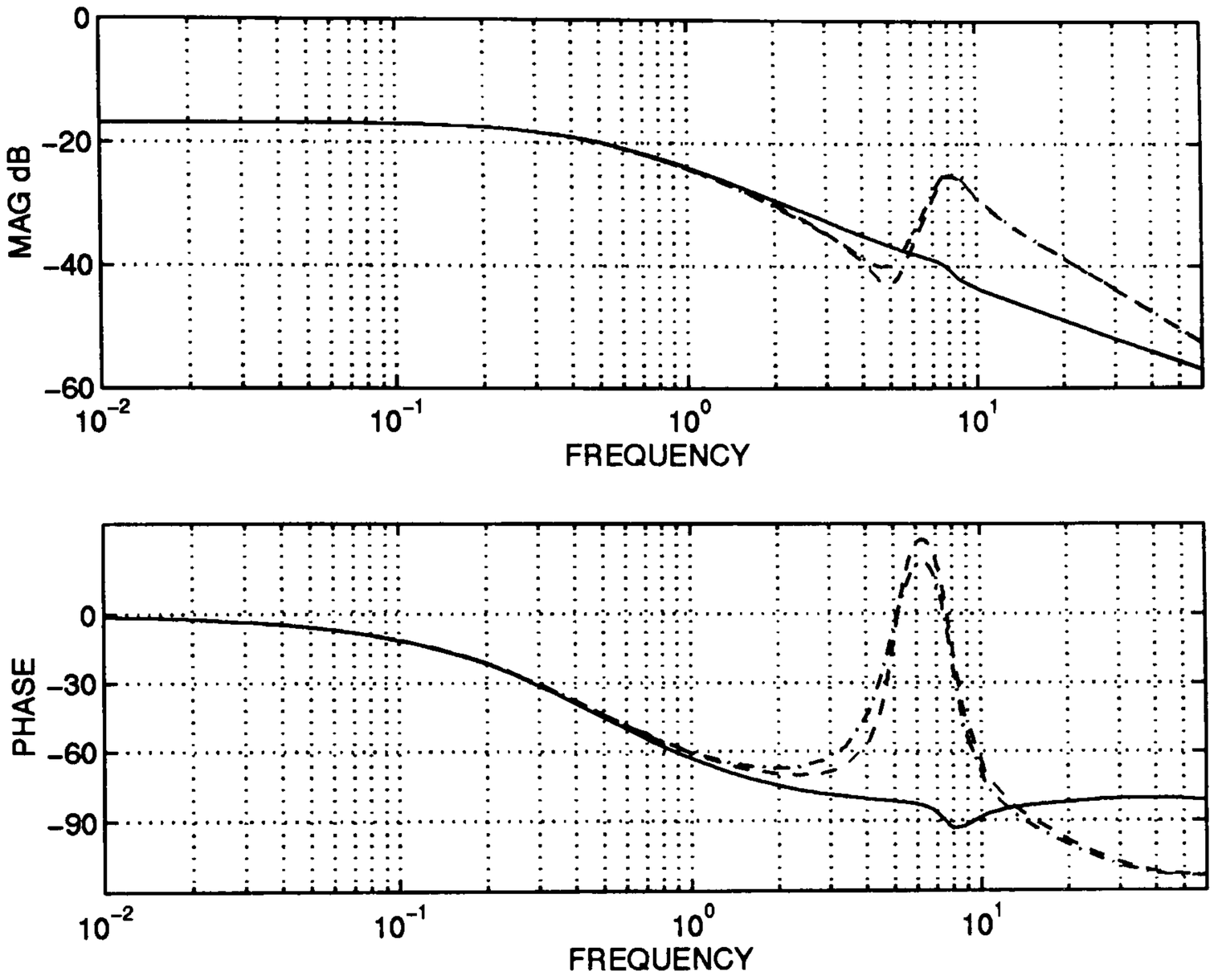

(_____) no PSS, (— — — —) CPSS, (—·—·—·—) APSS

Fig. 5.7 Bode plot of g_{22} and $g_{22} + pg_{12}$ for strong tie-line model

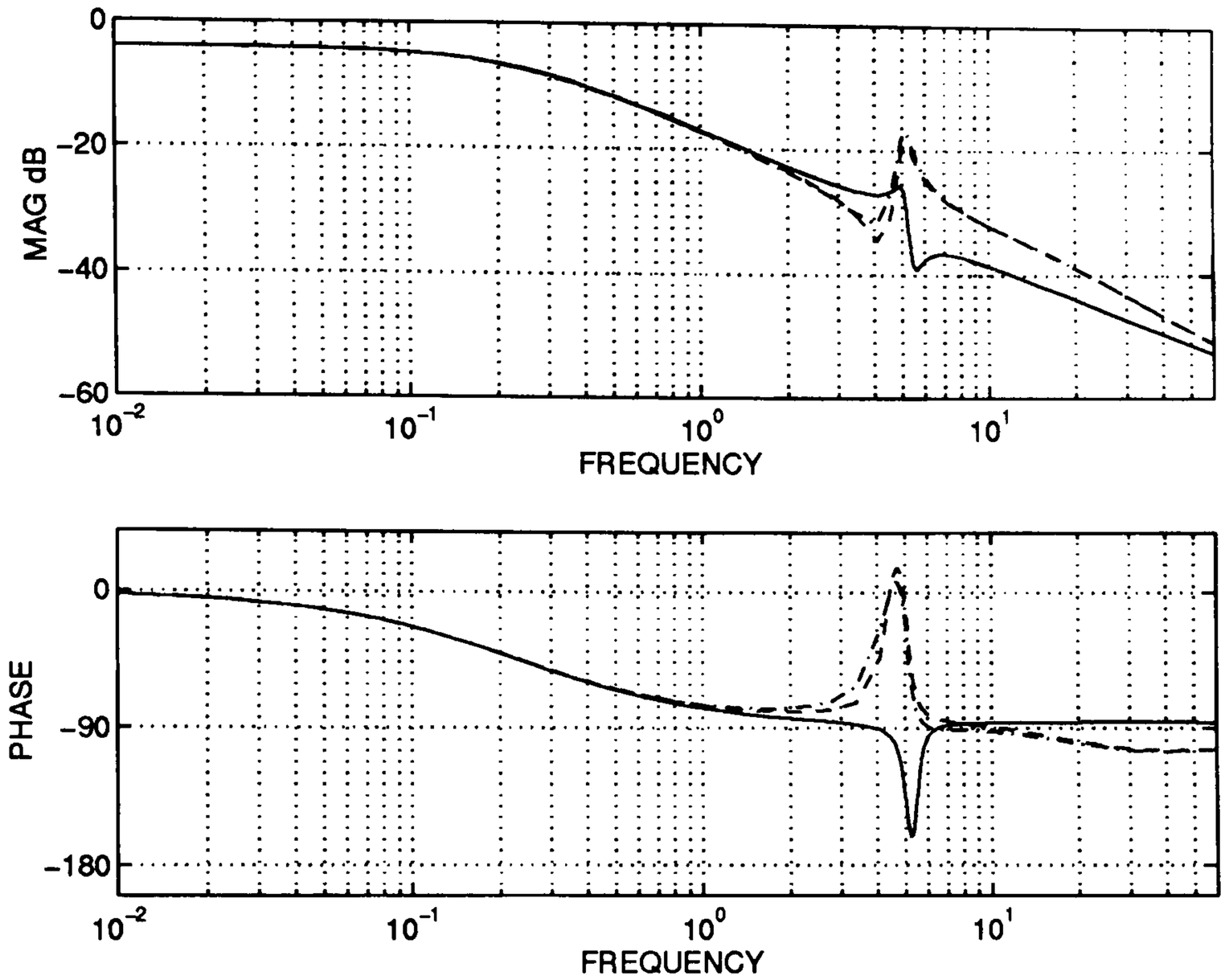

(————) no PSS, (— — — —) CPSS, (— . — . — . —) APSS

Fig. 5.8 Bode plot of g_{22} and $g_{22} + pg_{12}$ for weak tie-line model

From Fig. 5.8, it is clear that the augmented PSS has an slightly larger gain and phase advance than that provided by the conventional PSS; and the step response of the terminal voltage shown in Fig. 5.9, for the strong transmission line model, and Fig. 5.11 for the weak transmission line illustrate some improvement in the APSS case over the CPSS one. Fig. 5.10 and Fig. 5.12 show the effect of the Exciter input in the rotor speed output, form which also, it appears that the augmented PSS (APSS) has a better disturbance rejection.

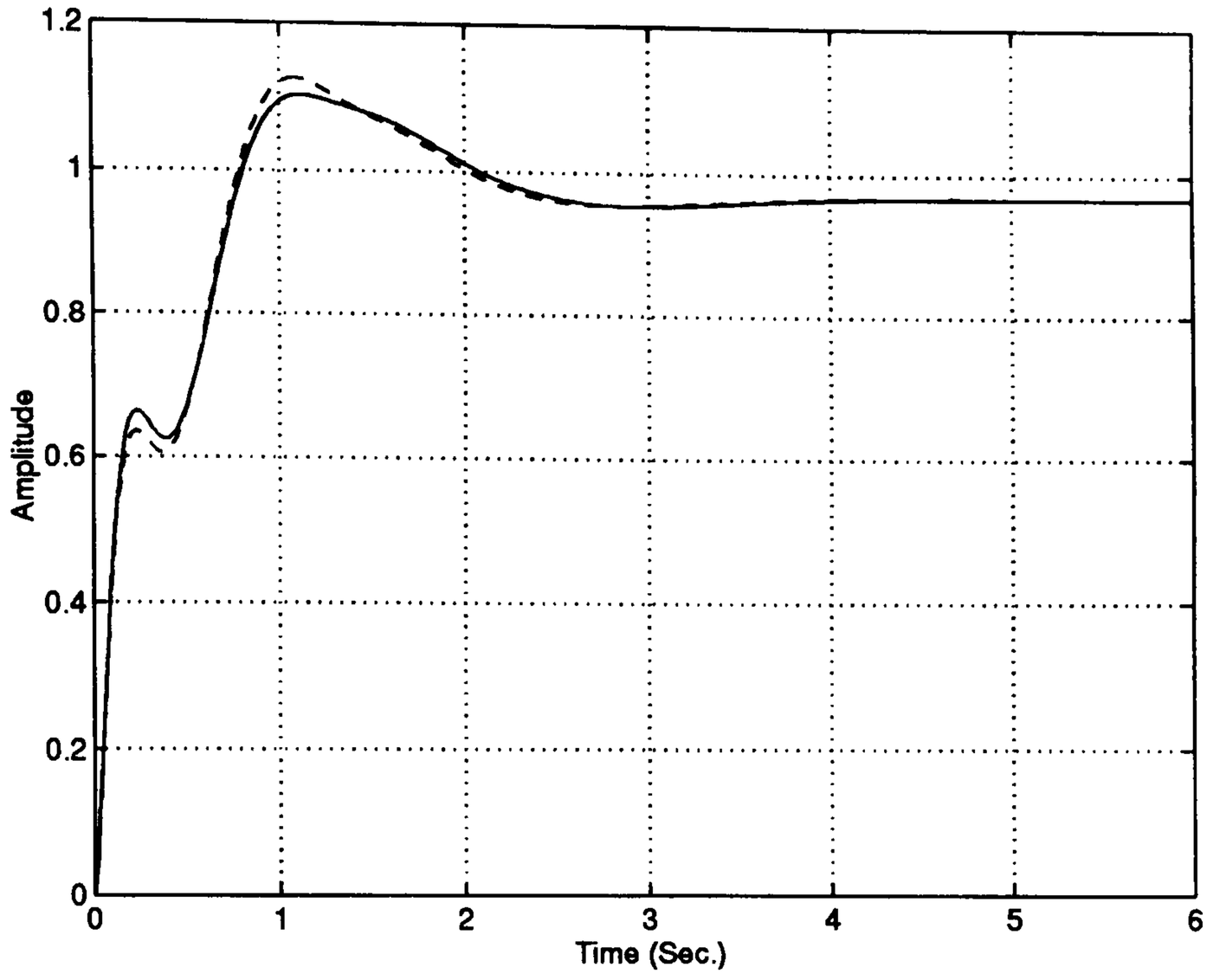

(———) plant with APSS, (– – – –) plant with CPSS

Fig. 5.9 Step response of terminal voltage of strong tie-line

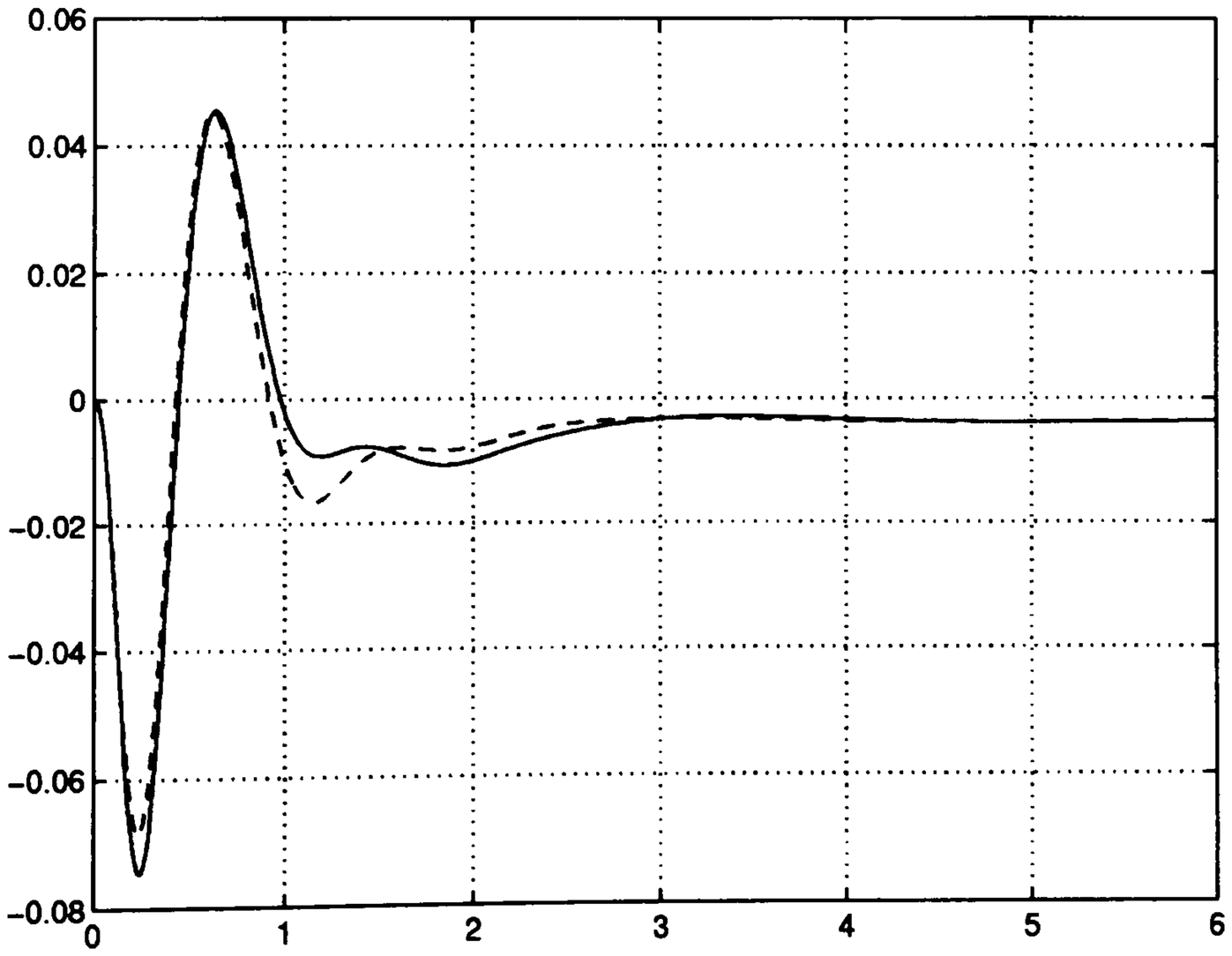

(———) plant with APSS, (— – – —) plant with CPSS

Fig. 5.10 Effect of speed on terminal voltage strong tie-line case

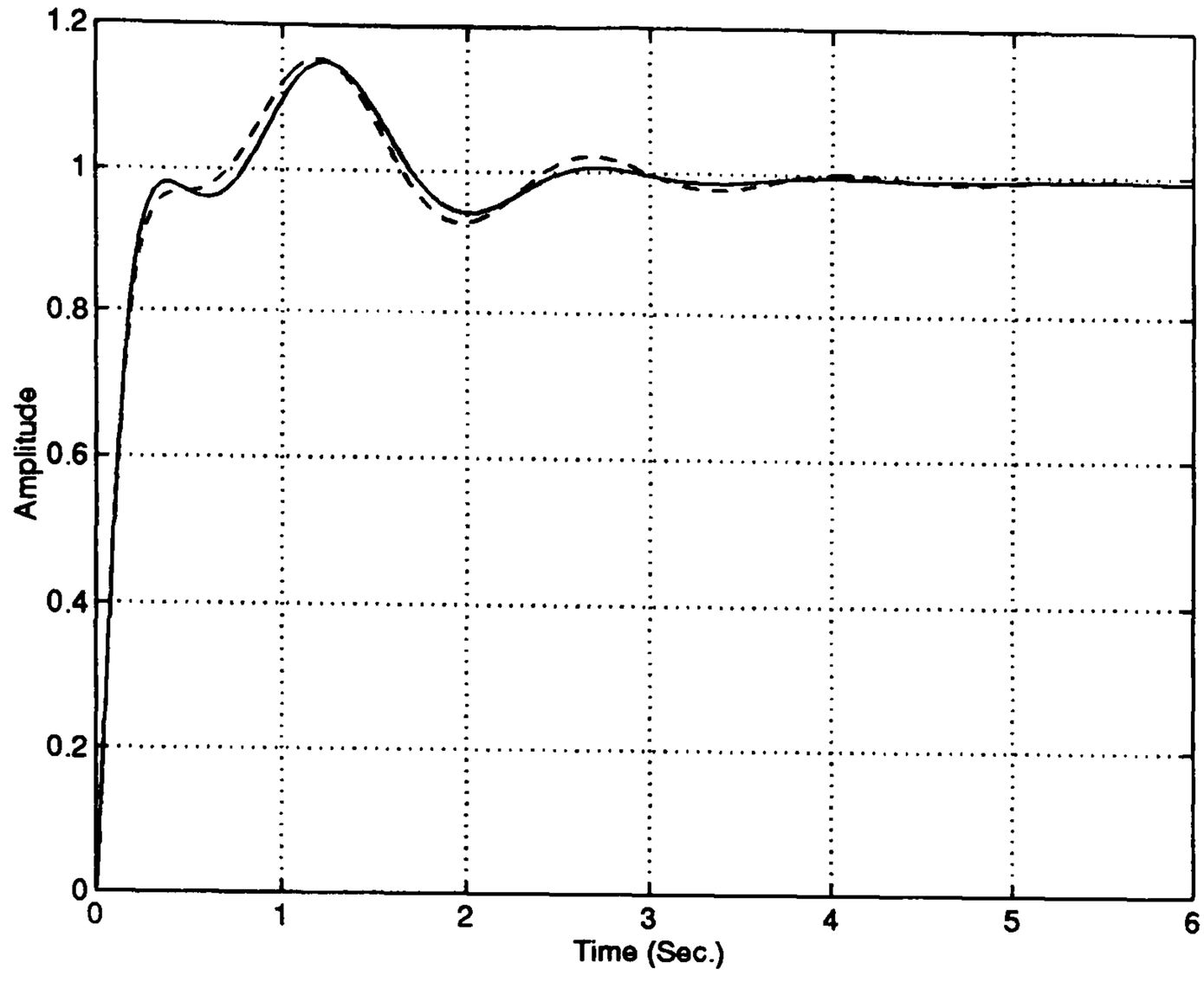

(———) plant with APSS, (– – – – –) plant with CPSS

Fig. 5.11 Step response of terminal voltage of strong tie-line

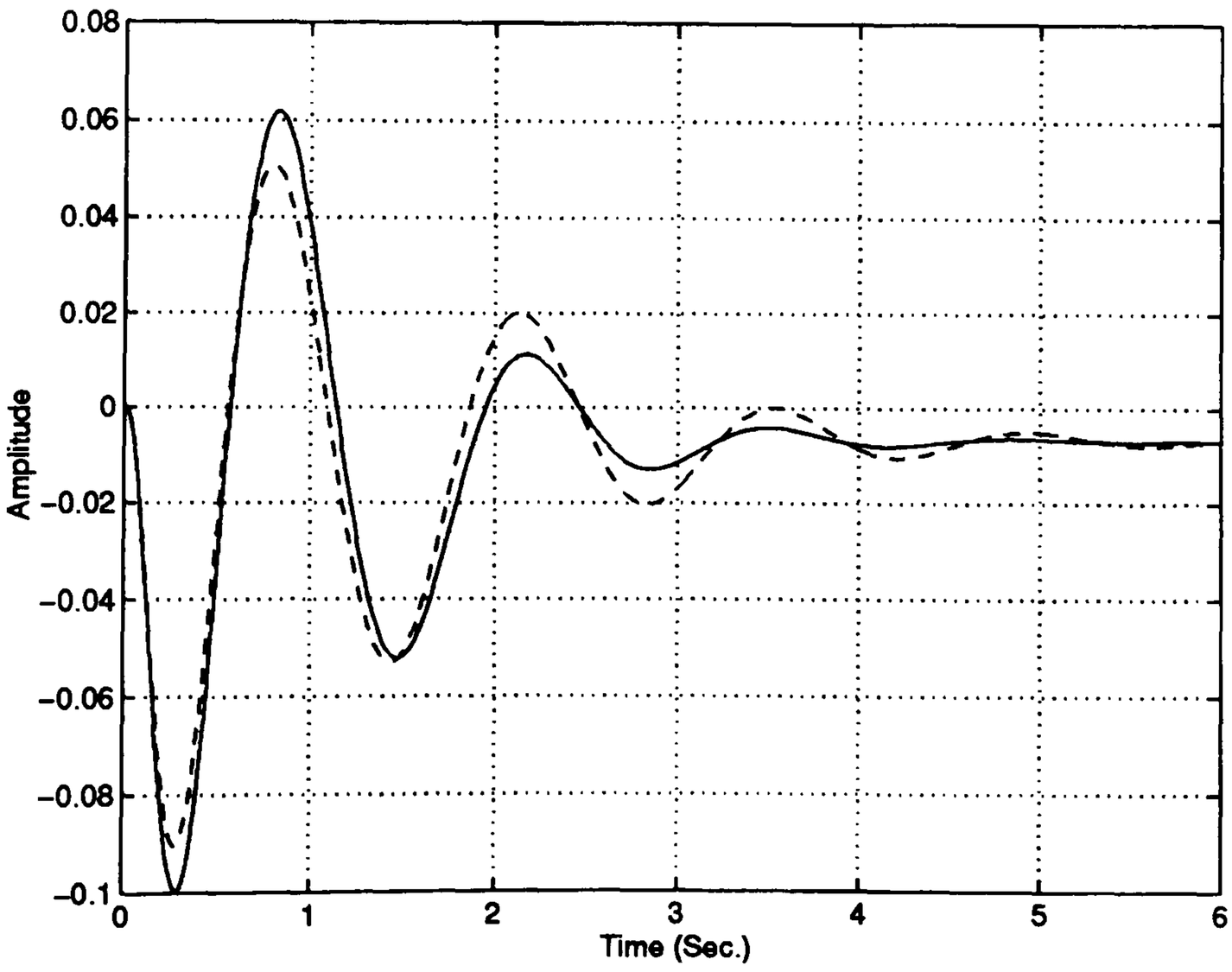

(———) plant with APSS, (– – – –) plant with CPSS

Fig. 5.12 Effect of speed on terminal voltage weak tie-line case

5.3- *Recent Method not involving PSS*

Some studies did investigate methods not involving the PSS to design controllers which improve the performance of a turbogenerator. Here, one of these methods will be analysed using the ICAD technique.

The method is based on the Inverse Nyquist Array technique proposed by Rosenbrock [29]. The design approach is to reduce the degree of interaction between the input signals (field voltage and mechanical torque in the case of a turbogenerator) and the measurable outputs (terminal voltage and speed) so that SISO methods become applicable; this reduction is referred to as *decoupling*. Once the system has been fairly well decoupled, the control loops can be designed separately, one at a time and the overall stability (and the stability margins) can be found from the distinct Nyquist diagrams of the distinct loops. Rosenbrock [29] devised a mathematical decoupling procedure which is applied to the inverse of the plant transfer function matrix, and which results in what is known as a diagonally dominant systems; the number of measurable outputs has to correspond to the number of input signals in order to have a square transfer matrix.

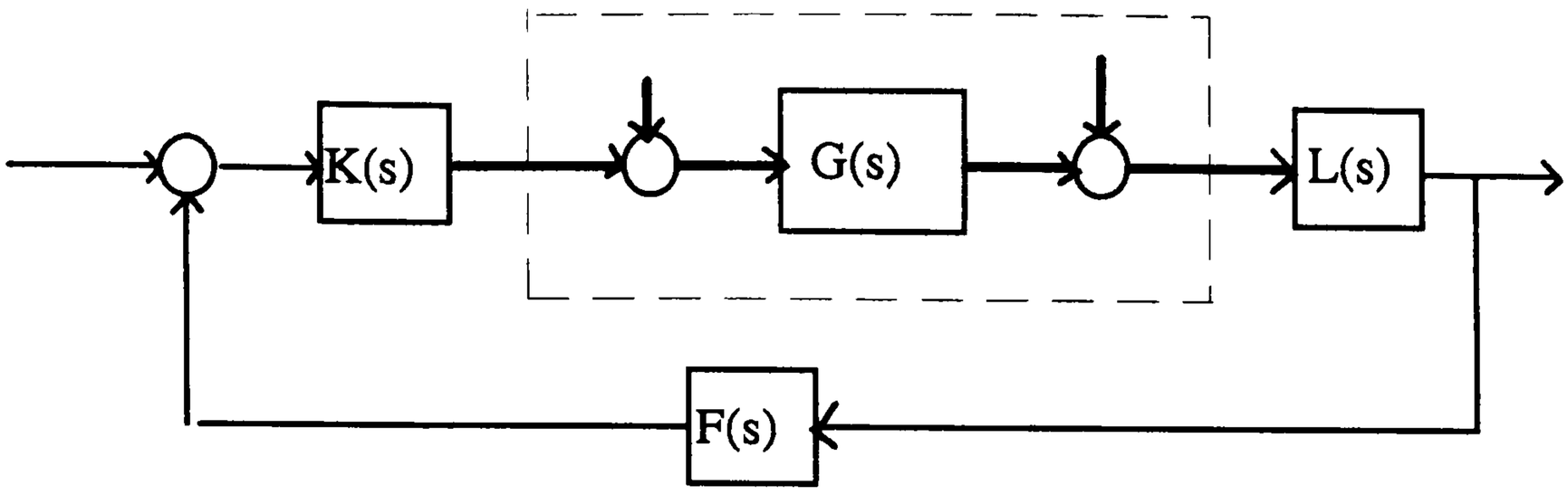

Fig. 5.13 an INA turbogenerator control problem

Fig. 5.13 above shows an INA turbogenerator system, where G(s) the turbogenerator system which include the synchronous machine, the exciter and the turbine/governor systems in a transfer function matrix, having an input vector U (mechanical torque and field voltage), and an output vector Y (speed and terminal voltage). The off-diagonal elements of [G(s)] are not zero, thus prohibiting the use of well-known SISO methods of designing stable feedback regulators. However, the addition of matrices [K(s)] and [L(s)] creates a new system with new inputs R and new outputs Z and a new plant transfer function Q(s) such that

$$[Q(s)] = [L(s)]\,[G(s)]\,[K(s)] \tag{5.4}$$

By carefully choosing the elements of the pre-compensator [K(s)] and the post-compensator [L(s)], a [Q(s)] can be found of which the off-diagonal terms are much smaller than the diagonal terms when compared to [G(s)]. The interaction between [R] as inputs and [Z] as

outputs is therefore greatly reduced and [Q(s)] is said to be diagonally dominant. This reduction is also referred to as decoupling.

In applying the INA to the turbogenerator control problem, it was noticed that the addition of lead compensation to either [K(s)] or [L(s)] is always necessary if higher gain values is to be used in the feedback matrix [F(s)], [78], [79].

A decoupler design developed using the INA method for a turbogenerator system by Bollinger et.el [80] will be analysed using the ICAD technique. The machine is a 3rd order linear model obtained from DeMello and Concordia [11], and the decoupler was designed on the basis of the following loading conditions and machine data :

(i) loading conditions :

P=1.0 pu; Q=0.5 pu; and X_e=0.1 pu.

(ii) machine data :

X_d =1.6 pu; X_q=1.55 pu; X'_d=0.32

M=3 pu; D=1.0 pu; and T'_{do}=5 pu.

From Appendix (3), the machine transfer function matrix [G(s)] is calculated using the machine data and the loading conditions above.

The decoupler (a pre-compensator) in a transfer function matrix form is :

$$P(s)=\begin{bmatrix} 1 & \dfrac{0.412(0.1s+1)}{(1.235s+1)} \\ \dfrac{3.48(s+77.6)}{(0.1s+1)\left(s^2+0.33s+226\right)} & 1 \end{bmatrix} \qquad (5.5)$$

in a block diagram, the plant G(s) , and the decoupler P(s) is shown in Fig. 5.14 below

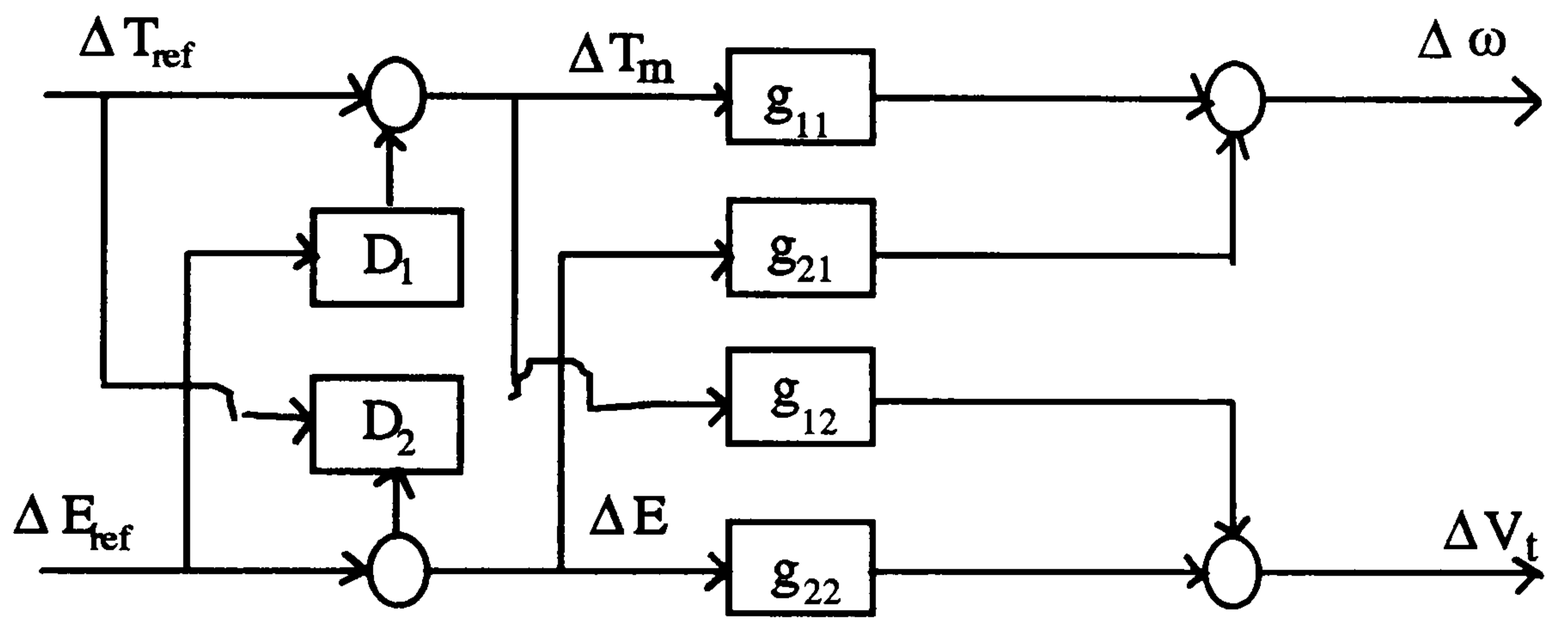

Fig. 5.14 a Turbogenerator system with a decoupler

From the machine data, the plant would not be expected to have a $\gamma(s)$ function near the (1,0) point; and although loading conditions are high, the effect of this high real power is offset by a very strong transmission line (tie line reactance Xe=0.1 pu).

After applying the pre-compensator, the new plant Q(s) is

$$Q(s)=G(s)\,.\,P(s)=\begin{bmatrix} g_{11} & g_{12} \\ g_{21} & g_{22} \end{bmatrix}\cdot\begin{bmatrix} 1 & D_1 \\ D_2 & 1 \end{bmatrix}=\begin{bmatrix} q_{11} & q_{12} \\ q_{21} & q_{22} \end{bmatrix} \qquad (5.6)$$

The $\gamma(s)$ function of the original plant and the $\gamma'(s)$ function of the pre-compensated plant are shown in Fig. 5.15 ; where it is observed that the pre-compensated plant has a very much smaller $\gamma(s)$ function, which means that, the pre-compensater has indeed reduced the cross-coupling effects in the original nominal plant model making it more diagonally dominant.

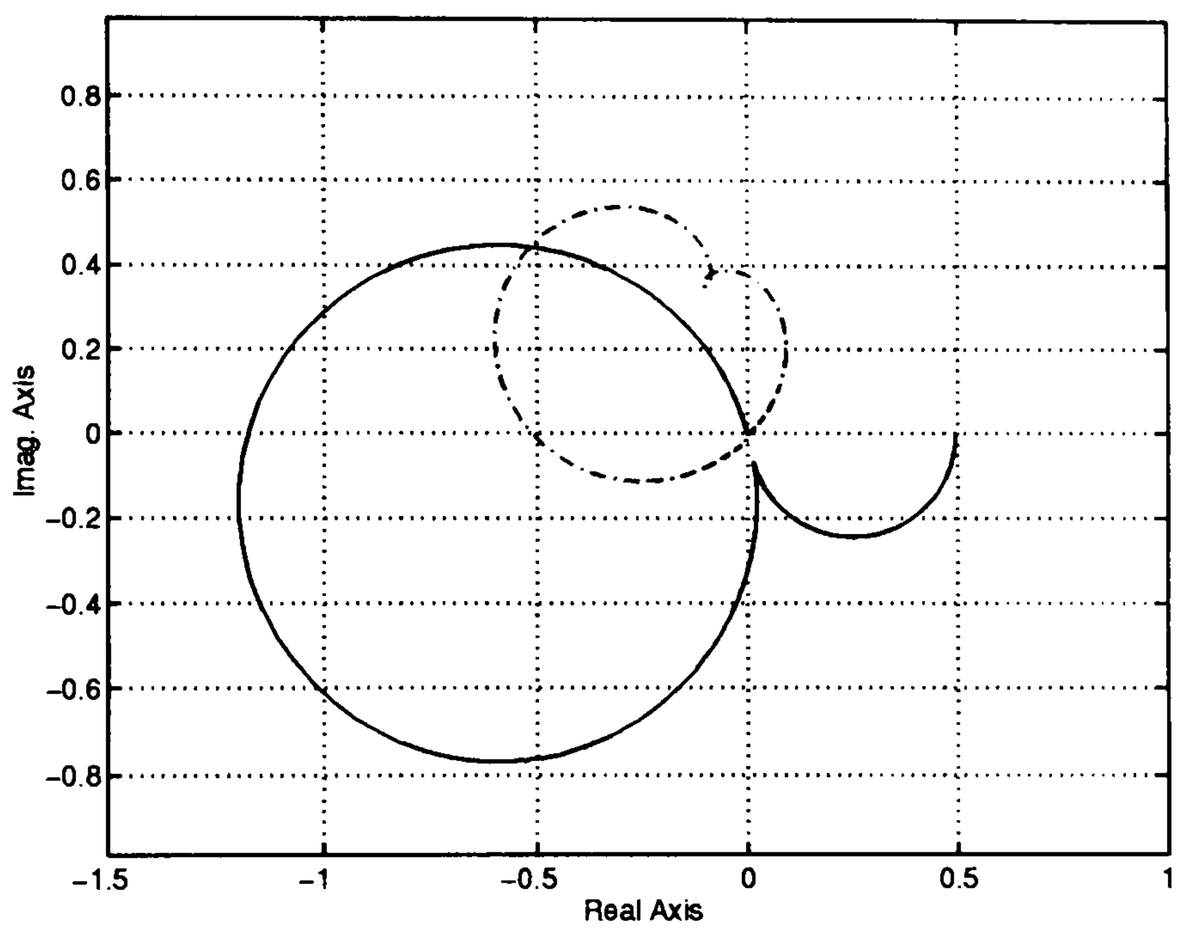

(————) nominal plant , (–·–·–·–·) compensated plant

Fig. 5.15 Nyquist plot of $\gamma(s)$

Nevertheless, the Bode plot of the $\gamma(s)$ of the uncompensated plant Fig. 5.16 shows some lack of robustness in the frequency range (12-18) rad/sec, where the switch-back characteristic occurs, Fig. 5.17.

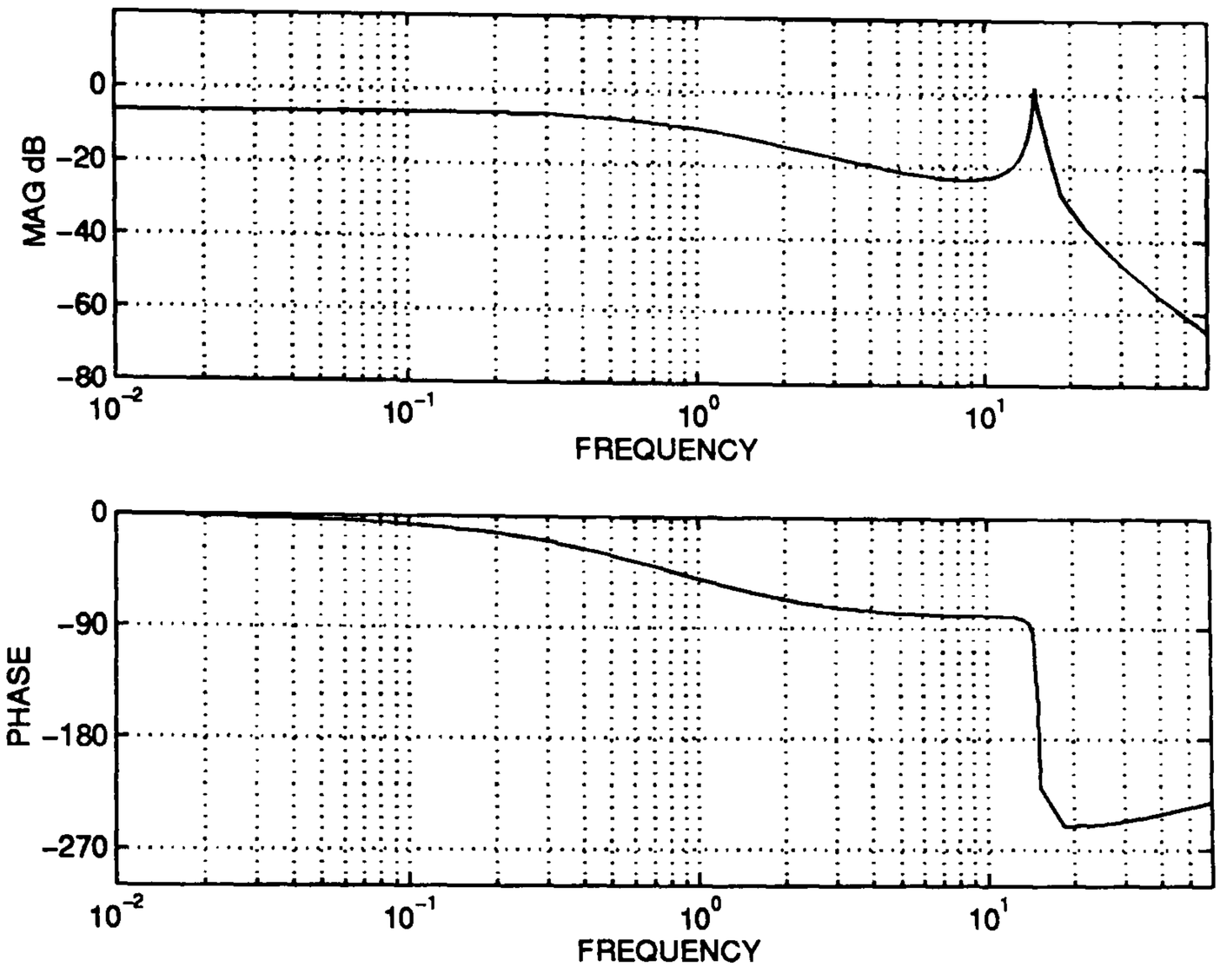

Fig. 5.16 Bode plot of $\gamma(s)$ for nominal plant

How is this pre-compensation effect compares to the power system stabiliser (PSS) effect discussed earlier in Chapter 4 ?. The answer lies in analysing the electrical subsystem g_{22} of the synchronous machine before and after the application of the pre-compensator.

The Bode plot of g_{22} (of the original plant) is shown in Fig. 5.17, where it is observed that the switch-back characteristic is not that severe. This is expected because the machine has a relatively small synchronous reactance and is connected to a strong transmission line (see Section 4.3, Chapter 4). The Bode plot of the electrical

subsystem of the pre-compensated plant q_{22} is shown in Fig. 5.18, together with g_{22} of the original plant.

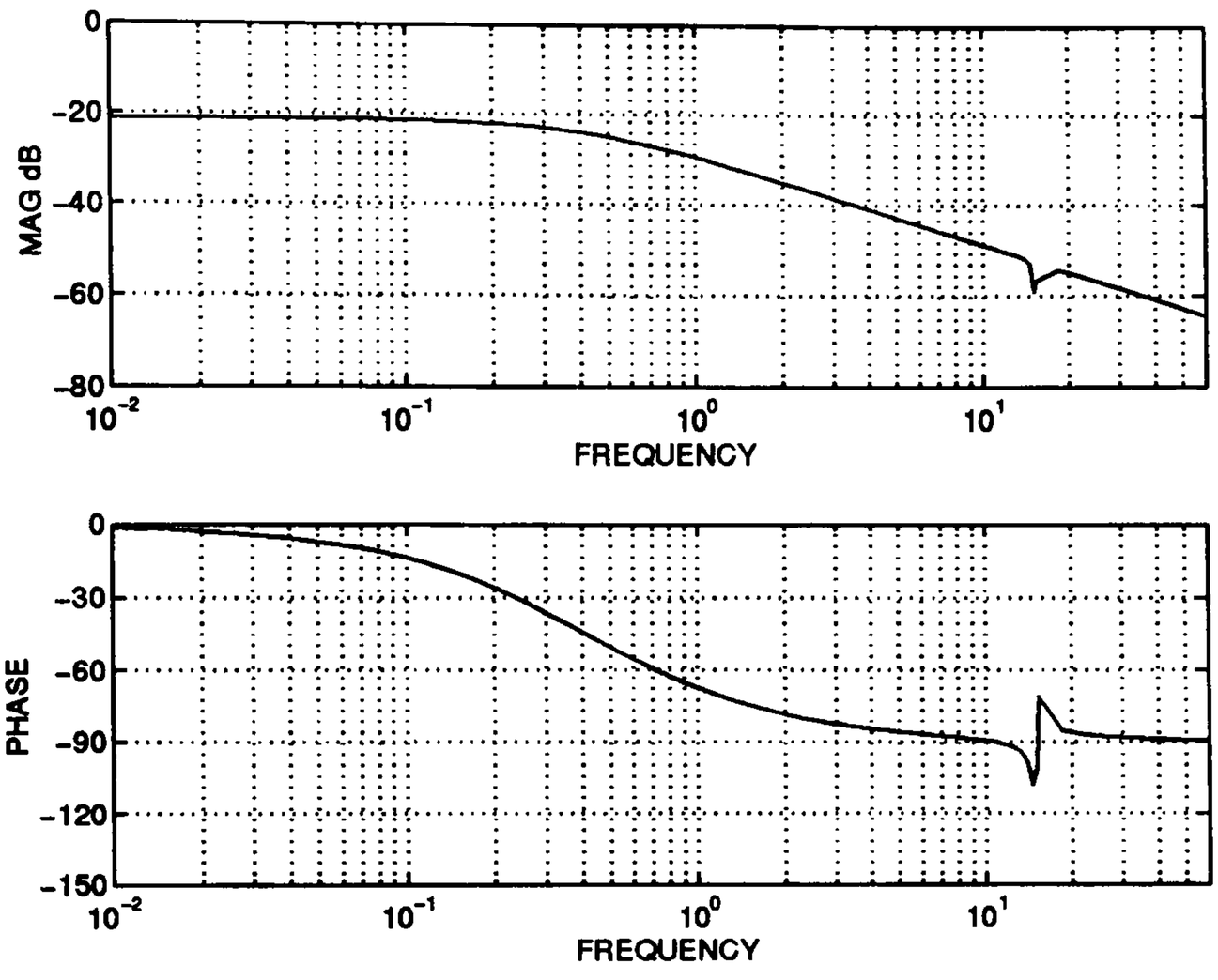

Fig. 5.17 Bode plot of g_{22} for the nopminal plant

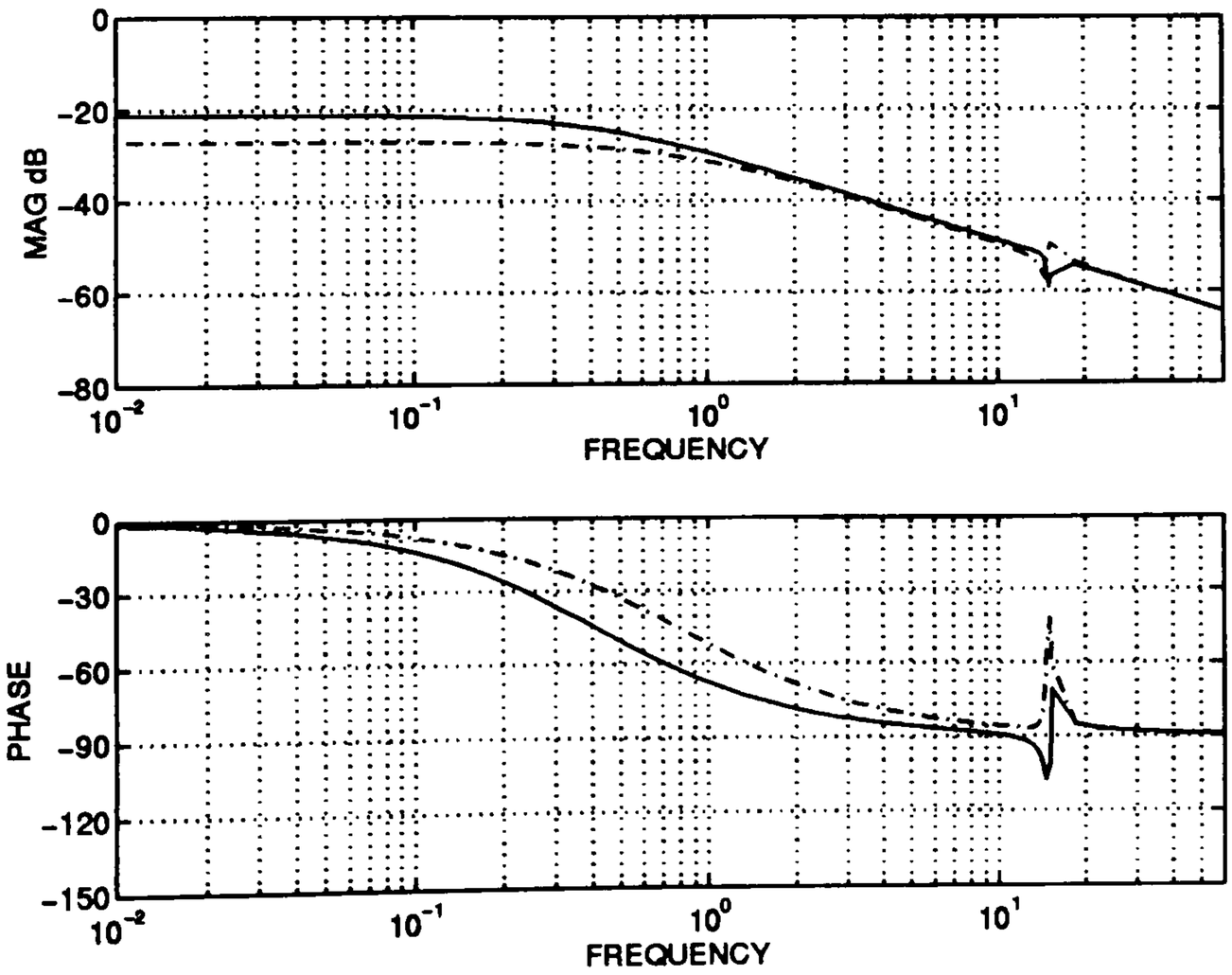

(———) g_{22}, (—·—·—·—) $g_{22} + pg_{12}$

Fig. 5.18 Bode plot of g_{22} and $g_{22} + pg_{12}$

It is clear that the switch-back characteristic, albeit very small, has been "buried" by the pre-compensator, thus permitting the very much sought after high gain of 50 pu or more to be used in the exciter/voltage loop without deteriorating the closed loop performance of the turbogenerator system.

A conventional turbine/governor is used to control the torque/speed loop of the form $[1/s(1+sT_g)(1+sT_t)]$, and this loop has a bandwidth less than 0.8 rad/sec. An exciter of the type IEEE-1s of the form $[K_e(1+sT_f)/(1+sT_f)(1+sT_e)+sK_eK_f]$ is used to control the second loop "exciter/voltage loop", and because of the presence of a direct gain reduction (DGR) in the exciter, the exciter/voltage loop has a bandwidth under 5 rad/sec.

The decoupler is used here for the sole purpose of disturbance rejection (the "switch-back" characteristic occurs at frequency above 10 rad/sec, while the exciter/voltage loop has a bandwidth less than 5 rad/sec.). That is, the decoupler reduces the effect of the excitation system input on the rotor speed output thus maintaining the synchronism of the power system; and the step response of the rotor speed output as affected by the excitation system input is shown in Fig. 5.19 for the system connected to a strong transmission line with and without the decoupler, and in Fig. 5.20 for the system

connected to a weak transmission line with and without the decoupler.

It is obvious that, the decoupler did indeed reduces the disturbance.

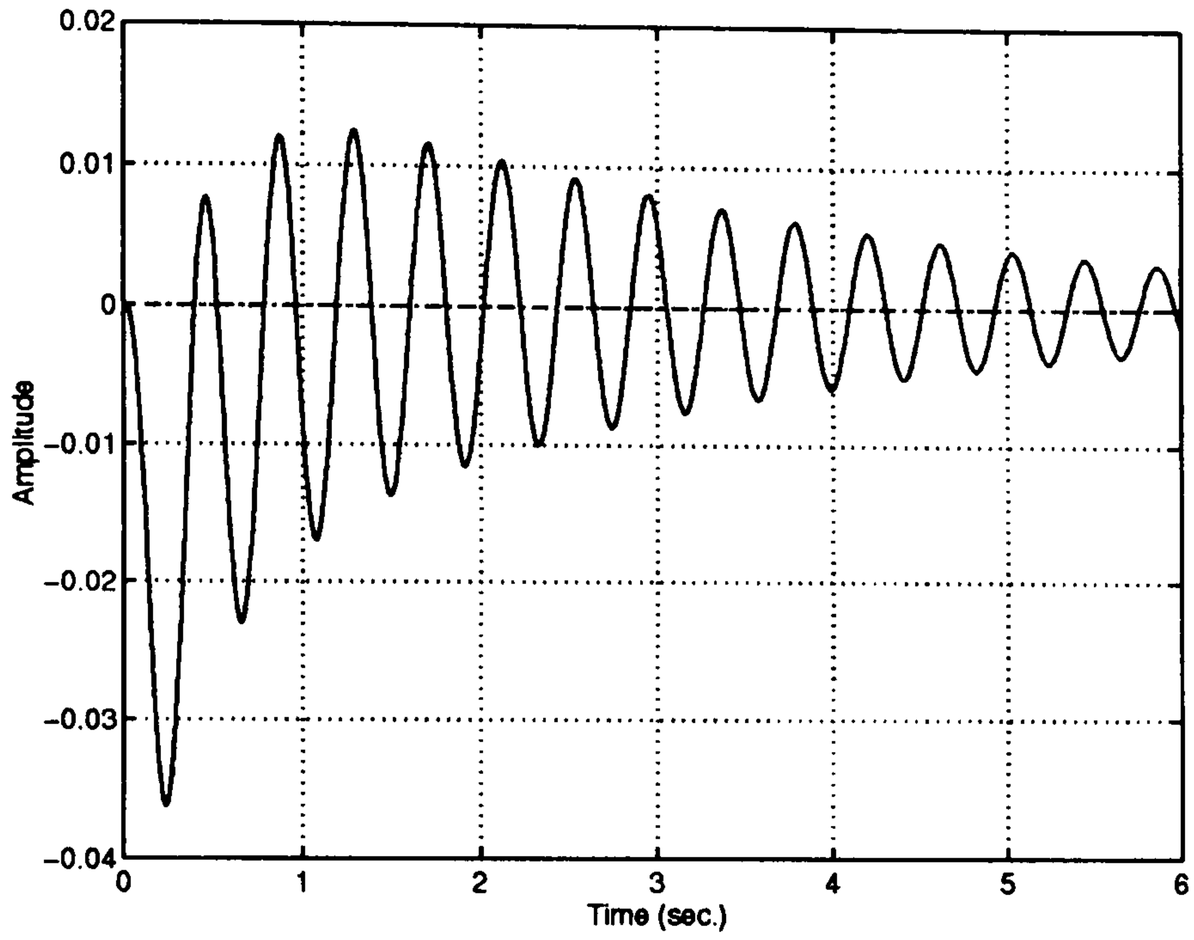

(———) un-compensated plant , (— - — - —-) compensated plant

Fig. 5.19 Effect of speed on volatge "strong tie-line case"

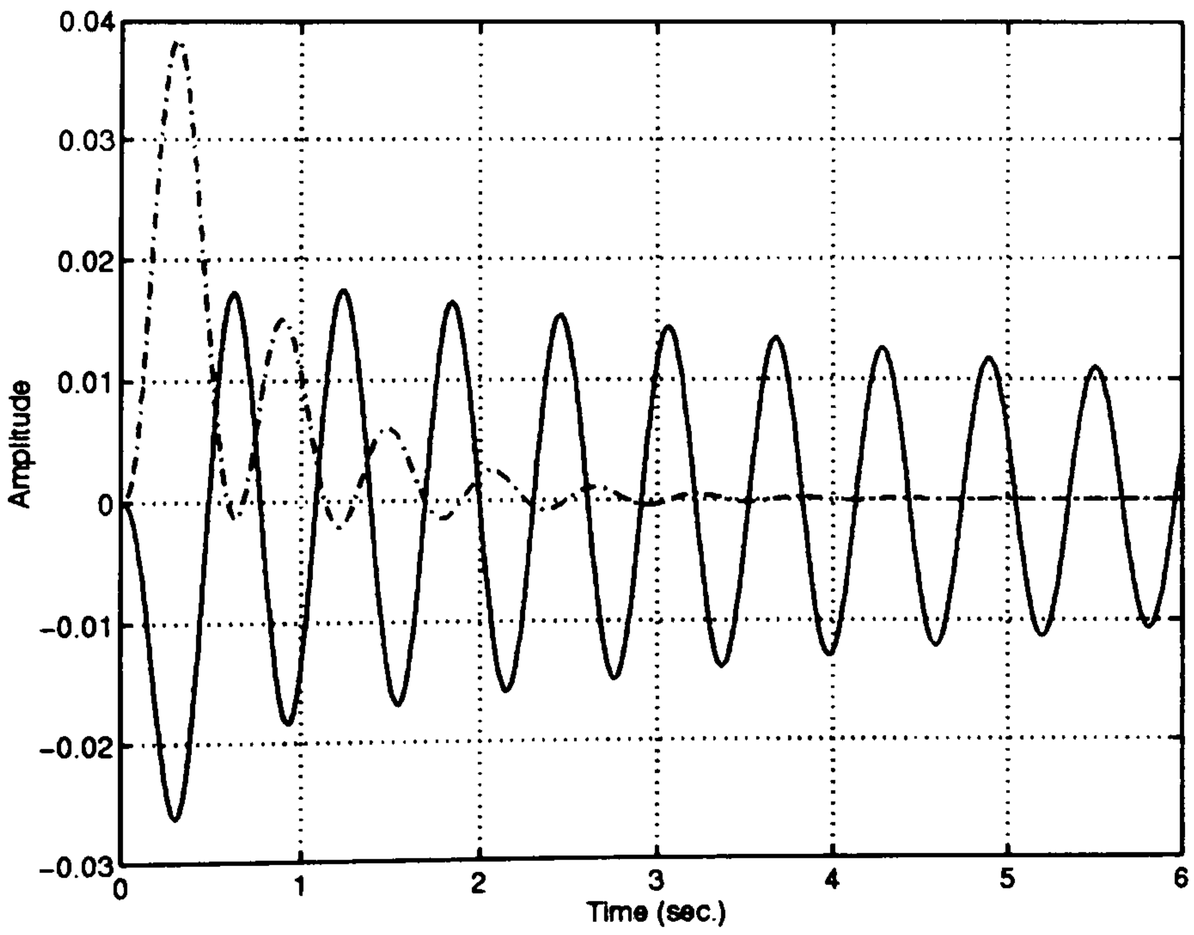

(———) un-compensated plant , (— - — - —) compensated plant

Fig. 5.20 Effect of speed on volatge "weak tie-line case"

5.4- *Non-diagonal control*

As mentioned in Chapter 2 and illustrated by examples in [36], the advantages of non-diagonal feedback control are not great, and there is no improvement in structure or robustness from non-diagonal feedback control beyond that attained by swapping the assignment of plant inputs to plant outputs. Nevertheless, the example of Section 5.3 shows some benefit in using a decoupler (pre-compensation), and in Chapter 4, Control option 2 also illustrate great advantages in using the PSS (post-compensation).

These advantages, however, are mainly due to the well-specified structure of the turbogenerator and its control specifications : By its well-defined structure, a small $\gamma(s)$ function for a turbogenerator model is always possible; e.g. if a high operating conditions (high real power) is required (leading to a strongly-coupled system), then a strong transmission line and/or a small pu synchronous reactance machine should be used (so, reducing the interconnection between the channels), also an increase number of damper windings in the synchronous machine will reduce the $\gamma(s)$ function. And with the $\gamma(s)$ function nowhere near the (1,0) point, then the system exhibits neither excessive phase sensitivity

nor excessive structural sensitivity, therefore the additional non-diagonal element will not increase the overall sensitivity.

On the other hand, in turbogenerator control specification, high-performance control (high channel bandwidth) is not a requirement for both channels, a considerable bandwidth separation exists between the two channels (the gov/speed loop, and the exciter/voltage loop), with only the latter requiring a high performance control. Some power system utilities use a Direct Gain reduction (DGR) in the exciter/voltage loop to ensure that the channel gain crossover frequency is well below the natural frequency of the mechanical mode of the turbogenerator (where the "switch-back" characteristic occur), hence eliminating the high-performance requirement even from this channel.

Chapter 6 : Conclusions

6.1- *Introduction*

Excitation/governor control with power system stabilisers (PSS) has been immensely successful for the control of turbogenerators connected to an infinite bus or as part of a multi-machine power system. This research provides a thorough multivariable analysis of a single turbogenerator system connected to an infinite bus using the control engineering analysis framework known as Individual Channel Analysis and Design (ICAD). This emphasis on the multivariable nature of the turbogenerator system, as compared with conventional power system analysis, provides a very interesting new interpretation of the small-signal (linearised) dynamical characteristics of a single machine connected to an infinite bus. Moreover, complete frequency-domain insight into the dynamic effects of machine and system parameters is made possible by their explicit parameterisation in the multivariable structure of what is a 2-input 2-output multivariable system.

6.2- *The Primary Result*

The main results concern the basic control function of the PSS and what control specification it sets out to achieve. First, it is shown that since the frequency response of the relatively slow governor/turbine channel rolls off above 1 rad/sec, the dynamic performance of the overall turbogenerator system is essentially determined by that of the electrical subsystem $g_{22}(s)$ in the typical

exciter frequency range of interest of 1 rad/sec to 10 rad/sec, [see Fig. 4.3]. Focusing therefore on the electrical subsystem $g_{22}(s)$, it is observed that its frequency response possesses the extremely awkward switch-back characteristic of a resonance (lightly damped left half-plane pole pair) closely followed by an inverted resonance (lightly damped left half-plane zero pair) round 7 rad/sec.

So, taking the above electrical subsystem frequency-response characteristics into account, what are the control specification options with or without the additional use of PSS ? If set point regulation of the terminal voltage and shaft speed are the only control requirements, then a relatively low excitation channel bandwidth of about 3 rad/sec suffices, well short of the awkward frequency characteristic at 7rad/sec. A PSS is not required. However, the sensitivity/disturbance rejection properties of the closed-loop excitation channel would be relatively poor. This is the first option and was the option exercised with smaller machines and smaller per unit synchronous reactance before the introduction of the PSS in the early 1960's [11].

A second control option is to seek an excitation channel bandwidth of up to 10 rad/sec; this is compatible with a control requirement to provide strong voltage disturbance rejection over this frequency range. But the lightly damped LHP zero pair round 7 rad/sec, shown in the frequency response of $g_{22}(s)$, prevents the attainment of the second option directly as discussed above. This is where the PSS

comes into play in a most ingenious way. The PSS transfer function multiplies the benign $g_{12}(s)$ subsystem transfer-function element (no lightly damped LHP zeros), so causing the electrical subsystem $g_{22}(s)$ to be amended to $g_{22}+pg_{12}$. In this way, the inverted notch characteristic of the PSS removes or dominates the problematic switch-back characteristic of the LHP pole-zero pairs round 7 rad/sec. In effect, an artificial system output is created which is the weighted sum of the terminal voltage output and the speed output. At low and high frequency, the artificial output is essentially terminal voltage; at frequencies round that of the LHP pole-zero pairs (7 rad/sec), the artificial output is dominated by the speed output. There is no longer any restriction on excitation channel bandwidth, as there was with the first option, needed to provide the required dynamical performance of $g_{22}+pg_{12}$ over the frequency range 0 to 10 rad/sec; the price paid in terms of the change of transient response of the terminal voltage round 7 rad/sec is small.

The PSS is shown to take the form of a non-diagonal (cross-coupled) system post-compensator on the terminal voltage and speed outputs. The price paid for the PSS post-compensator is that post-compensation leads to a general increase in system model uncertainty. In the case of PSS, it is established that the increase in system model uncertainty in the frequency range of interest (0 to 10 rad/sec.), under typical loading conditions, is not excessive.

This control interpretation as to the function of the PSS and the control specification it sets out to achieve in the face of a problematic machine dynamical characteristic is strikingly different from that afforded by conventional synchronising and damping torque analysis [24]. Interestingly, it is however supported by one other multivariable analysis carried out on the turbogenerator system [28], using the frequency-response methods of Rosenbrock and MacFarlane and pole-zero analysis. A similar mutlivariable control analysis to that carried out here could also be conducted into the use of stabilisers based on acceleration or electrical power feedback signals instead of the speed feedback based PSS [15].

A third and final control option considered is the use of excitation/governor control only with swapped input-output system pairings (system pre-compensation). While this third option has the advantages that a high bandwidth for the excitation channel can be used and the actual outputs are directly controlled unlike with the PSS, the option does suffer from two practical disadvantages: lack of system integrity in the face of actuator loop failure and the input of high-frequency signals to the governor. Consequently, the use of the conventional PSS remains the preferred option.

6.3- *Some Other Results*

Other results of the multivariable analysis of the turbogenerator system are as follows .

(a) It confirms that the system suffers an increasing lack of stability robustness to system uncertainty for increasing levels of real power P, in particular at heavy loading conditions in excess of P=0.9.

(b) It confirms that the system suffers an increasing lack of stability robustness to system uncertainty for increased values of synchronous reactance. For values of synchronous reactance in the usual range 1.6 pu to 2.6 pu, this is shown not to be a problem.

(c) For systems with a given synchronous reactance at a given operating condition, it is shown that the multivariable structures of the 3-rd order and 6-th order small-signal models are essentially the same, corroborating the widely held view that a 3-rd order model is adequate for control design.

(d) The multivariable structure of the turbogenerator system is encapsulated by the so-called multivariable structure function $\gamma(s)$. This is a scalar complex-frequency function, whose polar plot provides graphical information on the stability robustness to system uncertainty, in this case, the conventional use of excitation/governor control with PSS. Furthermore, for a 3-rd order turbogenerator model, the multivariable structure function $\gamma(s)$ is explicitly parameterised by all the key system parameters describing the machine dynamics.

6.4- *Future Work*

The multivariable analysis framework chosen, ICAD, provides a complete insight into why excitation/governor control with PSS has been so successful for

the control of turbogenerators connected to infinite bus. The multivariable analysis justifies treating the turbogenerator system as a pseudo-SISO system where the governor loop is first closed and the exciter loop is treated as a SISO system for the prime purpose of rejecting voltage disturbances. While the analysis has focused on the use of the PSS to remove local turbogenerator mode oscillation, due to an awkward frequency response characteristic round 1.2 Hz, it is readily extended to the use of the PSS to remove the slower inter-area mode oscillations in the frequency range 0.1 to 0.7 Hz [14] and the common low-frequency swing in the range 0.02 to 0.08 Hz [16]. Likewise, the use of notch filters to remove rotor torsional oscillations [13] and/or the use of additional compensation elements are all readily accommodated within the framework in a transparent and physically meaningful way. Furthermore, the approach lends itself to an examination of the effect of different tuning/gain scheduling strategies for the parameters of the PSS on the small-signal frequency-domain characteristics of the excitation channel in the neighbourhood of different system operating points.

The multivariable analysis framework itself is not confined to two-input two-output systems [68]. Also in future work, it would be of interest to analyse the performance of integrated control schemes for multi-machine power systems. Another area which deserve some attention is the desire to have a governor channel with bandwidth higher than 1 rad/sec, due to the ever growing technology of fast governing.

Appendix 1 : Bibliography

1 KIMBARK , EDWARD W., 'Power system stability Vol. I, II, III' John Wiley and sons Inc., N.Y. 1956.

2 ALDRED, A.S. and SHACKSHAFT, G. : 'A frequency-response method for the predetermination of synchronous machine stability' *Proc. IEE,* **Vol-105A**, 1959, pp 2

3 CONCORDIA, C. and BROWN, P.G. : 'Effects of trends in large steam turbine driven generator parameters on power system stability' *IEEE Trans* **PAS-89** , 1970, pp 2211

4 CONCORDIA, C. : ' Steady-state stability of synchronous machine as affected by voltage regulator characteristics' *AIEE.,* 1944 ,**Vol-63**, pp 215-220.

5 SCHLEIF, F.R. and WHITE, J.H. : ' Damping of northwest-southeast tie-line oscillations: an analogue study' *IEEE Trans.*, **PAS-85**, 1963, pp 1239-1247.

6 BERGEN, A. R. 'Power system analysis' Prentice-Hall Inc. 1986

7 KIMBARK , EDWARD W, : 'Improvement of power system stability by changes in the Network' *IEEE trans*, **PAS-88**, No. 5, 1969, pp 773-778

8 PARK, R.H. : 'Two-Reaction theory of synchronous machine pt 1&2' *trans. AIEE* , 1929 , **Vol-48**, pp 716-730.

9 DANDENO, P. L., KARAS, A.M., McCLYMONT, K.R., and WATSON, W.: 'Effect of high speed rectifier excitation systems on generator stability limits' *IEEE trans.*, 1968, **PAS-87**, pp 190-201.

10 SCHEIF, F.R., HUNKINS, H.D., MARTIN,G.E., and HAFFAN, E.: 'Excitation control to improve power line stability' *ibid.*, 1968, **PAS-87**, pp 1426-1434.

11 DEMELLO, F.P., and CONCORDIA, C. : 'Concepts of synchronous machine as effected by excitation control' *ibid.*, 1969, **PAS-88**, pp 316-328.

12 LI WANG ' A comparative study of damping schemes on damping generator oscillations' *IEEE Trans.*, **PWRS-8**, No. 2, 1993, pp 613-619.

13 KUNDUR, P., LEE, D.C., and ZEINELDIN, H.M. : 'Power system stabiliser for thermal units: Analytical techniques and on-site validations' *IEEE trans.*, 1981, **PAS-100**, pp 81-95.

14 KUNDUR, P., KLEIN, M., ROGERS, G.J., and ZYWNO, M.S. : 'Application of power system stabilisers for enhancement of overall system stability' *IEEE trans.*, 1989, **PWRS-4** , pp 614-626

15 LARSEN, E.V., SWANN, D.A.: 'Applying power system stabilisers pt. I, II and III' *IEEE Trans*, **PAS-100**, 1981, pp 3017-3046.

16 GRONDIN, R., KAMWA, I., SOULIERES, L., POTVIN, J., and CHAMPAGNE, R.,: 'An approach to PSS design for transient stability improvement through supplementary damping of the common low-frequency' *IEEE trans.*, 1993 **PWRS-8**, pp 954-963.

17 GIBBARD, M.J. 'Robust design of fixed-parameter PSS over a wide range of operating conditions' *IEEE trans.*, 1991, **PWRS-6**, pp 794

18 CHEN, S. and MALIK, O.P. : 'PSS design using μ synthesis' *IEEE trans.*, **EC-10**, No. 1, 1995, pp 175.

19 El-MATWALLY, K.A. ; HANCOCK, G.C ; and MALIK, O.P. : 'Implementation of a fuzzy logic PSS using a micro-controller' *ibid*, **EC-11**, No.1, 1996, pp 91-117.

20 YOUNG-MOON PARK and Y. LEE ' A self-organising PSS using fuzzy ARMA model' *ibid,* **EC-11**, No.2, 1996, pp 442-447.

21 ANDERSON, P., and FOUAD 'Power system control and stability' (Iowa state university Press, 1977, Ames.)

22 YAO, Y. N.,: 'Electric Power System Dynamics' (Academic Press, 1983, New York).

23 GUPTA, D.P., NARAHARI, N.G., BOYD, I., and HOGG, B. : 'An adaptive power system stabiliser which cancels the negative damping torque of a synchronous generator' *Proc. IEE* , 1985, **Vol-132**. pp 109-117.

24 KUNDUR, P.,: 'Power system stability and control' (McGraw-Hill 1994, NewYork)

25 HUGHES, F.M. : 'Improvement of turbogenerator transient performance by control means' *Proc. IEE* , 1973, **Vol-120**, pp 233-240.

26 CHOW, J.H., HARRIS, L.P., OTHMAN, M.A., and SANCHEZ-GASCA, J. : 'Robust control design of power system stabilisers using multivariable frequency domain technique' *Proc. of the 29th conf. on Decision and Control*, 1993 , Honolulu, HI, pp 2067-2073.

27 CHEN, S.; and MALIK, O.P. : ' H_∞ optimisation-based PSS design' *Proc-IEE*, Pt.C, **Vol-142**, No. 2, 1995, pp 179.

28 HAMDAN, A.M., and HUGHES, F.M. : 'Analysis and design of power system stabiliser' *International Journal of Control.*, 1977, **Vol-26**, pp 769-782.

29 ROSENBROCK, H.H. : 'Design of multivariable control system using the inverse Nyquist Array' *Proc-IEE*, **Vol-116**, No.11, 1969, pp 1929-1936.

30 MacFARLANE, A.G.J. : ' Multivariable control system design techniques: a guided tour' *Proc-IEE*, **Vol-117**, 1972, pp 1039-1047.

31 HANSON, C.W. ; GOODWIN, C.J.; and DANDENO, L.P. : ' Influence of excitation and speed control parameters in stabilizing intersystem oscillations' *IEEE Trans*, **PAS-87**, 1968, pp 1306-1313

32 SCHIER, R.M.; and BLYTHE, A.L. : 'Field tests of dynamic stability using a stabilising signal and computer program varifications' *IEEE Trans*, **PAS-87**, 1968, pp 315-322.

33 O'REILLY, J., and LEITHEAD, W.E. : 'Multivariable control by Individual Channel Design' *International Journal of Control*, 1991, **Vol-54**, pp 1-46.

34 LEITHEAD, W.E and O'REILLY, J : 'Performance issues in the individual channel design of 2-input 2-output systems : pt 1 structural issues' *ibid*, 1991, **Vol-54**, pp 47-82.

35 ROBERTSON, S., LEITHEAD, W.E., and O'REILLY, J. 'Graphically based multivariable frequency domain package' *Proc. EURACO Workshop on Recent Results in Robust and Adaptive Control*, September 1995, Florence, pp11-14.

36 LEITHEAD, W.E.,and O'REILLY, J. : 'Performance issues in ICD of 2-input 2-output system pt-3 :Non-diagonal control and related issues' *International Journal of Control*, 1992 , **Vol-55**, pp 265-312.

37 LICEAGA-CASTRO, J.; VERDE, C. ; O'REILLY, J., and LEITHEAD, W.E : ' Heliocopter flight control by ICD' *Proc-IEE*, pt. D, **Vol-142** , 1995, pp 58-72

38 LICEAGA-CASTRO, E.; and VANDERMOLEN, G. : 'A submarine depth control system design' *International Journal of Control*, No.1 1995, **Vol-61**, pp 279-308.

39 DOHERTY, R.; and NICKLE, C. : 'Synchronous machine I & II' *AIEE Trans.*, **Vol-45**, 1926, pp 912-942.

40 SHACKSHAFT, G.; and HENSER, P. : ' Model of generator saturation for use in power system studies' *Proc-IEE*, **Vol-126**, No.8, 1979, pp 759-763.

41 IEEE task force : 'Current usage and suggested practices in power system stability simulation for synchronous machines' *IEEE Trans*, **EC-1**, No.1, 1986, pp 77-93

42 CONCORDIA, C.: ' Synchronous machines: theory and performance' John Wiley and sons Inc. N.Y. 1951

43 BUSBY, E.L.; HURLY, J.; KEAY, F.W.; and RACZKOWSKI, C. : 'Dynamic stability improvement at Monticello station-Analytical study and field tests' *IEEE trans.*, 1977 , **PAS-98**, pp 889-897.

44 DANDENO, P. ; SCHULTZ, R.P. : ' Effects of synchronous machine modelling in large-scale system studies' *IEEE Trans.*, **PAS-92**, 1973, pp 574-582.

45 AHSON, S.I. : 'Multivariable control of turboalternator' **Ph.D. Thesis**, University of Sheffeild, UK, 1975.

46 SCHULTZ, R.P. : 'Synchronous machine modelling' in **IEEE Publication** *Adequacy and Philosophy of Modelling System Dynamic Performance*, 1972

47 DAVISON, E.J., and RAO, N.S. : 'The optimal output feedback control of a synchronous machine' *IEEE trans.*, 1971, **PAS-90**, pp 2123-2133.

48 HEFFERON, W.G., and PHILIPS, R.A. : 'Effect of a modern voltage regulator on under-excited operation of large turbine generator' *AIEE trans.*, 1952, **PAS-71**, pp 692-697.

49 SHSCKSHAFT, G. 'General-purpose turboalternator model' *Proc-IEE*, **Vol-110**, No.4, 1963, pp 703-713

50 AHSON, S.I., and NICHOLSON, H. : 'Improvement of turbo-alternator response using the Inverse Nyquist Array methods' *International Journal of Control*, 1976 , **Vol-23**, pp 657-672.

51 LAUGHTON, M.A. 'Matrix analysis of dynamic stability in synchronous multimachine systems' *Proc-IEE*, **Vol-113**, 1966, pp 325-336.

52 AGGOUNE, M.E., BOUDJEMA, F., and BENSENOUCI : 'Design of variable structure voltage regulator using pole assignement technique' *IEEE trans.*, **AC-39**, No. 10, 1994, pp 2106.

53 SAIDY, M., HUGHES, F. 'Block diagram transfer function model of generator including damper winding' *Proc-IEE*, **Vol-141**, No.6, 1994, pp 599-608

54 BAYNE, J., KUNDUR, P., WATSON, W. 'Static exciter control to improve transient stability' *IEEE Trans*. **PAS-94**, No.4, 1975, pp 1141-1146

55 IEEE Committee Report 'Excitation system models for power system stability studies' *IEEE Trans*. **PAS-100**, 1981, pp494-509.

56 WOODWARD, J. 'Hydraulic-turbine transfer function for use in governing studies' *Proc-IEE* **Vol-115**, No.3 1968, pp 424-426.

57 IEEE Committee Report 'Dynamic models for steam and Hydro turbines in power system studies' *IEEE Trans*. **PAS-92**, 1973, pp 1904-1915.

58 COOWAR, F., MAGDY, M., and GRAINGER, W.: 'Decoupling negative damping signals in a power system through Dynamic Gain Reduction measures' *IEEE-Trans*, **PWRS-7**, No 3, 1992, pp 1279-1284.

59 AHSON, S.I., and NICHOLSON, H. :'Inverse Nyquist Array design with minimum sensitivity' *Proc. IEE* , 1977, **123**, pp 457-461.

60 SALEH, A., and El-SHARBINI, M.K. 'Optimal design of an overall controller of saturated synchronous machine' *IEEE Trans*. **PAS-102**, 1983, pp 1651-1657

61 El-SHARBINI, M.K., and MEHTA, D. 'Dynamic system stability pt I' *IEEE Trans*. **PAS-92**, 1973, pp 1538-1546

62 HAMDAN, A.M.A. : 'Vector frequency response control applied to turbo-alternator control' **Ph.D. Thesis**, University of Machester, *UMIST*, 1977 , UK

63 HARELY, R.G., LAHOUD, M.A., and SECKER, A. : ' Optimal and multivariable control of a turbogenerator' models' *Electric power System research*, **Vol-10**, 1986, pp 35.

64 AHSON, S.I., and HOGG, B.W. : 'Application of multivariable frequency response methods to control of turbogenerator' *International Journal of Control*, 1979, **Vol-30**, pp 533-548.

65 HUGHES, F. and HAMDAN. A.M. 'Design of turboalternator excitation controllers using mutlivariable frequency-response methods' *Proc-IEE*, **Vol-123**, No. 9 1976, pp 901-905

66 FENWICK, D.R., and WRIGHT, W.F. : 'Review of trends in excitation systems and possible future development' *ibid.* , 1976 , **Vol-123**, pp 413-420.

67 VOURNAS, C.D., and PAPADIAS, B.C. : 'Excitation control schemes in the Hellenic Interconnected system for the improvement of system dynamic performance' *CIGRE paper 39-50*, 1984, Paris, France

68 LEITHEAD, W.E., and O'REILLY, J. : 'm-Input m-Output feedback control by ICD pt-1: structural issues' *International Journal of Control*, 1992 , **Vol-56**, pp 1347-1397.

69 El-SHARBINI, M.K. and El-SERAIFI , A.M. : 'Analysis of dynamic performance of a staurated machine and analog simulation' *IEEE Trans*. **PAS-101**, No. 7, 1982, pp 1899-1906.

70 BYERLY, R.T., and KIMBARK, W. :' Stability of large Electric Power Systems' **IEEE Press** Book, IEEE, N.Y. 1974.

71 DILLMAN, T., SKOOGLUND, J.W., KEAY, F., SOUTH , W. and RACZKOWSKI, C.'A high initial response brushless excitation system' *IEEE Trans*. **PAS-90**, 1971, pp2089-2094.

72 HURLY, J.D., and BALDWIN, M.S. 'High-response excitation systems on turbine generators: a stability assessement' *IEEE Trans*. **PAS-101**, No. 11, 1982, pp 4211-4221.

73 SAKAR, M., SOLIMAN, M. and El-SHARBINI, M.K. 'Power system control with minimum eignvalue sensitivity to operating conditions' *Computer & Electrical Engineering*, **Vol-13**, No. 13, 1987, pp 139-146.

74 CHOW, J.H. and SANCHEZ-GASCA, J.J.: 'Pole-placement designs of Power Systems Stabilisers' *IEEE trans.*, **PWRS-4**, No. 1, 1989, pp 271-278.

75 WANG, H.F., SWIFT, F.J., HOGG, B.W., CHEN, H. and TANG, G.: 'Rule-based variable-gain power system stabiliser' *Proc.IEE*, pt-C, 1995, **Vol-142**, No1, pp. 29-32.

76 KLIEN, M.; LE, L.X.; ROGERS, G.; FARROKHPAY, S.; BALU, N.: ' H_∞ damping controller design in large power systems' *IEEE trans.*, **PWRS-10**, No. 1, 1995 pp 158-166.

77 SAIDY, M., HUGHES, F. 'Performance improvement of a conventional PSS' *Electrical Power & Energy Systems*, **Vol-17**, 1995, pp 313-323.

78 LIMBEER, D., and HARLEY, R.G. : 'Synchronous machine stability using compsite governor and volatge regulator models' *Electric power System research*, **Vol-**1, 1977, pp 97.

79 PAPADOPOULOS, D. and PARASKEVOPOULOS, N. ' Design of a controller for an unregulated synchronous machine' *Proc-IEE*, **Vol-132**, 1985, pp 277-280.

80 WENYAN Gu, and BOLLINGER, K.E. ' A decoupler design method for synchronous machine infinite-bus system' *IEEE Trans*. **EC-4**, 1989, pp 54-61.

Appendix 2 : *Nomenclature*

Voltages, currents and fluxes

e_d : direct-axis armature voltage

e_q : quadrature-axis armature voltage

e_o : infinite bus voltage

E_{fd} : generator field voltage

E_{qo} : voltage proportional to direct-axis flux linkage

I_{fd} : generator field current

i_d : direct-axis armature current

i_q : quadrature-axis armature current

ψ_{fd} : field flux linkage

V_t : generator terminal voltage

ψ_d : direct-axis flux linkage

ψ_q : quadrature-axis flux linkage

P : real power

Q : reactive power

Reactances, resistances

x_d : direct-axis synchronous reactance

x_q : quadrature-axis synchronous reactance

x'_d : direct-axis transient reactance

R : machine stator resistance

G : resistive part of per phase parameter

B : reactive part of per phase parameter

x_e : machine stator reactance

δ : rotor angle

θ : angular position of direct-axis with respect to stator

ω : speed

ω_o : synchronous speed

T'_{do} : field open circuit time constant

T'_{dz} : effective field time constant under load

The subscript zero denotes an initial operating condition. Δ quantities denotes small changes about an initial operating point.

Mechanical symbols

T_m : mechanical torque

M : inertia constant (6 s)

D : damping constant (3 pu)

Exciter symbols

k_e : exciter gain

T_e : exciter time constant

V_{ref}: voltage input to the exciter

Governor/turbine

k_g : governor gain

T_g : governor time constant

T_t : turbine time constant

U_g: speed input to the governor

Appendix 3 : *Derivation of the small-signal 3-rd order synchronous machine model of Fig. 3.4 (equations (3.11) to (3.13))*

The general equations describing the performance of machine with no damper windings and connected to an infinite bus system, shown in Fig. A1, are [8],[22],[48] :

$$e_d = \dot{\psi}_d - \psi_q \dot{\theta} \tag{A1}$$

$$e_q = \dot{\psi}_q + \psi_d \dot{\theta} \tag{A2}$$

$$e_d = x_e \dot{i}_d - x_e i_q \dot{\theta} + e_o \sin\delta \tag{A3}$$

$$e_q = x_e \dot{i}_q + x_e i_d \dot{\theta} + e_o \cos\delta \tag{A4}$$

$$\psi_d = I_{fd} - x_d i_d \tag{A5}$$

$$\psi_q = -x_q i_q \tag{A6}$$

$$M\ddot{\theta} = T_m - \psi_d i_q + \psi_q i_d - D(\dot{\theta} - 1) \tag{A7}$$

$$\psi_{fd} = I_{fd} - (x_d - x'_d) i_d \tag{A8}$$

$$E_{fd} = I_{fd} + T'_{do} \dot{\psi}_{fd} \tag{A9}$$

$$V_t^{\,2} = e_d^{\,2} + e_q^{\,2} \tag{A10}$$

A particular initial operating point is assigned and the equations are rewritten to consider the effect of small Δ changes in currents, voltages, and so forth about their values at this point. The result is the following set of linear differential equations:-

$$\Delta e_d = [\dot{\psi}_d] - \Delta\psi_q - [\psi_{qo} \Delta\dot{\delta}] \tag{A11}$$

$$\Delta e_q = [\dot{\psi}_q] + \Delta\psi_d + [\psi_{do}\Delta\dot{\delta}] \tag{A12}$$

$$\Delta e_d = [x_e \Delta \dot{i}_d] - x_e \Delta i_q + (e_o \cos\delta_o)\Delta\delta - [i_{qo} x_e \Delta\dot{\delta}] \tag{A13}$$

$$\Delta e_q = [x_e \Delta \dot{i}_q] + x_e \Delta i_d - (e_o \sin\delta_o)\Delta\delta + [i_{do} x_e \Delta\dot{\delta}] \tag{A14}$$

$$\Delta\psi_d = \Delta I_{fd} - x_d \Delta i_d \tag{A15}$$

$$\Delta\psi_q = -x_q \Delta i_q \tag{A16}$$

$$(\ddot{M} + \dot{D})\Delta\delta = \Delta T_m - \psi_{do}\Delta i_q - i_{qo}\Delta\psi_d + \psi_{qo}\Delta i_d + i_{do}\Delta\psi_q \tag{A17}$$

$$\Delta\psi_{fd} = \Delta I_{fd} - (x_d - x'_d)\Delta i_d \tag{A18}$$

$$\Delta E_{fd} = \Delta I_{fd} + T'_{do}\Delta\dot{\psi}_{fd} \tag{A19}$$

$$\Delta V_t = \frac{e_{do}}{V_{to}}\Delta e_d + \frac{e_{qo}}{V_{to}}\Delta e_q \tag{A20}$$

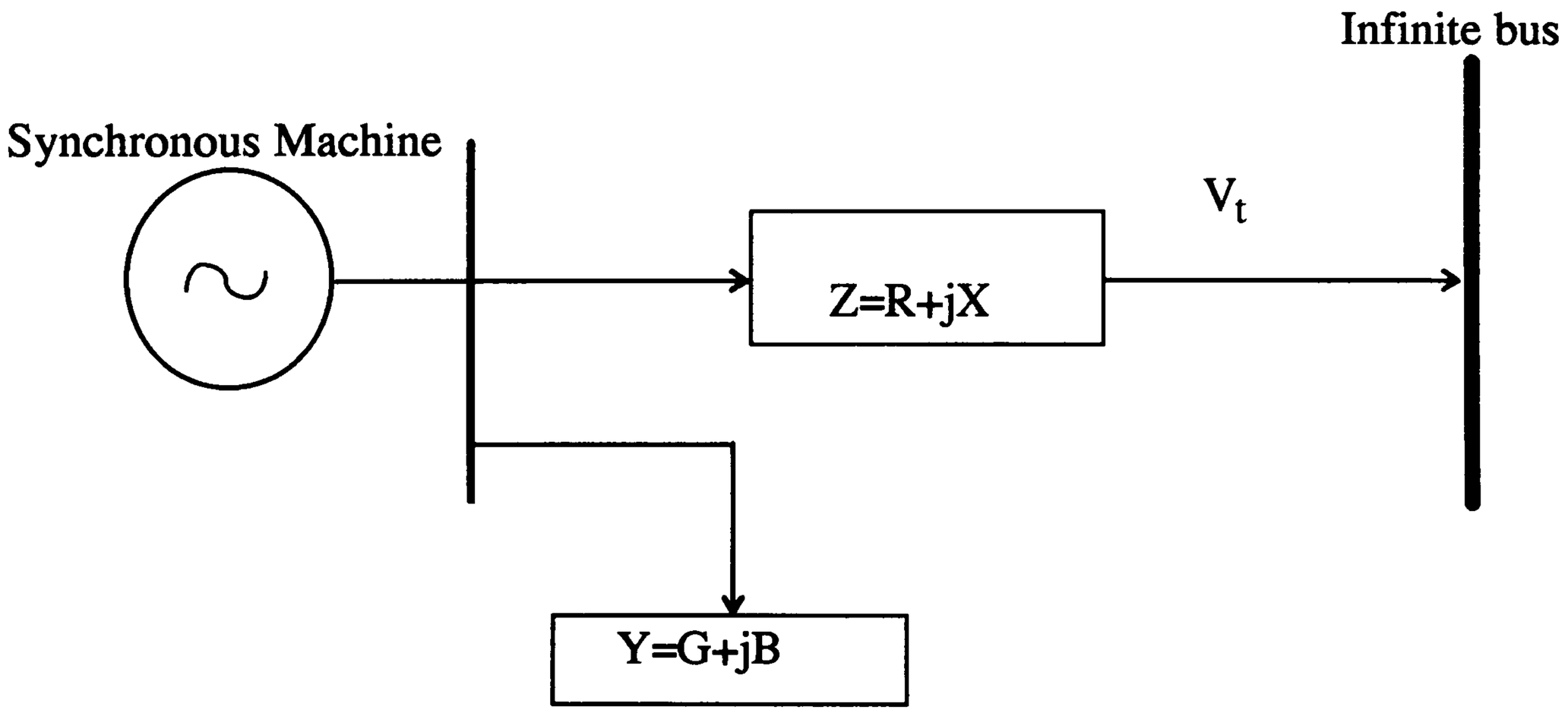

X=0.4 pu, R=G=B=0

Fig. A1 Single machine connected to an infinte bus [22]

The eight terms in brackets [equations (A11) to (A14)] are neglected; this is justified, because the quantities neglected have negligible effect [48]. Next, all variables except ΔV_t, $\Delta\delta$, $\Delta\psi_{fd}$, ΔT_m, and ΔE_{fd} are eliminated leaving three equations in three unknowns. ΔE_{fd} and ΔT_m are independent variables. The three final equations in ΔV_t, $\Delta\delta$, and $\Delta\psi_{fd}$ are :

$$(\ddot{M}+\dot{D})\Delta\delta = \Delta T_m - \frac{e_o \sin\delta_o}{x'_d + x_e}\Delta\psi_{fd} - \left[\frac{E_{qo} e_o \cos\delta_o}{x_e + x_q} + \left(\frac{e_{do} e_o \sin\delta_o}{x'_d + x_e}\right)\left(1 - \frac{x'_d}{x_q}\right)\right]\Delta\delta \qquad \text{(A21)}$$

$$\Delta\psi_{fd} = \frac{1}{1+\dot{T}'_{dz}}\left[\frac{x'_d + x_e}{x_e + x_d}\Delta E_{fd} - \frac{x_d - x'_d}{x_e + x_d} e_o \sin\delta_o \Delta\delta\right] \qquad \text{(A22)}$$

$$\Delta V_t = \frac{e_{qo}}{V_{to}}\frac{x_e}{x'_d + x_e}\Delta\psi_{fd} + \left[\frac{x_q}{x_e + x_q}\frac{e_{do}}{V_{to}} e_o \cos\delta_o - \frac{x'_d}{x'_d + x_e}\frac{e_{qo}}{V_{to}}\sin\delta_o\right]\Delta\delta \qquad \text{(A23)}$$

$$\text{where } T'_{dz} = \frac{x'_d + x_e}{x_d + x_e} T'_{do} \qquad \text{(A24)}$$

and if we define :

$$K_1 = \frac{E_{qo} e_o \cos\delta_o}{x_e + x_q} + \left(\frac{e_{do} e_o \sin\delta_o}{x'_d + x_e}\right)\left(1 - \frac{x'_d}{x_q}\right) \qquad \text{(A25)}$$

$$K_2 = \frac{e_o \sin\delta_o}{x'_d + x_e} \qquad \text{(A26)}$$

$$K_3 = \frac{x'_d + x_e}{x_d + x_e} \qquad \text{(A27)}$$

$$K_4 = \frac{e_o \sin\delta_o}{x'_d + x_e}(x_d - x'_d) \qquad \text{(A28)}$$

$$K_5 = \frac{x_q}{x_e + x_q}\frac{e_{do}}{V_{to}} e_o \cos\delta_o - \frac{x'_d}{x'_d + x_e}\frac{e_{qo}}{V_{to}} e_o \sin\delta_o \qquad \text{(A29)}$$

$$K_6 = \frac{e_{qo}}{V_{to}}\frac{x_e}{x'_d + x_e} \qquad \text{(A30)}$$

Then, the 3-rd order small-signal model, consistent with equations (3.11) to (3.13) or Fig. 3.4, is as follows :

$$(\ddot{M} + \dot{D})\Delta\delta = \Delta T_m - K_2\Delta\psi_{fd} - K_1\Delta\delta \qquad \text{(A31)}$$

$$\Delta\psi_{fd} = \frac{K_3}{1 + K_3\dot{T}'_{do}}(\Delta E_{fd} - K_4\Delta\delta) \qquad \text{(A32)}$$

$$\Delta V_t = K_6\Delta\psi_{fd} + K_5\Delta\delta \qquad \text{(A33)}$$

The 3-rd order small-signal model of equations (A31) to (A33) for a single synchronous machine connected to an infinite bus is defined by the parameters K_1 to K_6 of equations (A25) to (A30). These parameters in turn are determined by the initial currents, voltages and torque angle as follows .

The initial currents, voltages and torque angle in steady-state are usually found from a load flow study for a multi-machine system. For a single-machine infinite-bus system, they can be calculated as follows [22].

Given real and reactive power P and Q and the machine terminal voltage V_{to} we have :

$$P + jQ = (i_d + ji_q) * (e_d + je_q) \qquad \text{(A34)}$$

From equation (57) above ,

$$P = i_d e_d + i_q e_q \qquad \text{(A35)}$$

and

$$Q = i_d e_q - i_q e_d \tag{A36}$$

Also we have

$$e_d = x_q i_q \tag{A37}$$

$$e_q = E_{qo} - x'_d i_d \tag{A38}$$

$$V_t^{\,2} = e_d^{\,2} + e_q^{\,2} \tag{A39}$$

From these five independent equations, e_d, e_q, i_d, i_q, and Eqo can be calculated.

Thus :

$$e_d = \frac{PV_t}{\sqrt{P^2 + \left(Q + \frac{V_t^{\,2}}{x_q}\right)^2}} \tag{A40}$$

$$e_q = \sqrt{\left(V_t^{\,2} - e_d^{\,2}\right)} \tag{A41}$$

$$i_q = \frac{e_d}{x_q} \tag{A42}$$

$$i_d = \frac{\left(P - i_q e_q\right)}{e_d} \quad \text{or} \quad \frac{\left(Q + i_q e_d\right)}{e_q} \tag{A43}$$

$$E_{qo} = e_q + x'_d i_d \tag{A44}$$

The initial values of e_o (infinite bus voltage) and δ_o (rotor angle) remain to be determined. From Fig. A1, we define [22]

$$C_1 = 1 + RG - XB \tag{A45}$$

$$C_2 = XG - RB \tag{A46}$$

where $X = x_e$ and $R = G = B = 0$. Also we have

$$V_{od} = C_1 e_d - C_2 e_q - R i_d + X i_q \tag{A47}$$

$$V_{oq} = C_2 e_d + C_1 e_q - X i_d - R i_q \tag{A48}$$

Then

$$e_o = \sqrt{V_{od}{}^2 + V_{oq}{}^2} \tag{A49}$$

$$\delta_o = \tan^{-1}\left(\frac{V_{od}}{V_{oq}}\right) \tag{A50}$$

From (A40) to (A50) with V_t=1.0 pu, X=0.4 pu and R=G=B=0 and a given P and Q the machine parameters K_1 to K_6 are determined using equations (A25) to (A30).

Appendix 4 : *Derivation of 3-rd order model transfer-function matrix of Fig. 3.11 or equations (3.17) to (3.21) from equations (3.11) to (3.13) :*

From Fig. 3.4 :-

$$\Delta\omega = s\Delta\delta \tag{A51}$$

Substituting (A51) into (3.11) and (3.12)

$$(Ms+D)\Delta\omega = \Delta T_m - K_2\Delta\psi_{fd} - \frac{K_1\omega_o}{s}\Delta\omega \tag{A52}$$

$$\Delta\psi_{fd} = \frac{K_3}{1+sK_3T'_{do}}\left(\Delta E_{fd} - \frac{K_4\omega_o}{s}\Delta\omega\right) \tag{A53}$$

Substituting (A53) into (A52)

$$(Ms+D)\Delta\omega = \Delta T_m - \frac{K_2K_3}{1+sK_3T'_{do}}\Delta E_{fd} + \frac{K_2K_3K_4}{s\left(1+sK_3T'_{do}\right)}\Delta\omega - \frac{K_1\omega_o}{s}\Delta\omega \tag{A54}$$

which becomes

$$\left[(Ms+D) - \frac{K_2K_3K_4\omega_o}{s\left(1+sK_3T'_{do}\right)} + \frac{K_1\omega_o}{s}\right]\Delta\omega = \Delta T_m - \frac{K_2K_3}{1+sK_3T'_{do}}\Delta E_{fd} \tag{A55}$$

$$\therefore \Delta\omega = \frac{\left(1+sK_3T'_{do}\right)s}{den}\Delta T_m - \frac{K_2K_3s}{den}\Delta E_{fd} \tag{A56}$$

where

$$den = (Ms+D)\left(1+sK_3T'_{do}\right)s + K_1\left(1+sK_3T'_{do}\right)\omega_o - K_2K_3K_4\omega_o \tag{A57}$$

Therefore, equations (3.17) and (3.18) are obtained, namely

$$\bar{g}_{11}(s) = \left(1+sK_3T'_{do}\right)s \tag{A58}$$

$$\bar{g}_{12}(s) = -K_2K_3s \tag{A59}$$

Now, substituting (A51) and (A53) into equation (3.13) :-

$$\Delta V_t = \frac{K_3 K_6}{1+sK_3 T'_{do}} \Delta E_{fd} - \frac{K_3 K_4 K_6 \omega_o}{s(1+sK_3 T'_{do})} \Delta\omega + \frac{K_5 \omega_o}{s} \Delta\omega \qquad \text{(A60)}$$

or

$$\Delta V_t = \frac{K_3 K_6}{1+sK_3 T'_{do}} \Delta E_{fd} + \left[\frac{K_5(1+sK_3 T'_{do})\omega_o - K_3 K_4 K_6 \omega_0}{s(1+sK_3 T'_{do})} \right] \Delta\omega \qquad \text{(A61)}$$

Substituting (A56) into (A61)

$$\Delta V_t = K_3 \left[\frac{K_6(Ms+D)s + (K_1 K_6 - K_2 K_5)\omega_o}{den} \right] \Delta E_{fd} + \omega_o \left[\frac{K_5(1+sK_3 T'_{do}) - K_3 K_4 K_6}{den} \right] \Delta T_m \qquad \text{(A62)}$$

Therefore :-

$$\bar{g}_{22}(s) = K_3 \left[K_6(Ms+D)s + (K_1 K_6 - K_2 K_5)\omega_o \right] \qquad \text{(A63)}$$

$$\bar{g}_{21}(s) = \left[K_5(1+sK_3 T'_{do}) - K_3 K_4 K_6 \right] \omega_o \qquad \text{(A64)}$$

and this completes the 3-rd order model transfer-function representation of Fig. 3.11 or equations (3.17) to (3.21).

Appendix 5

The 3rd order model :-

$$a_{21} = -\frac{K_1}{M} \quad , \quad a_{22} = -\frac{D}{M} \quad , \quad a_{23} = -\frac{K_2}{M}, \quad a_{31} = -\frac{K_4}{T'_{do}} \quad , \quad a_{33} = -\frac{1}{K_3 T'_{do}}$$

$$b_{21} = \frac{1}{M}, \qquad b_{32} = \frac{1}{T'_{do}}, \qquad c_{21} = K_5, \qquad c_{33} = K_6$$

The 6th order model :-

$$a_{21} = -\frac{K_d}{M}, \quad a_{22} = -\frac{K_1}{M}, \quad a_{23} = -\frac{K_2}{M}, \quad a_{24} = -\frac{K_{21}}{M}, \quad a_{25} = -\frac{K_{22}}{M}, \quad a_{26} = -\frac{K_{23}}{M}$$

$$a_{31} = -\frac{\omega_o R_{fd}}{L_{fd}} m_1 L''_{ads}, \qquad a_{33} = -\frac{\omega_o R_{fd}}{L_{fd}} \left(1 - \frac{L''_{ads}}{L_{fd}} + m_2 L''_{ads} \right)$$

$$a_{34} = -\frac{\omega_o R_{fd}}{L_{fd}} \left(m_3 L''_{ads} - \frac{L''_{ads}}{L_{fd}} \right), \quad a_{35} = -\frac{\omega_o R_{fd}}{L_{fd}} m_4 L''_{ads}, \quad a_{36} = -\frac{\omega_o R_{fd}}{L_{fd}} m_5 L''_{ads}$$

$$a_{41} = -\frac{\omega_o R_{1d}}{L_{1d}} m_1 L''_{ads}, \qquad a_{43} = -\frac{\omega_o R_{1d}}{L_{1d}} \left(m_2 L''_{ads} - \frac{L''_{ads}}{L_{fd}} \right)$$

$$a_{44} = -\frac{\omega_o R_{1d}}{L_{1d}} \left(1 - \frac{L''_{ads}}{L_{fd}} + m_3 L''_{ads} \right), \quad a_{45} = -\frac{\omega_o R_{1d}}{L_{1d}} m_4 L''_{ads}, \quad a_{46} = -\frac{\omega_o R_{1d}}{L_{1d}} m_5 L''_{ads}$$

$$a_{51} = -\frac{\omega_o R_{1q}}{L_{1q}} n_1 L''_{aqs}, \qquad a_{53} = -\frac{\omega_o R_{1q}}{L_{1q}} n_2 L''_{aqs}, \qquad a_{54} = -\frac{\omega_o R_{1q}}{L_{1q}} n_3 L''_{aqs}$$

$$a_{55} = -\frac{\omega_o R_{1q}}{L_{1q}} \left(1 - \frac{L''_{aqs}}{L_{1q}} + n_4 L''_{aqs} \right), \qquad a_{56} = -\frac{\omega_o R_{1q}}{L_{1q}} \left(n_5 L''_{aqs} - \frac{L''_{aqs}}{L_{2q}} \right)$$

$$a_{61} = -\frac{\omega_o R_{2q}}{L_{2q}} n_1 L''_{aqs}, \qquad a_{63} = -\frac{\omega_o R_{2q}}{L_{2q}} n_2 L''_{aqs}, \qquad a_{64} = -\frac{\omega_o R_{2q}}{L_{2q}} n_3 L''_{aqs}$$

$$a_{65} = -\frac{\omega_o R_{2q}}{L_{2q}}\left(n_4 L''_{aqs} - \frac{L''_{aqs}}{L_{1q}}\right), \qquad a_{66} = -\frac{\omega_o R_{2q}}{L_{2q}}\left(1 - \frac{L''_{aqs}}{L_{2q}} + n_5 L''_{aqs}\right)$$

$$b_{21} = \frac{1}{M}, \qquad b_{32} = \frac{\omega_o R_{fd}}{L_{adu}}$$

$$c_{21} = \left[\frac{e_{do}}{e_{to}}\left(L_1 n_1 + m_1\left(L''_{ads} - R_a\right)\right) - \frac{e_{qo}}{e_{to}}\left(L_1 m_1 + n_1\left(L''_{aqs} + R_a\right)\right)\right]$$

$$c_{23} = \left[\frac{e_{do}}{e_{to}}\left(L_1 n_2 + m_2\left(L''_{ads} - R_a\right) - \frac{L''_{ads}}{L_{fd}}\right) - \frac{e_{qo}}{e_{to}}\left(L_1 m_2 + n_2\left(L''_{aqs} + R_a\right)\right)\right]$$

$$c_{24} = \left[\frac{e_{do}}{e_{to}}\left(L_1 n_3 + m_3\left(L''_{ads} - R_a\right) - \frac{L''_{ads}}{L_{1d}}\right) - \frac{e_{qo}}{e_{to}}\left(L_1 m_3 + n_3\left(L''_{aqs} + R_a\right)\right)\right]$$

$$c_{25} = \left[\frac{e_{do}}{e_{to}}\left(L_1 n_4 + m_4\left(L''_{ads} - R_a\right)\right) + \frac{e_{qo}}{e_{to}}\left(\frac{L''_{aqs}}{L_{1q}} - L_1 m_4 - n_4\left(L''_{aqs} + R_a\right)\right)\right]$$

$$c_{26} = \left[\frac{e_{do}}{e_{to}}\left(L_1 n_5 + m_5\left(L''_{ads} - R_a\right)\right) + \frac{e_{qo}}{e_{to}}\left(\frac{L''_{aqs}}{L_{2q}} - L_1 m_5 - n_5\left(L''_{aqs} + R_a\right)\right)\right]$$